Cell Reports
Medicine

Article

Robust SARS-CoV-2 T cell responses with common TCRαβ motifs toward COVID-19 vaccines in patients with hematological malignancy impacting B cells

Graphical abstract

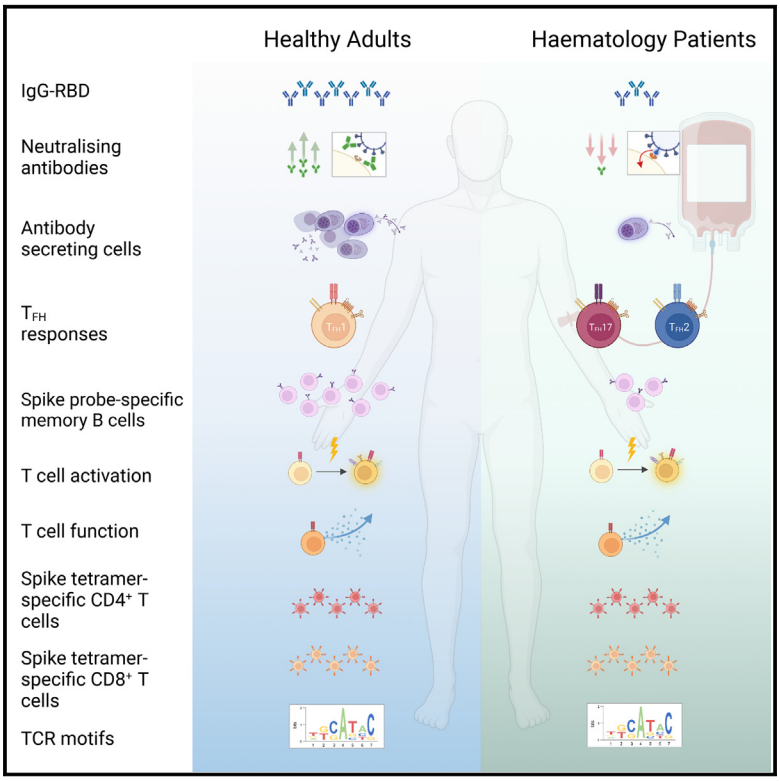

Highlights

- COVID-19 vaccines elicit robust SARS-CoV-2-specific T cells in hematology patients
- Prevalent TCRαβ motifs occur within tetramer$^+$ T cells in hematological patients
- Conversely, perturbed antibody responses and skewing of Tfh and ASC/Tfh kinetics occur
- Breakthrough infection patients have higher antibodies and comparable T cell responses

Authors

Thi H.O. Nguyen, Louise C. Rowntree, Lilith F. Allen, ..., Constantine S. Tam, Benjamin W. Teh, Katherine Kedzierska

Correspondence

ben.teh@petermac.org (B.W.T.), kkedz@unimelb.edu.au (K.K.)

In brief

Nguyen et al. define antibody, B, and T cell responses following COVID-19 vaccination in patients with hematological malignancy that are immunocompromised and vulnerable to severe COVID-19 infection. COVID-19 vaccination induces robust T cell immunity in hematology patients with diseases and treatments impacting B cell immunity irrespective of B cell numbers and antibody responses.

Nguyen et al., 2023, Cell Reports Medicine *4*, 101017
April 18, 2023
https://doi.org/10.1016/j.xcrm.2023.101017

CellPress

Cell Reports Medicine

CellPress
OPEN ACCESS

Article

Robust SARS-CoV-2 T cell responses with common TCRαβ motifs toward COVID-19 vaccines in patients with hematological malignancy impacting B cells

Thi H.O. Nguyen,[1,26] Louise C. Rowntree,[1,26] Lilith F. Allen,[1,26] Brendon Y. Chua,[1,2] Lukasz Kedzierski,[1,3] Chhay Lim,[4] Masa Lasica,[5,6] G. Surekha Tennakoon,[4] Natalie R. Saunders,[4] Megan Crane,[4] Lynette Chee,[7,8] John F. Seymour,[7,9] Mary Ann Anderson,[7,9,10] Ashley Whitechurch,[7] E. Bridie Clemens,[1] Wuji Zhang,[1] So Young Chang,[1] Jennifer R. Habel,[1] Xiaoxiao Jia,[1] Hayley A. McQuilten,[1] Anastasia A. Minervina,[11] Mikhail V. Pogorelyy,[11] Priyanka Chaurasia,[12]

(Author list continued on next page)

[1]Department of Microbiology and Immunology, University of Melbourne, at the Peter Doherty Institute for Infection and Immunity, Melbourne, VIC 3000, Australia
[2]Global Station for Zoonosis Control, Global Institution for Collaborative Research and Education (GI-CoRE), Hokkaido University, Sapporo, Hokkaido 060-0808, Japan
[3]Faculty of Veterinary and Agricultural Sciences, University of Melbourne, Melbourne, VIC 3000, Australia
[4]Department of Infectious Diseases, Peter MacCallum Cancer Centre, Melbourne, VIC 3000, Australia
[5]Department of Haematology, St Vincent's Hospital, Fitzroy, VIC 3065, Australia
[6]Department of Haematology, Eastern Health, Box Hill, VIC 3128, Australia
[7]Department of Clinical Haematology, The Royal Melbourne Hospital and Peter MacCallum Cancer Centre, Melbourne, VIC 3000, Australia
[8]Department of Medicine, University of Melbourne, Parkville, VIC 3010, Australia
[9]Sir Peter MacCallum Department of Oncology, University of Melbourne, Parkville, VIC 3010, Australia
[10]Walter and Eliza Hall Institute of Medical Research, Parkville, VIC 3052, Australia
[11]Department of Immunology, St. Jude Children's Research Hospital, Memphis, TN 38105, USA
[12]Infection and Immunity Program and Department of Biochemistry and Molecular Biology, Biomedicine Discovery Institute, Monash University, Clayton, VIC 3800, Australia
[13]ARC Centre of Excellence in Convergent Bio-Nano Science and Technology, University of Melbourne, Melbourne, VIC 3010, Australia
[14]Melbourne Sexual Health Centre, Infectious Diseases Department, Alfred Health, Central Clinical School, Monash University, Melbourne, VIC 3004, Australia
[15]World Health Organisation (WHO) Collaborating Centre for Reference and Research on Influenza, at The Peter Doherty Institute for Infection and Immunity, Melbourne, VIC 3000, Australia

(Affiliations continued on next page)

SUMMARY

Immunocompromised hematology patients are vulnerable to severe COVID-19 and respond poorly to vaccination. Relative deficits in immunity are, however, unclear, especially after 3 vaccine doses. We evaluated immune responses in hematology patients across three COVID-19 vaccination doses. Seropositivity was low after a first dose of BNT162b2 and ChAdOx1 (∼26%), increased to 59%–75% after a second dose, and increased to 85% after a third dose. While prototypical antibody-secreting cells (ASCs) and T follicular helper (Tfh) cell responses were elicited in healthy participants, hematology patients showed prolonged ASCs and skewed Tfh2/17 responses. Importantly, vaccine-induced expansions of spike-specific and peptide-HLA tetramer-specific $CD4^+$/$CD8^+$ T cells, together with their T cell receptor (TCR) repertoires, were robust in hematology patients, irrespective of B cell numbers, and comparable to healthy participants. Vaccinated patients with breakthrough infections developed higher antibody responses, while T cell responses were comparable to healthy groups. COVID-19 vaccination induces robust T cell immunity in hematology patients of varying diseases and treatments irrespective of B cell numbers and antibody response.

INTRODUCTION

Patients with hematological malignancies such as chronic lymphocytic leukemia (CLL) and multiple myeloma (MM) and those in the early period following hematopoietic stem cell transplantation (HCT) and chimeric antigen receptor T (CAR-T) therapy are at higher risk for viral respiratory tract infections, including COVID-19.[1–3] Up to half of hematology patients with COVID-19

Jan Petersen,[12] Tejas Menon,[1] Luca Hensen,[1] Jessica A. Neil,[1] Francesca L. Mordant,[1] Hyon-Xhi Tan,[1] Aira F. Cabug,[1] Adam K. Wheatley,[1]Stephen J. Kent,[1,13,14] Kanta Subbarao,[1,15] Theo Karapanagiotidis,[16] Han Huang,[16] Lynn K. Vo,[16] Natalie L. Cain,[16] Suellen Nicholson,[16] Florian Krammer,[17] Grace Gibney,[18] Fiona James,[18] Janine M. Trevillyan,[18,23] Jason A. Trubiano,[4,8,19,20] Jeni Mitchell,[21] Britt Christensen,[8,21] Katherine A. Bond,[1,16,22] Deborah A. Williamson,[10,16,23] Jamie Rossjohn,[12,24] Jeremy Chase Crawford,[11] Paul G. Thomas,[11] Karin A. Thursky,[4,9,20] Monica A. Slavin,[4,9,20,23,25] Constantine S. Tam,[7,8,25] and Benjamin W. Teh,[4,9,20,25,*] and Katherine Kedzierska[1,2,25,27,*]

[16]Victorian Infectious Diseases Reference Laboratory (VIDRL), at the Peter Doherty Institute for Infection and Immunity, Melbourne, VIC 3000, Australia
[17]Department of Microbiology, Icahn School of Medicine at Mount Sinai, New York, NY 10029, USA
[18]Department of Infectious Diseases, Austin Health, Heidelberg, VIC 3084, Australia
[19]Centre for Antibiotic Allergy and Research, Department of Infectious Diseases, Austin Health, Heidelberg, VIC 3084, Australia
[20]National Centre for Infections in Cancer, Peter MacCallum Cancer Centre, Melbourne, VIC 3000, Australia
[21]Department of Gastroenterology, Royal Melbourne Hospital, Melbourne, VIC 3050, Australia
[22]Department of Microbiology, Royal Melbourne Hospital, Melbourne, VIC 3050, Australia
[23]Department of Infectious Diseases, University of Melbourne at the Peter Doherty Institute for Infection and Immunity, Melbourne, VIC 3000, Australia
[24]Institute of Infection and Immunity, Cardiff University School of Medicine, Heath Park, CF14 4XN Cardiff, UK
[25]Senior author
[26]These authors contributed equally
[27]Lead contact
*Correspondence: ben.teh@petermac.org (B.W.T.), kkedz@unimelb.edu.au (K.K.)
https://doi.org/10.1016/j.xcrm.2023.101017

present with severe disease and require hospital admission, 15% require intensive care, and mortality rates can reach 30%–40%.[1,2] Furthermore, immune suppression from underlying disease, immune reconstitution following cellular therapies (HCT, CAR-T), and ongoing treatments such as anti-CD20 monoclonal antibody therapies continue to drive risk for COVID-19 infection but concurrently impact protective responses from vaccination.[4–6] To prevent severe SARS-CoV-2 (severe acute respiratory syndrome coronavirus 2) infection in this immunosuppressed high-risk group of patients, there is an urgent need to comprehensively profile their immune response to COVID-19 vaccination to better understand the interplay between underlying disease, treatment and optimal correlates of protection so that vaccination strategies can be enhanced.

Detection of circulating SARS-CoV-2-specific receptor-binding domains (RBDs) and neutralizing antibodies are widely utilized as surrogate endpoints for evaluation of vaccine efficacy in hematology patients,[7,8] yet it is unclear whether these are appropriate endpoints, especially in the setting of B cell depletion. Patients with B cell hematological malignancies such as CLL, patients in the early period following HCT and CAR-T therapy, and those receiving active therapy and B cell-depleting therapies (anti-CD20, BTK inhibitors) within 12 months have low humoral response rates to SARS-CoV-2 vaccination.[7,9]

Serological endpoints offer only a glimpse of the potential breadth of immune response to vaccination and may not be the best predictor of efficacy. Cellular responses reported to date relied on limited measurements of SARS-CoV-2-specific T cell responses.[9–11] Early data suggest a lack of correlation between humoral and cellular responses in patients with hematological malignancy, and cellular responses tend to be higher in B cell-depleted patients than non-B cell-depleted patients.[9,12] Furthermore, the majority of studies in hematology patients were performed following 2 COVID-19 vaccine doses.[13–15]

In hematology patients hospitalized with COVID-19, robust $CD8^+$ T cell responses correlated with better outcomes, including among those treated with anti-CD20 therapy.[16] Similarly, in patients with multiple sclerosis (MS), SARS-CoV-2-specific antibody and memory B cell responses were reduced in patients on monoclonal anti-CD20 treatment following SARS-CoV-2 mRNA vaccination; however, all patients generated robust spike-specific $CD4^+$ and $CD8^+$ T cell responses.[17]

We have previously compared and contrasted *ex vivo* SARS-CoV-2-specific $CD8^+$ and $CD4^+$ T cell responses and their T cell receptor (TCR) repertoires in SARS-CoV-2-infected children and adults,[18–21] pre-pandemic children and adults,[18,19] and following COVID-19 mRNA vaccination versus infection,[22,23] revealing diverse TCR repertoires with prominent TCR$\alpha\beta$ motifs that were shared between different individuals.[18,20–24] Whether these prominent TCR$\alpha\beta$ signatures are observed in hematology patients following COVID-19 vaccination remains to be elucidated, particularly in those with B cell malignancies or following ChAdOx1 vaccination.

We evaluate the breadth of immune responses following COVID-19 vaccination in hematology patients with diseases and treatments impacting B cell immunity, where scant data exist after the third dose. Our study shows that hematology patients who fail to seroconvert and generate memory B cell responses post-vaccination can still generate robust SARS-CoV-2-specific T cell immunity to protect against severe and fatal COVID-19.

RESULTS

COVID-19 vaccination cohort

To assess immunological responses toward COVID-19 vaccines in hematology patients, 95 SARS-CoV-2-unexposed, seronegative patients were recruited between April and December 2021 (Figure 1A; Table S1). Patients were predominantly male compared with healthy individuals (71% versus 29%). For comparison, 58 healthy SARS-CoV-2-unexposed, seronegative participants were recruited during the same period (26 ChAdOx1, 32

CellPress
OPEN ACCESS

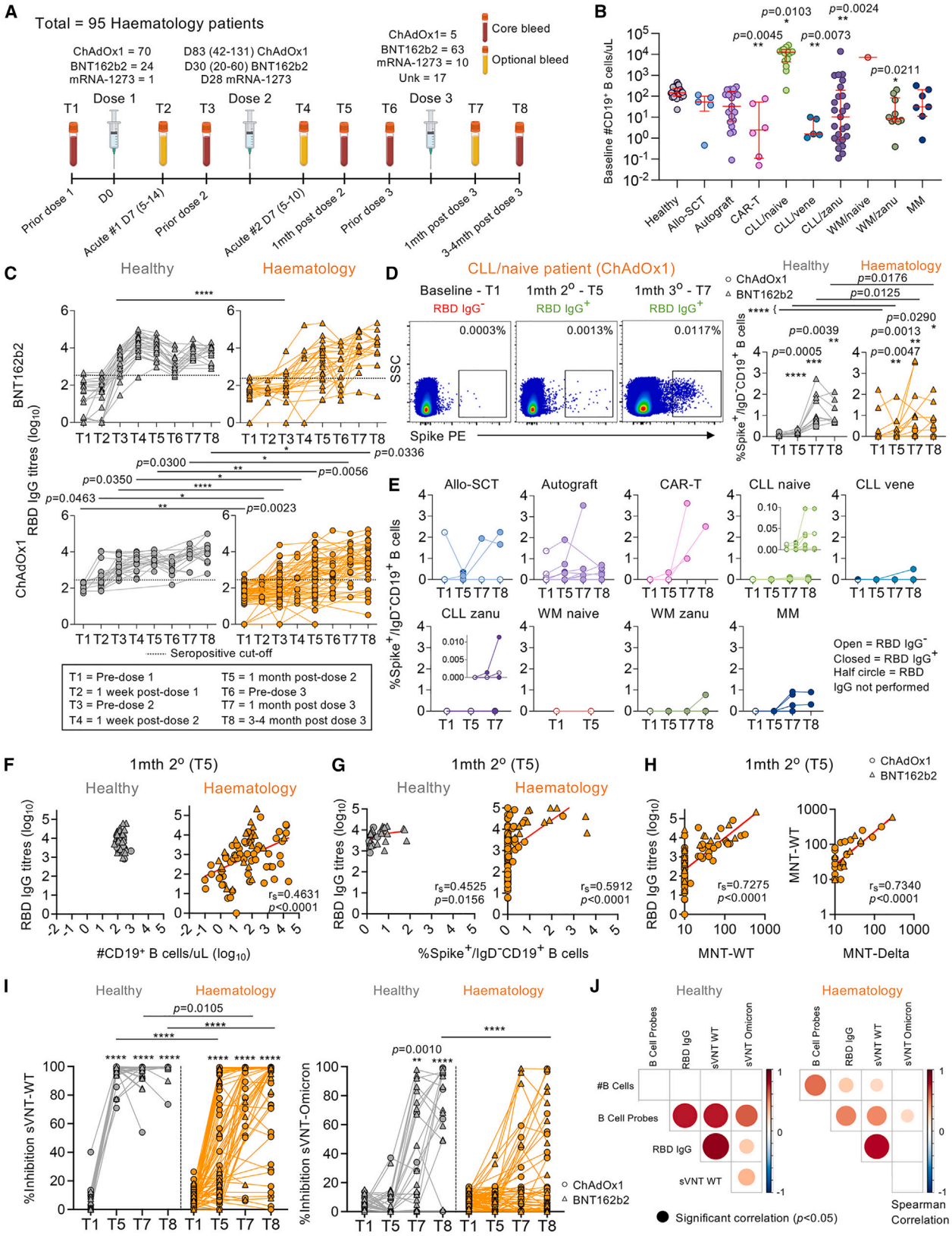

(legend on next page)

BNT162b2). During the study, 12 patients and 8 healthy individuals had breakthrough SARS-CoV-2 infection (Table S1). ChAdOx1 and BNT162b2 vaccine responses were analyzed separately or grouped together with different symbols. Subjects labeled as having BNT162b2 or ChAdOx1 were based on their two doses.

Hematology patients have reduced RBD-specific IgG antibodies, memory spike-specific B cells, and neutralizing antibodies following COVID-19 vaccination

Given the heterogeneity in the hematology cohort, blood B cell numbers varied in patients compared with healthy individuals (Figure 1B), with higher numbers in patients with CLL not on treatment but lower numbers in CAR-T patients, patients with CLL on venetoclax, patients with CLL on zanubrutinib, and patients with Waldenstrom macroglobulinemia on zanubrutinib. ELISA immunoglobulin G (IgG) antibody responses directed at RBDs corresponding to the ancestral vaccine strain (herein called RBD IgG) were lower in BNT162b2-vaccinated hematology patients compared with healthy individuals prior to the second vaccine dose (T3) but were comparable after the second and third doses (Figure 1C). RBD IgG antibody responses in ChAdOx1-vaccinated patients were lower than healthy individuals at all time points. Patient seropositivity was lower after first dose (26%, T3, n = 87), then increased to 65% 1 month after the second dose (T5, n = 82) and 87% 1 month after the third dose (T7, n = 30). Seropositivity remained stable at 84% ~3–4 months post-third dose (T8, n = 56), indicating that a small proportion of patients, particularly patients with CLL on zanubrutinib (CLL/zanu), still did not have any robust RBD IgG antibody responses after 3 COVID-19 vaccinations. Healthy individuals were 91% seropositive after the primary vaccination and 100% seropositive after the second- (T5) and third-dose vaccinations (T7 and T8). Heterogeneity of RBD IgG antibody responses were observed when hematology patients were grouped by low, normal, or high B cell numbers or by disease/treatment group (Figures S1A–S1C).

COVID-19 vaccination induced gradual significant increases in memory spike probe-specific IgD^- B cells in both healthy individuals and hematology patients of the same magnitude range (Figures 1D and S2A). However, hematology patients' spike-specific B cell responses were significantly lower than healthy individual responses after vaccination due to some of the patients not having detectable memory spike-specific B cell responses, particularly those with B cell malignancies (CLL, Waldenstrom macroglobulinemia [WM], MM) (Figures 1D and 1E) or abnormal B cell numbers (Figure S1D). Total B cell numbers and frequencies of memory spike-specific B cells correlated with RBD IgG antibody titers in hematology patients ~1 month after the second vaccine, but only memory spike-specific B cell frequencies correlated with antibody titers in healthy individuals given the narrower range in B cell numbers (Figures 1F and 1G). Patients' RBD IgG antibody titers strongly correlated with microneutralizing titers (MNTs) against the ancestral strain (Figure 1H) and, to a lesser extent, the Delta strain (r_s = 0.5994, $p < 0.0001$, data not shown), whereas ancestral and Delta MNTs were strongly correlative (Figure 1H).

Ancestral surrogate virus neutralization test (sVNT) neutralizing antibodies increased following COVID-19 vaccination in both healthy individuals and hematology patients, but increases in Omicron (B.1.1.529; BA.1-like) sVNT antibodies were only observed in healthy individuals (Figure 1I). Neutralizing sVNT responses were lower in hematology patients compared with healthy individuals after the second and third doses using the ancestral strain and were also lower ~3–4 months after the third dose using the B.1.1.529 Omicron strain.

Correlation matrix of antibody and B cell responses showed B cell numbers only correlating with spike-specific memory B cells in hematology patients (Figure 1J). Correlations of spike-specific memory B cells with antibody responses were also stronger for healthy individuals compared with patients. Thus, antibody and B cell responses following COVID-19 vaccination were reduced compared with otherwise healthy individuals, likely due to their disease state and immunosuppressive treatment, thus explaining the low B cell numbers.

COVID-19 vaccination induces non-prototypical activation of ASCs, Tfh cells, and $CD8^+$ T cells in hematology patients

Transient activation of $CD27^{hi}CD38^{hi}$ antibody-secreting cells (ASCs) and circulating $PD\text{-}1^+ICOS^+$ $CXCR5^+$ T follicular helper (Tfh) cells peak in the blood ~7–10 days after SARS-CoV-2 infection using whole-blood flow cytometry assays.[25,26] Induction of activated Tfh cells also occurs in the blood and draining lymph nodes following COVID-19 mRNA vaccination.[22,27] Dual ASC and Tfh cell responses have also been observed following

Figure 1. RBD-specific IgG antibodies, neutralizing antibodies, and memory spike-specific B cell responses following COVID-19 vaccination

(A) Study design and sampling timepoints.

(B) B cell numbers per μL with median and interquartile range (IQR) shown (hematology n = 94; healthy n = 39). Statistical significance determined by Dunn's multiple comparisons set on healthy versus all other disease groups.

(C) Endpoint IgG titers of ancestral RBD antibodies (hematology n = 94, 24 BNT162b2, 70 ChAdOx1; healthy n = 53, 27 BNT162b2, 26 ChAdOx1). Seropositive cutoff defined by baseline mean + 2 SD per group.

(D and E) Spike-probe staining of spike-specific memory B cells in (D) healthy (n = 16) and hematology groups (n = 64) and (E) per malignancy and treatment groups.

(F and G) Spearman's correlation (r_s) of RBD IgG titers with (F) B cell numbers (hematology n = 82; healthy n = 45) and (G) spike-specific memory B cells (hematology n = 64; healthy n = 16).

(H) r_s of RBD IgG titers with ancestral MNT and ancestral versus Delta MNT (hematology n = 82).

(I) Percentage sVNT inhibition assay against wild-type (WT) ancestral and Omicron strains (haematology n = 63; healthy n = 29).

(J) r_s matrix of B cell and antibody parameters at T1/T5/T7/T8.

Statistical significance determined by Wilcoxon test for time point comparisons against T1 or by Mann-Whitney for comparisons between healthy and patient time points. ****$p < 0.0001$. Experiments were performed once for each sample. Refer to Figure S2A.

CellPress
OPEN ACCESS

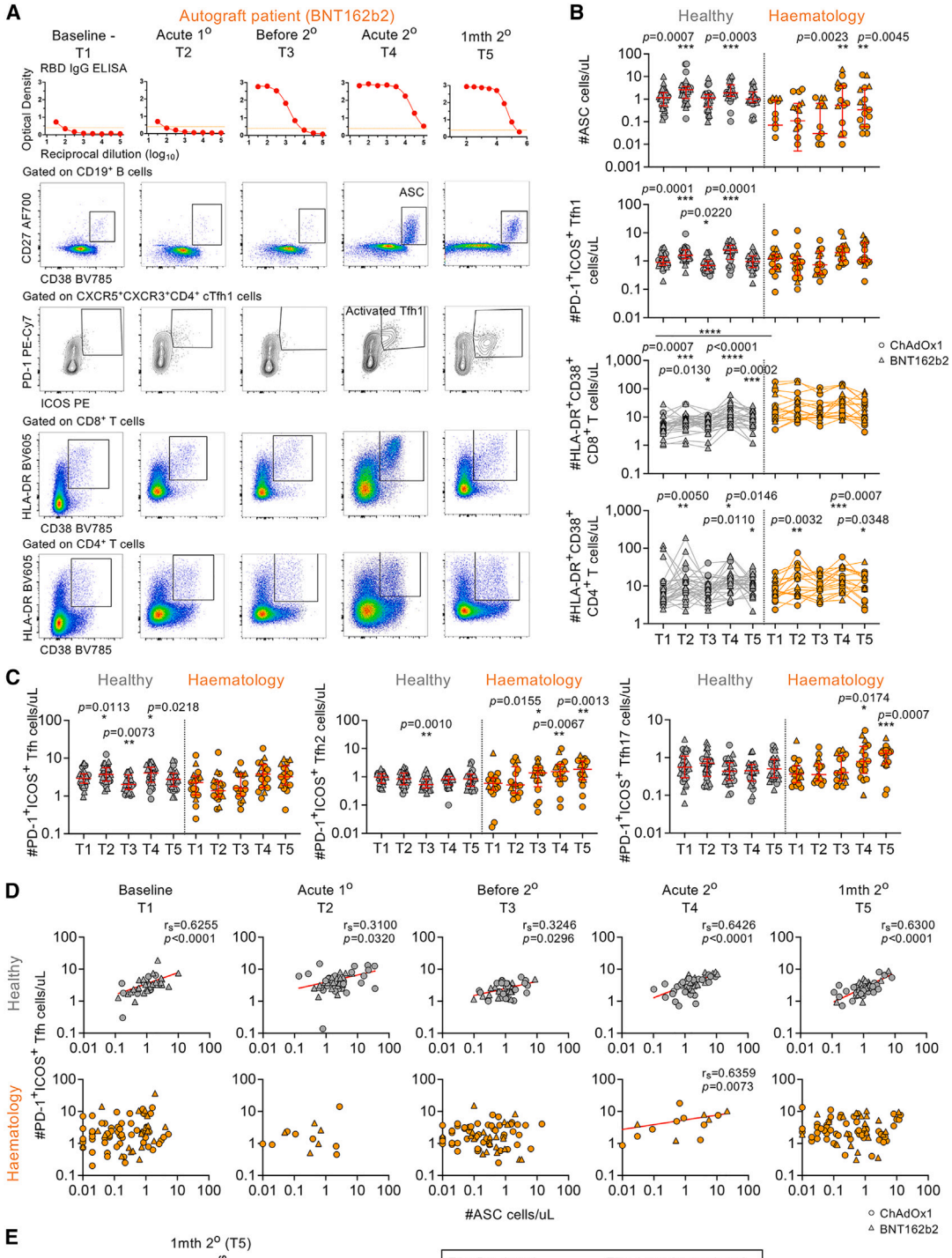

(legend on next page)

influenza virus infection[28] and influenza vaccination,[29] with the predominant Tfh subset being Tfh type 1 cells (Tfh1 cells; $CXCR3^+CCR6^-$). We performed whole-blood staining on a subset of 30 hematology patients that underwent intense blood sampling to capture transient acute responses following first and second COVID-19 vaccination doses (Figures 2A and S2B).

Healthy individuals showed prototypical vaccine-induced responses with transient increases in $CD27^{hi}CD38^{hi}$ ASCs, $PD\text{-}1^+ICOS^+$-activated Tfh1 cells, and $HLA\text{-}DR^+CD38^+$-activated $CD8^+$ and $CD4^+$ T cells acutely observed at ~7 days after the first (T2) and second COVID-19 vaccination doses (T4) when compared with baseline T1 levels (Figure 2B). In hematology patients, ASCs only increased at ~7 days after the second dose (T4) and remained high at ~1 month post-second dose (T5) (Figures 2A and 2B). $PD\text{-}1^+ICOS^+$ Tfh responses were skewed toward type 2 (Tfh2; $CXCR3^-CCR6^-$) and type 17 subsets (Tfh17; $CXCR3^-CCR6^+$), which similarly increased and remained high after the second dose (Figure 2C). Since hematology patients had higher baseline levels of activated $HLA\text{-}DR^+CD38^+CD8^+$ T cells compared with healthy individuals, $HLA\text{-}DR^+CD38^+CD8^+$ T responses were not further induced by two doses of COVID-19 vaccination (Figure 2B). In contrast, $HLA\text{-}DR^+CD38^+$ $CD4^+$ T cell responses were prototypical of those observed in healthy individuals with acute transient increases after the first and second doses (Figure 2B).

Numbers of ASCs typically correlated with Tfh numbers across all time points measured (T1–T5) in healthy individuals, but this correlation was only observed at ~7 days post-second dose (T4) in hematology patients (Figure 2D). At T4, ASCs correlated with each Tfh subset in healthy individuals, whereas Tfh1 cells, but not Tfh2 or Tfh17 cells, correlated with ASCs in hematology patients (Figure S3A), even though we did not observe significant increases in Tfh1 responses but rather observed significant increases in the other Tfh2/17 subsets. $HLA\text{-}DR^+CD38^+$ $CD8^+$ and $CD4^+$ T cells correlated with each other across all time points in both healthy individuals and hematology patients except for ~7 days after the first vaccine dose (T2) in hematology patients (Figure S3B).

Overall, hematology patients needed two vaccination doses to generate ASC and Tfh responses, but there was prolonged activation of ASCs, skewing of Tfh2/17 responses, and high basal levels of activated $CD8^+$ T cells.

Comparable spike-specific $CD4^+$ and $CD8^+$ T cell responses in hematology patients and healthy individuals post-COVID-19 vaccination

To evaluate COVID-19 vaccine-induced spike-specific T cell responses, we performed activation-induced marker (AIM) and intracellular cytokine staining (ICS) assays (Figures 3A, S2C, S2D, and S4A). AIM frequency of $CD134^+CD137^+CD4^+$ and $CD69^+CD137^+$ $CD8^+$ cells increased at ~1 month post-second dose (T5) compared with baseline (T1) by a mean 32- and 31-fold for healthy individuals and a higher mean 87- and 75-fold for patients, respectively (Figure 3B), which was not due to any differences in baseline threshold levels at T1. These increases in AIM $CD4^+$ and $CD8^+$ T cell responses were maintained after the third dose (T7 and T8) in both healthy individuals and hematology patients. Unlike antibody and memory B cell responses, there was no difference in AIM responses between healthy individuals and hematology patients at any time point (Figure 3B).

Similarly, functional ICS assay showed increased interferon γ ($IFN\gamma$)$^+$tumor necrosis factor α ($TNF\text{-}\alpha$)$^+$ $CD4^+$ and $CD8^+$ T cell responses for both healthy individuals and hematology patients at all time points post-COVID-19 vaccination (T5, T7, and T8) with mean 3- to 19-fold and 6- to 36-fold increases for healthy individuals and mean 11- to 31-fold and 10- to 44-fold for hematology patients, respectively (Figure 3C). Frequencies of $IFN\gamma^+TNF\text{-}\alpha^+$ $CD4^+$ and $CD8^+$ T cells were higher for patients at baseline (T1) and ~1 month post-second dose (T5) compared with healthy individuals, but frequencies were comparable after the third dose. Importantly, T cell responses were observed across disease groups by AIM (Figure 3D) or ICS assay (Figure S4B). Autograft patients had overall higher $CD134^+CD137^+$ and $IFN\gamma^+TNF\text{-}\alpha^+$ $CD4^+$ T cell frequencies at ~1 month post-second dose (T5) when compared with healthy individuals, whereas CLL/naive patients had higher $IFN\gamma^+TNF\text{-}\alpha^+$ $CD4^+$ and $CD8^+$ T cell frequencies (Figures 3E and S4C).

Correlations of $CD4^+$ versus $CD8^+$ T cell responses and of AIM versus ICS responses were more observed in healthy individuals compared with hematology patients (Figure S4D). AIM Tfh responses showed increases in $CXCR5^+$ Tfh and $CXCR5^+CXCR3^+$ Tfh1 responses in both groups following COVID-19 vaccination, while $CXCR5^+CXCR3^-$ Tfh2/17 responses decreased (Figures 3F and S5A). Based on serostatus, RBD IgG^+ patients generated more robust AIM and ICS $CD4^+$ and $CD8^+$ T cell responses compared with RBD IgG^- patients (Figure 3G). Correlations of T cell responses against antibody and B cell responses were stronger and more frequent in healthy individuals compared with hematology patients (Figure 3H).

Spike-specific $CD4^+$ and $CD8^+$ T cell responses were fairly similar between ChAdOx1- or BNT162b2-vaccinated patients and compared with healthy groups (Figures S5B and S5C). T cell responses were also comparable between hematology patients with low, normal, or high B cell numbers (Figure S1E). This was exemplified by volcano plot analyses combining antibodies with spike-specific memory B and T cell responses (Figures 3I and S6), where humoral responses were more enriched in

Figure 2. Whole-blood analyses of acute ASC, Tfh cell, and activated $CD8^+$ and $CD4^+$ T cell responses

(A) RBD IgG ELISA titration curves and fluorescence-activated cell sorting (FACS) plots of ASCs and activated Tfh1/$CD8^+$/$CD4^+$ T cells. Orange dotted lines indicate endpoint titer cutoffs.

(B) Numbers of ASCs and activated Tfh1 cells and $CD8^+$ and $CD4^+$ T cells per μL (hematology n = 17; healthy n = 39).

(C) Numbers of Tfh, Tfh2, and Tfh17 subsets per μL.

(D) r_s of ASCs and activated Tfh1 cells per time point T1–T5 (T1/T3/T5 hematology n = 94; T2/T4 hematology n = 17). Statistical significance determined by Wilcoxon test for time point comparisons against T1 (floating values) or by Mann-Whitney for comparisons between healthy and patient time points (connecting line). ****$p < 0.0001$. Experiments were performed once for each sample. Refer to Figures S2B and S3. Zero data points not shown but included in statistics.

CellPress
OPEN ACCESS

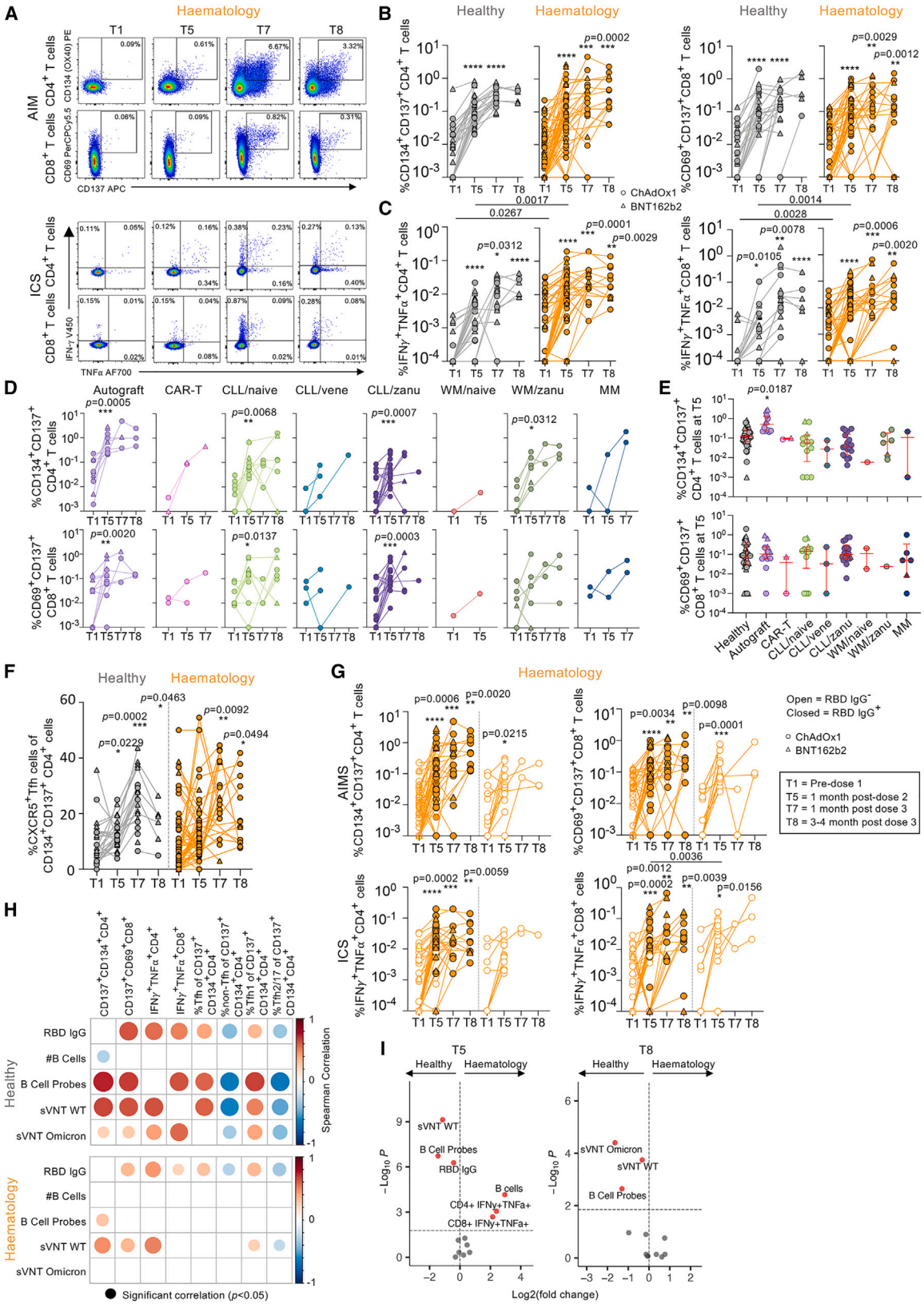

(legend on next page)

healthy individuals after the second and third doses compared with hematology patients, irrespectively of whether they had low or normal to high B cells.

Following three-dose COVID-19 vaccination, hematology patients of varying diseases and immunosuppressive treatments, including those with B cell deficiencies, can still generate robust and functional spike-specific T cell responses.

SARS-CoV-2 peptide-HLA tetramer-specific T cell responses increase post-COVID-19 vaccination in hematology patients

To define SARS-CoV-2 epitope-specific $CD4^+$ and $CD8^+$ T cell responses, peptide-HLA tetramers combined with tetramer-associated magnetic enrichment (TAME)[18,21] (Figures 4A and S2E) were used to measure directly *ex vivo* $CD4^+$ T cell responses directed against the prominent DPB4/S_{167} epitope[21,22] and $CD8^+$ T cell responses against 6 immunodominant $CD8^+$ T cell epitopes (A1/S_{865}, A2/S_{269}, A3/S_{378}, A24/S_{1208}, B15/S_{919}, and B35/S_{321}).[18–20,23,30,31] These epitopes originated from the ancestral SARS-CoV-2 spike and are highly conserved across variant of concern (VOC) strains.[21,32] B15/S_{919} shares similar homology and is highly cross-reactive to common cold coronaviruses (HKU1/OC43).[23]

Two doses of mRNA COVID-19 vaccination have previously been shown to induce robust $CD4^+$ and $CD8^+$ $tetramer^+$ T cell responses.[22,23,33] We observed robust expansions of pooled $tetramer^+$ $CD4^+$ and $CD8^+$ T cell frequencies after the third dose with either vaccine (Figure 4B). Baseline tetramer precursor frequencies weakly correlated with tetramer responses at T5 and T7/T8 (Figure 4C). There was no correlation between tetramer-specific T cell responses and B cell numbers at T1 or T5, with weak correlations based on RBD serostatus (Figures 4D and S7A). Patients' $tetramer^+$ T cell frequencies increased following three-dose COVID-19 vaccination, irrespective of RBD IgG serostatus (Figure 4E) or B cell numbers (Figure S1F), similar to healthy individuals (Figure S7B). Cross-reactive B15/S_{919} epitope had comparable or lower baseline frequency (mean 3.26×10^{-6}) than other $CD8^+$ epitopes in patients and healthy individuals (4.47×10^{-5}), suggesting no numerical cross-reactive advantage. Importantly, increase and maintenance of SARS-CoV-2-epitope T cell responses following COVID-19 vaccination were observed across all malignancy and treatment groups, except for the WM/naive group, which was small in number and not followed up with after the second dose (Figure 4F). Most patient groups generated similar response magnitudes to healthy individuals at T5, except for CLL/venetoclax (vene) patients and patients with MM (Figure 4G). CLL/vene patients also had lower $tetramer^+$ T cell frequencies at T1 baseline and ~3 months post-third dose (T8) (Figure S7C). Venetoclax also targets T cells, which may explain the lower responses for CLL/vene patients.

Baseline $tetramer^+$ phenotypes differed between healthy and hematology patients but converged post-vaccination (Figures 4H and S7D). This was attributed by overall baseline $CD4^+$/$CD8^+$ T cell phenotypes (Figure S7E) rather than individual epitope specificities (Figure S7F). Baseline $tetramer^+$ T cell profiles from healthy individuals were more of a prototypical $CD45RA^+CD27^+CD95^-$ naive-like phenotype compared with those of hematology patients, which gradually decreased post-vaccination. $Tetramer^+$ cells from hematology patients displayed activated profiles, with elevated baseline $CD45RA^-CD27^-$ T effector memory (Tem)-like and $CD45RA^+CD27^-$ T effector memory CD45RA (Temra)-like features. Nevertheless, both groups had increasing $CD45RA^-CD27^+$ T central memory (Tcm)-like $tetramer^+$ populations post-vaccination (Figure 4H), which is highly desirable for any T cell-based vaccine. Differences in phenotype profiles were also somewhat related to certain disease and treatment groups (Figure 4I).

Overall, hematology patients can generate robust SARS-CoV-2-specific T cell responses to a range of immunodominant spike epitopes following vaccination.

Hematology patients with COVID-19 breakthrough infections generate higher antibody responses than non-COVID-19 patients

During our study, 12 hematology patients had COVID-19 breakthrough infections (Figure 5). 2, 1, and 9 patients had COVID-19 after the first, second, and third vaccine doses, respectively. 3 patients were infected during the Delta period (June–July 2022), 6 during the emergence of Omicron (strain unknown, December 2021–January 2022), and 3 during the BA.1 Omicron wave (post-February 2022) where Delta was absent from circulation (Figure 5A). 8 healthy individuals had breakthrough COVID-19 after the third vaccine dose, which occurred during or after the emergence of BA.1 Omicron. All had mild COVID-19 infections, although 1 patient was hospitalized but not treated with any monoclonal antibodies, and 2 were treated with monoclonal antibody sotrovimab as outpatients (Figure 5B).

$COVID\text{-}19^+$ patients had higher RBD IgG antibodies than $COVID\text{-}19^-$ patients with 100% seropositivity at T8, consistent with an anamnestic response to the infection (Figure 5C). This was still significant when the 2 $COVID\text{-}19^+$ patients treated with sotrovimab were excluded from the analysis ($p = 0.0077$, data not shown). There were no differences in MNT and

Figure 3. Comparable spike-specific $CD4^+$ and $CD8^+$ T cell responses between hematology patients and healthy individuals

(A) AIM and ICS FACS plots.

(B and C) AIM (B) and ICS (C) frequencies of $CD4^+$ and $CD8^+$ T cells in healthy (n = 35, 23 BNT162b2, 12 ChAdOx1) and hematology groups (n = 56, 8 BNT162b2, 48 ChAdOx1).

(D and E) AIM frequency (D) per malignancy and treatment group and (E) at T5 where median and IQR are shown. Statistical significance determined by Dunn's multiple comparisons set on healthy versus all other disease groups.

(F) $CXCR5^+CD4^+$ Tfh response of total $CD134^+CD137^+$ $CD4^+$ T cells.

(G) AIM and ICS frequency between IgG RBD^+ and RBD^- patients.

(H) r_s matrix of antibody/B cell and T cell responses.

(I) Volcano plots at T5 and T8 comparing healthy individuals and hematology patients.

Statistical significance determined by Wilcoxon test for time point comparisons against T1 (floating values) or by Mann-Whitney for comparisons between healthy and patient time points (connecting line). ****$p < 0.0001$. Experiments were performed once for each sample. Refer to Figures S2C, S2D, and S4–S6.

CellPress
OPEN ACCESS

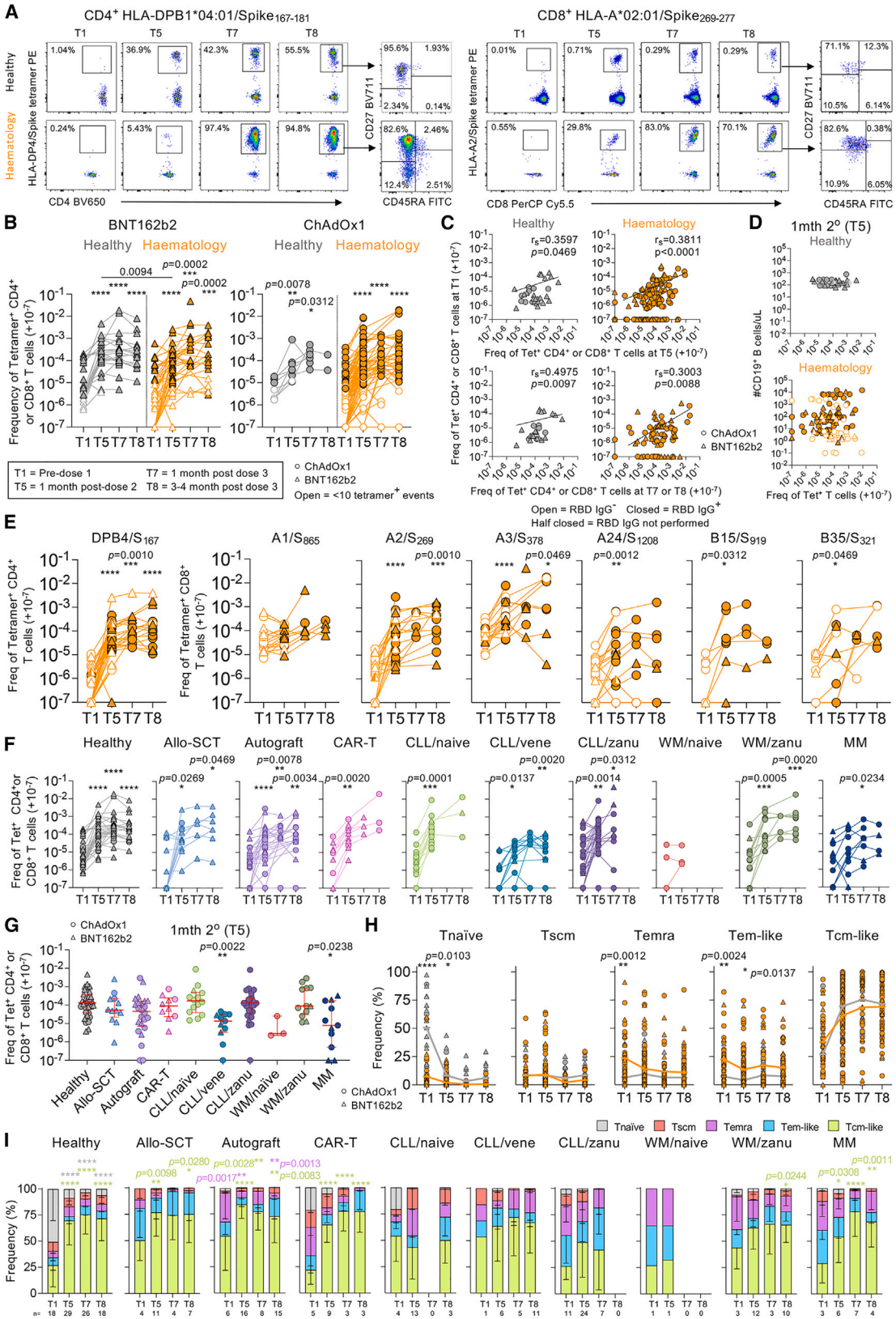

(legend on next page)

sVNT neutralizing responses (Figures 5D and 5E), although COVID-19$^+$ patients had higher sVNT neutralization toward the ancestral strain at T8 compared with COVID-19$^-$ patients. Spike-specific T cell responses were comparable between COVID-19$^-$ and COVID-19$^+$ healthy individuals and hematology patients (Figures 5F, 5G, 5H, S8A, and S8B). Tetramer+ phenotypes were comparable between breakthrough COVID-19$^+$ patients and healthy individuals, although the activation status of one patient sampled during acute infection showed increased PD-1 expression (Figures 5I and S8C). Our hematology patient data agree with previous reports in healthy individuals,[23] showing that vaccination or vaccination plus infection can elicit robust spike epitope-specific T cell responses.

We also performed tetramer staining directed against non-spike epitopes for 3 breakthrough patients and 3 healthy participants (Figure S9A). Spike, ORF1a, and nucleocapsid-specific CD8$^+$ T cells increased in breakthrough patients, while spike CD8$^+$ T cell frequencies were maintained in healthy participants (Figure S9B) with phenotype changes post-infection (Figure S9C) but similar activation profiles for spike and non-spike-specific CD8$^+$ T cells (Figure S9D).

SARS-CoV-2-specific T cells in hematology patients display prominent gene segment usage

TCR$\alpha\beta$ repertoires of dominant SARS-CoV-2 T cell epitopes have been identified as sharing similar motifs and gene usage in immunocompetent healthy individuals following SARS-CoV-2 infection[18,20–24] and COVID-19 mRNA vaccination.[23] To determine whether the molecular signatures underpinning epitope-specific T cell responses were conserved in our cohort of COVID-19-vaccinated hematology patients, we determined TCR$\alpha\beta$ repertoires for 3 of the most prominent spike-specific CD4$^+$ and CD8$^+$ T cell epitopes, DPB4/S_{167}, A2/S_{269}, and A24/S_{1208}, using single-cell TCR$\alpha\beta$ multiplex-nested RT-PCR after *ex vivo* tetramer enrichment.[34] A total of 637 paired TCR$\alpha\beta$ clonotypes from up to 17 hematology patients were analyzed across DPB4/S_{167} (n = 17), A2/S_{269} (n = 17), and A24/S_{1208} (n = 12) epitopes in terms of their clonotype composition and clonal expansion. These TCR$\alpha\beta$ repertoires were compared with previously published TCR datasets from healthy SARS-CoV-2-infected (DPB4/S_{167}, A2/S_{269}, and A24/S_{1208}) and COVID-19-vaccinated (A2/S_{269} and A24/S_{1208} only) individuals.[18,21–23]

In line with previous reports,[21,22] DPB4/S_{167}-specific CD4$^+$ T cells in hematology patients displayed a heavy bias for TRAV35/TRAJ42 gene segments (Figures 6A and S10; Table S2), which were paired with different TRBV/TRBJ genes. The A2/S_{269}-specific TCR repertoire in healthy infected and vaccinated cohorts is generally dominated by TRAV12-1 pairing with TRBV20-1 or TRBV7-9.[18,21,23,24] In contrast, TRAV29 had the highest number of different clonotypes observed in hematology patients, followed by TRAV12-1, both of which were paired with TRBV2. In addition, both TRAV29 and TRAV12-1 were only observed in 4/17 donors tested with very little clonal expansions, while some hematology patients had very large clonal expansions of non-TRAV12-1 clonotypes pairing with the common TRBV20-1 gene (donor P46: 86% TRAV8-1; donor P51: 96% TRAV13-2) (Table S2). The A24/S_{1208}-specific CD8$^+$ TCR repertoire was more diverse in hematology patients, which has been observed previously[20]; however, all 3 cohorts shared common TRAV19, TRAV21, and TRBV20-1 genes.

TCR sequence similarity network for each epitope identified prominent sharing of dominant motifs between vaccinated hematology and healthy infected cohorts for DPB4/S_{167}, followed by a smaller network for A2/S_{269} connecting all 3 cohorts available, and the smallest network was for A24/S_{1208} (Figure 6B). The DPB4/S_{167} network generated a common TRAV35/TRAJ42 sequence motif that represented both vaccinated hematology and healthy infected cohorts when motifs were analyzed separately per cohort (Figures 6B and S11), whereas TCRβ motifs were very different between groups. Interestingly, the TCRα and TCRβ network motifs for A2/S_{269} were only observed in the healthy vaccinated and infected cohorts and not in vaccinated hematology patients, which mainly comprised of TRAV29/TRAJ45 and TRBV2-TRBJ2-2 motifs. The A24/S_{1208} TCRα and TCRβ network motifs were only observed in vaccinated hematology patients, given the low number of sequences identified, while another TRBV5-6 motif was observed for healthy vaccinated individuals (Figures 6B and S11).

Strikingly, clonal expansions of diverse TCR clonotypes were most evident in hematology patients for A2/S_{269} and A24/S_{1208} CD8$^+$ T cells compared with healthy infected and healthy vaccinated cohorts. However, similarly to the network analyses, these clonotypes did not cluster as closely with each other compared with the DPB4/S_{167} repertoire, which was closely clustered and sharing the same gene usage but had less evidence of clonal expansions from either vaccinated hematology and healthy infected cohorts (Figure 6C). Nevertheless, the probability to

Figure 4. COVID-19 vaccination induces expansion of SARS-CoV-2-specific tetramer$^+$ T cell responses

(A) FACS plots of TAME-enriched CD4$^+$ and CD8$^+$ tetramer populations.

(B) Tetramer CD4$^+$ and CD8$^+$ T cell frequencies of healthy (n = 16, ChAdOx1 = 4, BNT162b2 = 12) and hematology groups (n = 54, ChAdOx1 = 35, BNT162b2 = 19) per vaccine type. Any samples with <10 tetramer$^+$ events are shown as open symbols. 1–3 tetramer responses shown per donor.

(C) r_s of T1 tetramer frequencies versus T5 or T7/T8.

(D) r_s of tetramer frequencies versus B cell numbers at T5.

(E–G) Tetramer frequencies per (E) epitope, (F) malignancy and immunosuppressive treatment, or (G) at T5 where median and IQR are shown.

(H) Phenotype frequencies of tetramer$^+$ cells from healthy (gray line) and hematology patients (orange line).

(I) Tetramer$^+$ phenotype per malignancy and immunosuppressive treatment.

The frequency of tetramer$^+$ cells are right shifted by 10^{-7} (i.e., no detected tetramer$^+$ events displayed as 10^{-7}). Only samples with 10 or more tetramer$^+$ events are included for (H) and (I). Statistical significance determined by Wilcoxon test for time point comparisons against T1 (floating values); Mann-Whitney for comparisons between healthy and patient timepoints (connecting line); (G) Dunn's multiple comparisons set on healthy versus all other disease groups; and (H) Sidak's multiple comparison test and (I) Dunnett's multiple comparison test for time point comparisons against T1. ****$p < 0.0001$. Experiments were performed once for each sample. Refer to Figures S2E and S7.

CellPress
OPEN ACCESS

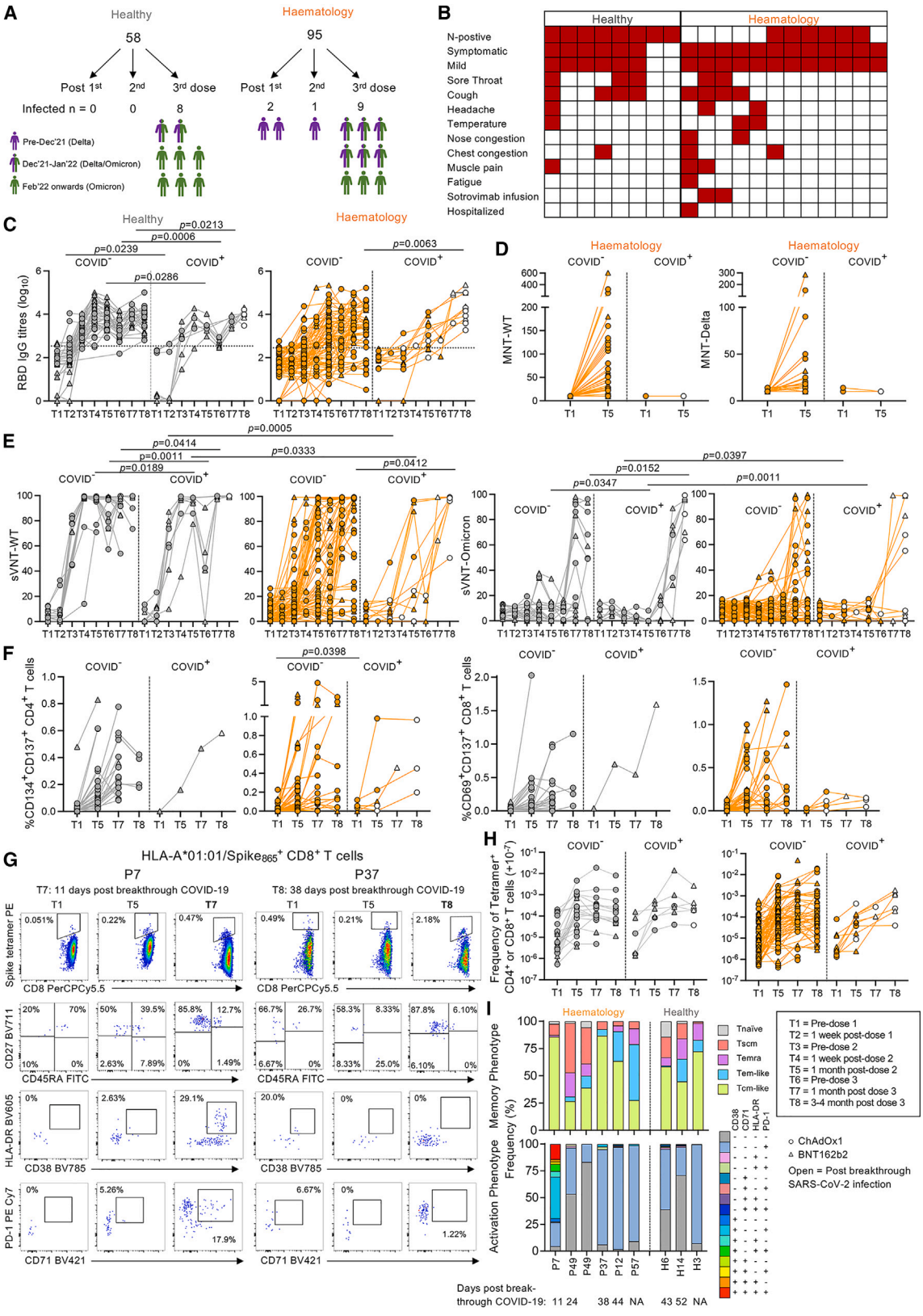

(legend on next page)

generate TCRs were comparable across the cohort groups for each epitope (Figure 6D).

Overall, following COVID-19 vaccination, hematology patients could generate robust SARS-CoV-2-specific T cells that shared many common TCR signatures with healthy vaccinated and infected cohorts.

DISCUSSION

Our study provides comprehensive insights into humoral and cellular immune responses following COVID-19 vaccination in hematology patients with malignancies and treatments expected to eradicate or profoundly impair B cell function. We demonstrate that hematology patients mount effective SARS-CoV-2-specific T cell responses to COVID-19 vaccines irrespective of their B cell malignancy or B cell-depleting therapies, with which B cell numbers are greatly affected. Importantly, these T cell responses, detected directly *ex vivo* with peptide-HLA tetramers, are comparable to healthy individuals with respect to the magnitude, phenotype, TCR$\alpha\beta$ diversity, clonal composition, and motifs. Conversely, B cell numbers relating to disease status markedly impacted SARS-CoV-2-specific antibody levels and memory spike-specific B cell responses, together with ASC and Tfh skewing.

Our cohort is representative of a hematological malignancy population with B cell deficiencies arising from disease and/or therapies. Apart from patients with CLL, WM, and myeloma, other hematological malignancies and prior treatments are well represented in our post-cellular therapies cohort (allogeneic transplant, autologous transplant, and CAR-T therapy), including patients with non-Hodgkin's lymphoma treated with prior anti-CD20 antibody exposure. While our patient group is heterogeneous, breakdown of immune response is provided by individual disease/treatment group in the individual figures to allow a reader to consider/assess responses by a particular group of interest (Figure S12).

Consistent with previous studies, hematology patients had lower seroconversion rates following the first and second doses compared with healthy individuals. We highlight that the third dose observed close to 90% seropositivity by RBD IgG in hematology patients, which is an excellent outcome for immunocompromised patients and comparable to the seropositivity rates observed after 2 doses in healthy individuals.

RBD-specific IgG antibody responses toward two doses of ChAdOx1 vaccine in hematology patients were lower than BNT162b2-vaccinated patients, when compared with healthy individuals, and remained lower after the third mRNA dose. This could partially be explained by the age difference, where ChAdOx1-vaccinated patients were older than BNT162b2-vaccinated patients or healthy individuals. Another explanation could be related to the type of vaccine, as it has been reported that two-dose ChAdOx1 vaccination provides lower protective efficacy (~60%) in terms of neutralizing antibodies compared with BNT162b2 (~90%).[35] A recent study comparing antibody and memory B cell responses following two-dose ChAdOx1, two-dose mRNA, or combined ChAdOx1/mRNA vaccination also observed inferior antibody responses with the ChAdOx1 vaccine.[36] Importantly, there were no differences in T cell responses between vaccine type.

Spike-specific $CD4^+$ and $CD8^+$ T cell responses following COVID-19 vaccination were also measured by AIM and ICS assays, as previously used in other SARS-CoV-2 infection studies.[37,38] The skewing of PD-$1^+$$ICOS^+$-activated Tfh2/Tfh17 in the whole-blood assay aligned with our AIM data, where the majority of the AIM Tfh response was made up of Tfh2/Tfh17 cells rather than Tfh1 cells. Our data support Apostolidis et al.'s study[17] where all patients with MS on anti-CD20 monoclonal antibody treatment (n = 20) generated robust spike-specific $CD4^+$ and $CD8^+$ T cell responses following BNT162b2 or mRNA-1273 mRNA vaccination in the absence of B cells.

Two doses of mRNA COVID-19 vaccination can induce robust $CD4^+$ and $CD8^+$ $tetramer^+$ T cell responses.[22,23,33] Here, both hematology patients and healthy individuals can generate robust $CD4^+$ and $CD8^+$ T cell responses to 7 immunodominant spike-specific epitopes after two doses of ChAdOx1 or BNT162b2 vaccines and after the third dose. Importantly, patients lacking RBD-specific IgG antibodies could still generate robust epitope-specific T cell responses. Furthermore, TCR repertoires from hematology patients shared common TCR signatures with healthy vaccinated and infected cohorts.

Breakthrough SARS-CoV-2 infections are increasingly becoming more common in the vaccinated community. Although SARS-CoV-2-infected patients had higher RBD-specific IgG antibody responses, T cell responses were

Figure 5. Vaccine responses between non-COVID-19 and breakthrough COVID-19

(A) COVID-19 following SARS-CoV-2 vaccination.

(B) Clinical symptoms and monoclonal antibody treatment for SARS-CoV-2 breakthrough infections.

(C) Endpoint IgG titers of ancestral RBD antibodies (44 $COVID^-$ and 8 $COVID^+$ healthy individuals; 83 $COVID^-$ and 12 $COVID^+$ patients). Seropositive cutoff defined by baseline mean + 2 SD per group.

(D) MNT titers at T5 against WT ancestral and Delta strains (74 $COVID^-$ and 2 $COVID^+$ patients).

(E) Percentage of inhibition by sVNT assay against WT ancestral and Omicron strains (44 $COVID^-$ and 8 $COVID^+$ healthy individuals; 83 $COVID^-$ and 12 $COVID^+$ patients).

(F) AIM between $COVID^-$ and $COVID^+$ groups (33 $COVID^-$ and 1 $COVID^+$ healthy individuals; 51 $COVID^-$ and 5 $COVID^+$ patients).

(G) TAME-enriched FACS plots depicting tetramer and memory and activation phenotypes.

(H) Tetramer frequencies between $COVID^-$ and $COVID^+$ groups (12 $COVID^-$ and 3 $COVID^+$ healthy individuals; 49 $COVID^-$ and 5 $COVID^+$ patients). 1–2 tetramer responses per donor.

(I) $CD8^+tetramer^+$ phenotypes from individuals with breakthrough COVID-19.

The frequency of $tetramer^+$ cells has been right shifted by 10^{-7} (i.e., no detected $tetramer^+$ events displayed as 10^{-7}).

Statistical significance determined by Mann-Whitney for comparisons between $COVID^-$ and $COVID^+$ time points (connecting line). ****$p < 0.0001$. Experiments were performed once for each sample. Refer to Figures S8 and S9.

CellPress
OPEN ACCESS

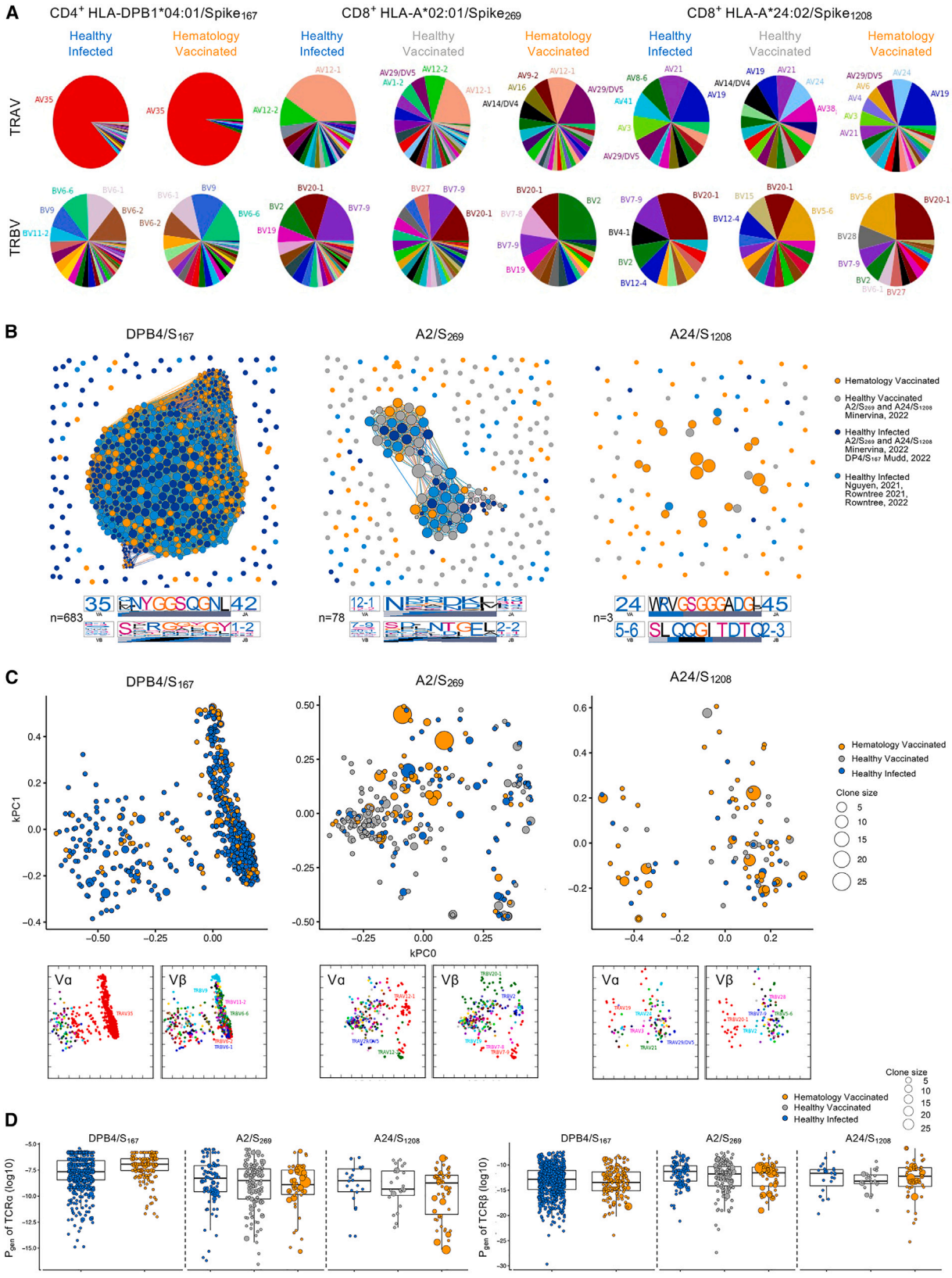

(legend on next page)

indistinguishable between infected and non-infected individuals in both patient and healthy groups, which aligns with previous reports in healthy individuals,[23] showing that vaccination alone or vaccination followed by subsequent infection can elicit comparable spike epitope-specific T cell responses.

Overall, our study shows that hematology patients who fail to seroconvert and generate memory B cell responses post-vaccination can nevertheless generate robust SARS-CoV-2-specific T cell immunity. Our findings are particularly relevant for reducing disease severity in hematology patients who acquire breakthrough infections since robust $CD8^+$ T cell responses correlate with better outcomes in hematology patients hospitalized with COVID-19, including those treated with anti-CD20 therapy, while B cells had no impact on survival.[16] Our data also support development of vaccines targeted to immunocompromised patients, such as those that have shown to induce potent and prolonged T cell responses to multiple SARS-CoV-2 antigens in healthy individuals.[39] Therefore, COVID-19 vaccination can still be immunogenic, especially with respect to SARS-CoV-2-specific $CD4^+$ and $CD8^+$ T cell responses, in hematology patients of varying diseases and treatment.

Limitations of the study

Our patient cohort is heterogeneous, and so we were not always powered to statistically analyze the data per disease, treatment, or vaccine group for all assays. Some assays were not performed for all patients, but patient numbers per assay are included in figure legends. Larger prospective studies are needed to demonstrate protection against severe and fatal disease with patient stratification based on antibody/B cell and T cell responses. SARS-CoV-2 infections occurred after 1/2/3 vaccinations in patients but only after 3 vaccinations in healthy individuals, although numbers are small. ChAdOx1-vaccinated patients were older than BNT162b2-vaccinated or healthy individuals.

STAR★METHODS

Detailed methods are provided in the online version of this paper and include the following:

SUPPLEMENTAL INFORMATION

Supplemental information can be found online at https://doi.org/10.1016/j.xcrm.2023.101017.

ACKNOWLEDGMENTS

We thank B. Cox, M. Fezollari, E. Shilling, and L. Davies for support with the healthy cohort; G. Au-Yeung for support with patients; Melbourne Cytometry Platform for technical assistance; and BEI Resources, NIAID, NIH, for providing the peptide array, SARS-related coronavirus 2 spike (S) glycoprotein, NR-52402. This work was supported by NHMRC L1 to K.K. (#1173871) and M.A.S. (#1173791); NHMRC L2 to K.S. (#1177174); NHMRC EL1 to T.H.O.N. (#1194036) and A.K.W. (#1173433); NHMRC EL2 to B.W.T. (#1195894) and D.A.W. (#1174555); Research Grants Council of the Hong Kong Special Administrative Region, China (#T11-712/19-N) to K.K.; the Victorian government (S.J.K. and A.K.W.); a MRFF Award (#2016062) to K.K., T.H.O.N., L.C.R., A.K.W., S.J.K., J.R., and B.W.T.; a MRFF award (#2002073) to S.J.K. and A.K.W.; a MRFF Award (#1202445) to K.K.; a MRFF Award (#2005544) to K.K., S.J.K., and A.K.W.; NHMRC program grant 1149990 (S.J.K.); NHMRC project grant 1162760 (A.K.W.); NHMRC Synergy grant 2011100 (M.A.S.); and NIH contract CIVC-HRP (HHS-NIH-NIAID-BAA2018) to P.G.T. and K.K. E.B.C. is supported by a NHMRC Peter Doherty Fellowship (#1091516). W.Z., S.Y.C and J.R.H were supported by a Melbourne Research Scholarship from the University of Melbourne. S.J.K. is supported by NHMRC Senior Principal Research Fellowship (#1136322). J.R. is supported by an ARC Laureate Fellowship. J.C.C. and P.G.T. are supported by NIH NIAID R01 AI136514-03 and ALSAC at St. Jude. We acknowledge BeiGene for supporting a part of the study. C.S.T. receives research funding from the CLL Global Research Foundation.

AUTHOR CONTRIBUTIONS

K.K. led the study. K.K., B.W.T., C.S.T., M.A.S., and T.H.O.N. supervised the study. K.K., T.H.O.N., L.C.R., L.F.A., B.Y.C., L.K., L.H., J.A.N., F.L.M., H.-X.T., K.S., T.K., S.N., and D.A.W. designed the experiments. T.H.O.N., L.C.R., L.F.A., B.Y.C., L.K., E.B.C., W.Z., S.Y.C., J.R.H., X.J., L.H., J.A.N., F.L.M., H.-X.T., A.F.C., and T.K. performed and analyzed experiments. H.A.M., T.M., A.A.M., M.V.P., A.F.C., J.C.C., and P.G.T. analyzed data. P.C., J.P., A.K.W., S.J.K., K.S., and J.R. provided crucial reagents. C.L., M.L.,

Figure 6. TCR sequence similarity network identifies sharing of dominant motifs between the groups

(A) Pie charts of TRAV and TRBV usage for TCR$\alpha\beta$ clonotypes specific to DPB4/S_{167} (n = 18 patients), A2/S_{269} (n = 18 patients), and A24/S_{1208} (n = 13 patients). Clonally expanded TCRs were reduced to a single data point for this analysis.

(B) TCR$\alpha\beta$ sequence similarity networks. Each vertex is a different clonotype, and edges connect clonotypes with highly similar amino acid TCR$\alpha\beta$ sequences (TCR distance [TCRdist] $\leq$ 120). Size of the vertex is proportional to number of neighbors. TCRdist sequence logos for TCRα and TCRβ chains are shown for central largest cluster for each panel. Each TCR motif depicts the V (left side) and J (right side) gene frequencies, the CDR3 amino acid sequence (middle), and the inferred rearrangement structure (bottom bars colored by source region; V-region, light gray; insertions, blue; diversity [D]-region, black; and J-region dark gray).

(C) TCR landscapes displayed using kernel principal-component analysis (PCA) projections. Vα/Vβ usage shown below.

(D) P_{gen} for TCRα and TCRβ. Boxplots represent the median (middle bar), 75% quantile (upper hinge), and 25% quantile (lower hinge), with whiskers extending 1.5 times the IQR.

Experiments were performed once for each sample. Refer to Figures S10 and S11.

G.S.T., N.R.S., M.C., L.C., J.F.S., M.A.A., A.W., K.A.T., M.A.S., C.S.T., and B.W.T. recruited the vaccinated hematology patients. G.G., F.J., J.M.T., J.A.T., J.M., B.C., K.A.B., and D.A.W. recruited the healthy vaccinated cohorts. T.H.O.N., L.C.R., L.F.A., B.W.T., and K.K. wrote the manuscript. All authors reviewed and approved the manuscript.

DECLARATION OF INTERESTS

The Icahn School of Medicine at Mount Sinai has filed patent applications relating to SARS-CoV-2 serological assays and NDV-based SARS-CoV-2 vaccines, which list F.K. as co-inventor. Mount Sinai has spun out a company, Kantaro, to market serological tests for SARS-CoV-2. F.K. has consulted for Merck and Pfizer (before 2020) and is currently consulting for Pfizer, Seqirus, and Avimex. The Krammer laboratory is also collaborating with Pfizer on animal models of SARS-CoV-2. H.A.M. and B.Y.C. are currently consulting for Ena Respiratory. B.W.T. has received research funding from MSD, Seqirus, and Sanofi and is on the advisory board for Moderna, CSL-Behring, and Takeda.

Received: November 3, 2022
Revised: February 21, 2023
Accepted: March 22, 2023
Published: March 27, 2023

REFERENCES

1. Sharma, A., Bhatt, N.S., St Martin, A., Abid, M.B., Bloomquist, J., Chemaly, R.F., Dandoy, C., Gauthier, J., Gowda, L., Perales, M.A., et al. (2021). Clinical characteristics and outcomes of COVID-19 in haematopoietic stem-cell transplantation recipients: an observational cohort study. Lancet. Haematol. *8*, e185–e193. https://doi.org/10.1016/S2352-3026(20)30429-4.
2. Wood, W.A., Neuberg, D.S., Thompson, J.C., Tallman, M.S., Sekeres, M.A., Sehn, L.H., Anderson, K.C., Goldberg, A.D., Pennell, N.A., Niemeyer, C.M., et al. (2020). Outcomes of patients with hematologic malignancies and COVID-19: a report from the ASH research collaborative data hub. Blood Adv. *4*, 5966–5975. https://doi.org/10.1182/bloodadvances.2020003170.
3. Hirsch, H.H., Martino, R., Ward, K.N., Boeckh, M., Einsele, H., and Ljungman, P. (2013). Fourth European Conference on Infections in Leukaemia (ECIL-4): guidelines for diagnosis and treatment of human respiratory syncytial virus, parainfluenza virus, metapneumovirus, rhinovirus, and coronavirus. Clin. Infect. Dis. *56*, 258–266. https://doi.org/10.1093/cid/cis844.
4. Mato, A.R., Roeker, L.E., Lamanna, N., Allan, J.N., Leslie, L., Pagel, J.M., Patel, K., Osterborg, A., Wojenski, D., Kamdar, M., et al. (2020). Outcomes of COVID-19 in patients with CLL: a multicenter international experience. Blood *136*, 1134–1143. https://doi.org/10.1182/blood.2020006965.
5. Chari, A., Samur, M.K., Martinez-Lopez, J., Cook, G., Biran, N., Yong, K., Hungria, V., Engelhardt, M., Gay, F., García Feria, A., et al. (2020). Clinical features associated with COVID-19 outcome in multiple myeloma: first results from the International Myeloma Society data set. Blood *136*, 3033–3040. https://doi.org/10.1182/blood.2020008150.
6. Yri, O.E., Torfoss, D., Hungnes, O., Tierens, A., Waalen, K., Nordøy, T., Dudman, S., Kilander, A., Wader, K.F., Ostenstad, B., et al. (2011). Rituximab blocks protective serologic response to influenza A (H1N1) 2009 vaccination in lymphoma patients during or within 6 months after treatment. Blood *118*, 6769–6771. https://doi.org/10.1182/blood-2011-08-372649.
7. Teh, J.S.K., Coussement, J., Neoh, Z.C.F., Spelman, T., Lazarakis, S., Slavin, M.A., and Teh, B.W. (2022). Immunogenicity of COVID-19 vaccines in patients with hematologic malignancies: a systematic review and meta-analysis. Blood Adv. *6*, 2014–2034. https://doi.org/10.1182/bloodadvances.2021006333.
8. Haggenburg, S., Lissenberg-Witte, B.I., van Binnendijk, R.S., den Hartog, G., Bhoekhan, M.S., Haverkate, N.J.E., de Rooij, D.M., van Meerloo, J., Cloos, J., Kootstra, N.A., et al. (2022). Quantitative analysis of mRNA-1273 COVID-19 vaccination response in immunocompromised adult hematology patients. Blood Adv. *6*, 1537–1546. https://doi.org/10.1182/bloodadvances.2021006917.
9. Jiménez, M., Roldán, E., Fernández-Naval, C., Villacampa, G., Martinez-Gallo, M., Medina-Gil, D., Peralta-Garzón, S., Pujadas, G., Hernández, C., Pagès, C., et al. (2022). Cellular and humoral immunogenicity of the mRNA-1273 SARS-CoV-2 vaccine in patients with hematologic malignancies. Blood Adv. *6*, 774–784. https://doi.org/10.1182/bloodadvances.2021006101.
10. Lindemann, M., Klisanin, V., Thummler, L., Fisenkci, N., Tsachakis-Muck, N., Ditschkowski, M., Schwarzkopf, S., Klump, H., Reinhardt, H.C., Horn, P.A., and Koldehoff, M. (2021). Humoral and cellular vaccination responses against SARS-CoV-2 in hematopoietic stem cell transplant recipients. Vaccines *9*. https://doi.org/10.3390/vaccines9101075.
11. Jarisch, A., Wiercinska, E., Daqiq-Mirdad, S., Hellstern, H., Ajib, S., Cremer, A., Nguyen, N.T.T., Dukat, A., Ullrich, E., Ciesek, S., et al. (2022). SARS-CoV-2-specific T cells are generated in less than half of allogeneic HSCT recipients failing to seroconvert after COVID-19 vaccination. Eur. J. Immunol. *52*, 1194–1197. https://doi.org/10.1002/eji.202149771.
12. Monin, L., Laing, A.G., Muñoz-Ruiz, M., McKenzie, D.R., Del Molino Del Barrio, I., Alaguthurai, T., Domingo-Vila, C., Hayday, T.S., Graham, C., Seow, J., et al. (2021). Safety and immunogenicity of one versus two doses of the COVID-19 vaccine BNT162b2 for patients with cancer: interim analysis of a prospective observational study. Lancet Oncol. *22*, 765–778. https://doi.org/10.1016/S1470-2045(21)00213-8.
13. Gavriatopoulou, M., Terpos, E., Ntanasis-Stathopoulos, I., Briasoulis, A., Gumeni, S., Malandrakis, P., Fotiou, D., Migkou, M., Theodorakakou, F., Eleutherakis-Papaiakovou, E., et al. (2021). Poor neutralizing antibody responses in 106 patients with WM after vaccination against SARS-CoV-2: a prospective study. Blood Adv. *5*, 4398–4405. https://doi.org/10.1182/bloodadvances.2021005444.
14. Kakkassery, H., Carpenter, E., Patten, P.E.M., and Irshad, S. (2022). Immunogenicity of SARS-CoV-2 vaccines in patients with cancer. Trends Mol. Med. *28*, 1082–1099. https://doi.org/10.1016/j.molmed.2022.07.006.
15. Gao, Y., Cai, C., Wullimann, D., Niessl, J., Rivera-Ballesteros, O., Chen, P., Lange, J., Cuapio, A., Blennow, O., Hansson, L., et al. (2022). Immunodeficiency syndromes differentially impact the functional profile of SARS-CoV-2-specific T cells elicited by mRNA vaccination. Immunity *55*, 1732–1746.e5. https://doi.org/10.1016/j.immuni.2022.07.005.
16. Bange, E.M., Han, N.A., Wileyto, P., Kim, J.Y., Gouma, S., Robinson, J., Greenplate, A.R., Hwee, M.A., Porterfield, F., Owoyemi, O., et al. (2021). CD8(+) T cells contribute to survival in patients with COVID-19 and hematologic cancer. Nat. Med. *27*, 1280–1289. https://doi.org/10.1038/s41591-021-01386-7.
17. Apostolidis, S.A., Kakara, M., Painter, M.M., Goel, R.R., Mathew, D., Lenzi, K., Rezk, A., Patterson, K.R., Espinoza, D.A., Kadri, J.C., et al. (2021). Cellular and humoral immune responses following SARS-CoV-2 mRNA vaccination in patients with multiple sclerosis on anti-CD20 therapy. Nat. Med. *27*, 1990–2001. https://doi.org/10.1038/s41591-021-01507-2.
18. Nguyen, T.H.O., Rowntree, L.C., Petersen, J., Chua, B.Y., Hensen, L., Kedzierski, L., van de Sandt, C.E., Chaurasia, P., Tan, H.X., Habel, J.R., et al. (2021). CD8(+) T cells specific for an immunodominant SARS-CoV-2 nucleocapsid epitope display high naive precursor frequency and TCR promiscuity. Immunity *54*, 1066–1082.e5. https://doi.org/10.1016/j.immuni.2021.04.009.
19. Habel, J.R., Nguyen, T.H.O., van de Sandt, C.E., Juno, J.A., Chaurasia, P., Wragg, K., Koutsakos, M., Hensen, L., Jia, X., Chua, B., et al. (2020). Suboptimal SARS-CoV-2-specific CD8(+) T cell response associated with the prominent HLA-A*02:01 phenotype. Proc. Natl. Acad. Sci. USA *117*, 24384–24391. https://doi.org/10.1073/pnas.2015486117.
20. Rowntree, L.C., Petersen, J., Juno, J.A., Chaurasia, P., Wragg, K., Koutsakos, M., Hensen, L., Wheatley, A.K., Kent, S.J., Rossjohn, J., et al. (2021). SARS-CoV-2-specific CD8(+) T-cell responses and TCR signatures in the

context of a prominent HLA-A*24:02 allomorph. Immunol. Cell Biol. *99*, 990–1000. https://doi.org/10.1111/imcb.12482.

21. Rowntree, L.C., Nguyen, T.H.O., Kedzierski, L., Neeland, M.R., Petersen, J., Crawford, J.C., Allen, L.F., Clemens, E.B., Chua, B., McQuilten, H.A., et al. (2022). SARS-CoV-2-specific T cell memory with common TCRalphabeta motifs is established in unvaccinated children who seroconvert after infection. Immunity *55*, 1299–1315.e4. https://doi.org/10.1016/j.immuni.2022.06.003.
22. Mudd, P.A., Minervina, A.A., Pogorelyy, M.V., Turner, J.S., Kim, W., Kalaidina, E., Petersen, J., Schmitz, A.J., Lei, T., Haile, A., et al. (2022). SARS-CoV-2 mRNA vaccination elicits a robust and persistent T follicular helper cell response in humans. Cell *185*, 603–613.e15. https://doi.org/10.1016/j.cell.2021.12.026.
23. Minervina, A.A., Pogorelyy, M.V., Kirk, A.M., Crawford, J.C., Allen, E.K., Chou, C.H., Mettelman, R.C., Allison, K.J., Lin, C.Y., Brice, D.C., et al. (2022). SARS-CoV-2 antigen exposure history shapes phenotypes and specificity of memory CD8(+) T cells. Nat. Immunol. *23*, 781–790. https://doi.org/10.1038/s41590-022-01184-4.
24. Goncharov, M., Bagaev, D., Shcherbinin, D., Zvyagin, I., Bolotin, D., Thomas, P.G., Minervina, A.A., Pogorelyy, M.V., Ladell, K., McLaren, J.E., et al. (2022). VDJdb in the pandemic era: a compendium of T cell receptors specific for SARS-CoV-2. Nat. Methods *19*, 1017–1019. https://doi.org/10.1038/s41592-022-01578-0.
25. Thevarajan, I., Nguyen, T.H.O., Koutsakos, M., Druce, J., Caly, L., van de Sandt, C.E., Jia, X., Nicholson, S., Catton, M., Cowie, B., et al. (2020). Breadth of concomitant immune responses prior to patient recovery: a case report of non-severe COVID-19. Nat. Med. *26*, 453–455. https://doi.org/10.1038/s41591-020-0819-2.
26. Koutsakos, M., Rowntree, L.C., Hensen, L., Chua, B.Y., van de Sandt, C.E., Habel, J.R., Zhang, W., Jia, X., Kedzierski, L., Ashhurst, T.M., et al. (2021). Integrated immune dynamics define correlates of COVID-19 severity and antibody responses. Cell Rep. Med. *2*, 100208. https://doi.org/10.1016/j.xcrm.2021.100208.
27. Wragg, K.M., Lee, W.S., Koutsakos, M., Tan, H.X., Amarasena, T., Reynaldi, A., Gare, G., Konstandopoulos, P., Field, K.R., Esterbauer, R., et al. (2022). Establishment and recall of SARS-CoV-2 spike epitope-specific CD4(+) T cell memory. Nat. Immunol. *23*, 768–780. https://doi.org/10.1038/s41590-022-01175-5.
28. Nguyen, T.H.O., Koutsakos, M., van de Sandt, C.E., Crawford, J.C., Loh, L., Sant, S., Grzelak, L., Allen, E.K., Brahm, T., Clemens, E.B., et al. (2021). Immune cellular networks underlying recovery from influenza virus infection in acute hospitalized patients. Nat. Commun. *12*, 2691. https://doi.org/10.1038/s41467-021-23018-x.
29. Koutsakos, M., Wheatley, A.K., Loh, L., Clemens, E.B., Sant, S., Nüssing, S., Fox, A., Chung, A.W., Laurie, K.L., Hurt, A.C., et al. (2018). Circulating TFH cells, serological memory, and tissue compartmentalization shape human influenza-specific B cell immunity. Sci. Transl. Med. *10*, eaan8405. https://doi.org/10.1126/scitranslmed.aan8405.
30. Schulien, I., Kemming, J., Oberhardt, V., Wild, K., Seidel, L.M., Killmer, S., Sagar; Daul, F., Salvat Lago, M., Decker, A., et al. (2021). Characterization of pre-existing and induced SARS-CoV-2-specific $CD8^+$ T cells. Nat. Med. *27*, 78–85. https://doi.org/10.1038/s41591-020-01143-2.
31. Ferretti, A.P., Kula, T., Wang, Y., Nguyen, D.M.V., Weinheimer, A., Dunlap, G.S., Xu, Q., Nabilsi, N., Perullo, C.R., Cristofaro, A.W., et al. (2020). Unbiased screens show $CD8^+$ T cells of COVID-19 patients recognize shared epitopes in SARS-CoV-2 that largely reside outside the spike protein. Immunity *53*, 1095–1107.e3. https://doi.org/10.1016/j.immuni.2020.10.006.
32. Kedzierska, K., and Thomas, P.G. (2022). Count on us: T cells in SARS-CoV-2 infection and vaccination. Cell Rep. Med. *3*, 100562. https://doi.org/10.1016/j.xcrm.2022.100562.
33. Sahin, U., Muik, A., Vogler, I., Derhovanessian, E., Kranz, L.M., Vormehr, M., Quandt, J., Bidmon, N., Ulges, A., Baum, A., et al. (2021). BNT162b2 vaccine induces neutralizing antibodies and poly-specific T cells in humans. Nature *595*, 572–577. https://doi.org/10.1038/s41586-021-03653-6.
34. Valkenburg, S.A., Josephs, T.M., Clemens, E.B., Grant, E.J., Nguyen, T.H.O., Wang, G.C., Price, D.A., Miller, A., Tong, S.Y.C., Thomas, P.G., et al. (2016). Molecular basis for universal HLA-A*0201-restricted CD8+ T-cell immunity against influenza viruses. Proc. Natl. Acad. Sci. USA *113*, 4440–4445. https://doi.org/10.1073/pnas.1603106113.
35. Khoury, D.S., Cromer, D., Reynaldi, A., Schlub, T.E., Wheatley, A.K., Juno, J.A., Subbarao, K., Kent, S.J., Triccas, J.A., and Davenport, M.P. (2021). Neutralizing antibody levels are highly predictive of immune protection from symptomatic SARS-CoV-2 infection. Nat. Med. *27*, 1205–1211. https://doi.org/10.1038/s41591-021-01377-8.
36. Wang, Z., Muecksch, F., Muenn, F., Cho, A., Zong, S., Raspe, R., Ramos, V., Johnson, B., Ben Tanfous, T., DaSilva, J., et al. (2022). Humoral immunity to SARS-CoV-2 elicited by combination COVID-19 vaccination regimens. J. Exp. Med. *219*, e20220826. https://doi.org/10.1084/jem.20220826.
37. Juno, J.A., Tan, H.-X., Lee, W.S., Reynaldi, A., Kelly, H.G., Wragg, K., Esterbauer, R., Kent, H.E., Batten, C.J., Mordant, F.L., et al. (2020). Humoral and circulating follicular helper T cell responses in recovered patients with COVID-19. Nat. Med. *26*, 1428–1434. https://doi.org/10.1038/s41591-020-0995-0.
38. Grifoni, A., Weiskopf, D., Ramirez, S.I., Mateus, J., Dan, J.M., Moderbacher, C.R., Rawlings, S.A., Sutherland, A., Premkumar, L., Jadi, R.S., et al. (2020). Targets of T Cell responses to SARS-CoV-2 coronavirus in humans with COVID-19 disease and unexposed individuals. Cell *181*, 1489–1501.e15. https://doi.org/10.1016/j.cell.2020.05.015.
39. Chiuppesi, F., Zaia, J.A., Faircloth, K., Johnson, D., Ly, M., Karpinski, V., La Rosa, C., Drake, J., Marcia, J., Acosta, A.M., et al. (2022). Vaccine-induced spike- and nucleocapsid-specific cellular responses maintain potent cross-reactivity to SARS-CoV-2 Delta and Omicron variants. iScience *25*, 104745. https://doi.org/10.1016/j.isci.2022.104745.
40. Amanat, F., Stadlbauer, D., Strohmeier, S., Nguyen, T.H.O., Chromikova, V., McMahon, M., Jiang, K., Arunkumar, G.A., Jurczyszak, D., Polanco, J., et al. (2020). A serological assay to detect SARS-CoV-2 seroconversion in humans. Nat. Med. *26*, 1033–1036. https://doi.org/10.1038/s41591-020-0913-5.
41. Saini, S.K., Hersby, D.S., Tamhane, T., Povlsen, H.R., Amaya Hernandez, S.P., Nielsen, M., Gang, A.O., and Hadrup, S.R. (2021). SARS-CoV-2 genome-wide T cell epitope mapping reveals immunodominance and substantial CD8(+) T cell activation in COVID-19 patients. Sci. Immunol. *6*, eabf7550. https://doi.org/10.1126/sciimmunol.abf7550.
42. Peng, Y., Mentzer, A.J., Liu, G., Yao, X., Yin, Z., Dong, D., Dejnirattisai, W., Rostron, T., Supasa, P., Liu, C., et al. (2020). Broad and strong memory CD4(+) and CD8(+) T cells induced by SARS-CoV-2 in UK convalescent individuals following COVID-19. Nat. Immunol. *21*, 1336–1345. https://doi.org/10.1038/s41590-020-0782-6.
43. R Core Team (2022). R: A Language and Environment for Statistical Computing (R Foundation for Statistical Computing). https://www.R-project.org/.
44. Schattgen, S.A., Guion, K., Crawford, J.C., Souquette, A., Barrio, A.M., Stubbington, M.J.T., Thomas, P.G., and Bradley, P. (2022). Integrating T cell receptor sequences and transcriptional profiles by clonotype neighbor graph analysis (CoNGA). Nat. Biotechnol. *40*, 54–63. https://doi.org/10.1038/s41587-021-00989-2.
45. Csárdi, G., and Nepusz, T. (2006). The igraph software package for complex network research. InterJournal Complex Systems.
46. Dash, P., Fiore-Gartland, A.J., Hertz, T., Wang, G.C., Sharma, S., Souquette, A., Crawford, J.C., Clemens, E.B., Nguyen, T.H.O., Kedzierska, K., et al. (2017). Quantifiable predictive features define epitope-specific T cell receptor repertoires. Nature *547*, 89–93. https://doi.org/10.1038/nature22383.
47. Jacomy, M., Venturini, T., Heymann, S., and Bastian, M. (2014). ForceAtlas2, a continuous graph layout algorithm for handy network visualization designed for the Gephi software. PLoS One *9*, e98679. https://doi.org/10.1371/journal.pone.0098679.

48. Wei, T., and Simko, V. (2021). R package 'corrplot': visualization of a correlation matrix. (Version 0.92). https://github.com/taiyun/corrplot.

49. Kassambara, A. (2021). Rstatix: pipe-friendly framework for basic statistical tests. R package version 0.7.0. https://CRAN.R-project.org/package=rstatix.

50. Blighe, K., Rana, S., and Lewis, M. (2022). EnhancedVolcano: publication-ready volcano plots with enhanced colouring and labeling. R package version 1.14.0. https://github.com/kevinblighe/EnhancedVolcano.

51. Nguyen, T.H.O., Lim, C., Lasica, M., Whitechurch, A., Tennakoon, S., Saunders, N.R., Allen, L.F., Rowntree, L.C., Chua, B.Y., Kedzierski, L., et al. (2023). Prospective comprehensive profiling of immune responses to COVID-19 vaccination in patients on zanubrutinib therapy. EJHaem *4*, 216–220. https://doi.org/10.1002/jha2.639.

52. Chappell, K.J., Mordant, F.L., Li, Z., Wijesundara, D.K., Ellenberg, P., Lackenby, J.A., Cheung, S.T.M., Modhiran, N., Avumegah, M.S., Henderson, C.L., et al. (2021). Safety and immunogenicity of an MF59-adjuvanted spike glycoprotein-clamp vaccine for SARS-CoV-2: a randomised, double-blind, placebo-controlled, phase 1 trial. Lancet Infect. Dis. *21*, 1383–1394. https://doi.org/10.1016/S1473-3099(21)00200-0.

53. Rowntree, L.C., Chua, B.Y., Nicholson, S., Koutsakos, M., Hensen, L., Douros, C., Selva, K., Mordant, F.L., Wong, C.Y., Habel, J.R., et al. (2021). Robust correlations across six SARS-CoV-2 serology assays detecting distinct antibody features. Clin. Transl. Immunology *10*, e1258. https://doi.org/10.1002/cti2.1258.

54. Zhang, W., Chua, B.Y., Selva, K.J., Kedzierski, L., Ashhurst, T.M., Haycroft, E.R., Shoffner-Beck, S.K., Hensen, L., Boyd, D.F., James, F., et al. (2022). SARS-CoV-2 infection results in immune responses in the respiratory tract and peripheral blood that suggest mechanisms of disease severity. Nat. Commun. *13*, 2774. https://doi.org/10.1038/s41467-022-30088-y.

STAR★METHODS

KEY RESOURCES TABLE

REAGENT or RESOURCE	SOURCE	IDENTIFIER
Antibodies		
CD71 M-A712 BV421	BD Biosciences	Cat#562995; RRID: AB_2737939
CD4 SK3 BV650	BD Biosciences	Cat#563875; RRID: AB_2744425
CD27 L128 BV711	BD Biosciences	Cat#563167; RRID: AB_2738042
CD38 HIT2 BV786	BD Biosciences	Cat#563964; RRID: AB_2738515
CCR7 150503 AF700	BD Biosciences	Cat#561143; RRID: AB_10562031
CD14 MΦP9 APC-H7	BD Biosciences	Cat#560180; RRID: AB_1645464
CD19 SJ25C1 APC-H7	BD Biosciences	Cat#560177; RRID: AB_1645470
CD45RA HI100 FITC	BD Biosciences	Cat#555488; RRID: AB_395879
CD8a SK1 PerCP-Cy5.5	BD Pharmingen	Cat#565310; RRID: AB_2687497
CD95 DX2 PE-CF594	BD Biosciences	Cat#562395; RRID: AB_11153666
PD-1 EH12.1 PE-Cy7	BD Biosciences	Cat#561272; RRID: AB_10611585
CD3 OKT3 BV510	BioLegend	Cat#317332; RRID: AB_2561943
HLA-DR L243 BV605	BioLegend	Cat#307640; RRID: AB_2561913
CXCR5 RF8B2 BV421	BD Biosciences	Cat#562747; RRID: AB_2737766
CD19 SJ25C1 BV510	BD BioSciences	Cat#562947; RRID: AB_2737912
CCR6 11A9 BV650	BD Biosciences	Cat#563922; RRID: AB_2738488
CD20 2H7 BV711	BD Biosciences	Cat#563126; RRID: AB_2313579
CD27 M-T271 AF700	BD Biosciences	Cat#560611; RRID: AB_1727454
CD4 RPA-T4 APC-H7	BD Biosciences	Cat#560158; RRID: AB_1645478
CD3 UCHT1 PE-CF594	BD Biosciences	Cat#562280; RRID: AB_11153674
CXCR3 (CD183) 1C6 APC	BD Biosciences	Cat#550967; RRID: AB_398481
CD8 SK1 FITC	BD Biosciences	Cat#555634; RRID: AB_395996
CD45 HI30 PerCPCy5.5	BD Biosciences	Cat#340953; RRID: AB_400194
ICOS (CD278) DX29 PE	BD Biosciences	Cat#557802; RRID: AB_396878
CD8a SK1 BV605	BD Biosciences	Cat#564116; RRID: AB_2869551
CD25 2A3 BV711	BD Biosciences	Cat#563159; RRID: AB_2738037
CXCR3 G025H7 BV785	BioLegend	Cat#353738; RRID: AB_2565924
APC (4-1BB) 4B4-1 CD137	BioLegend	Cat#309810; RRID: AB_830672
CD69 FN50 PerCPCy5.5	BioLegend	Cat#310926; RRID: AB_2074956
CD134 L106 PE	BD Biosciences	Cat#340420; RRID: AB_400027
CD45RA L48 PECy7	BD Biosciences	Cat#337167; RRID: AB_647424
CD19 J4.119 ECD	Beckman Coulter	Cat#IM2708U; RRID:AB_130854
IgM G20-127 BUV395	BD Biosciences	Cat#563903; RRID:AB_2721269
CD21 B-ly4 BUV737	BD Biosciences	Cat#564437; RRID:AB_2738807
IgD IA6-2 PE-Cy7	BD Biosciences	Cat#561314; RRID:AB_10642457
IgG G18-145 BV786	BD Biosciences	Cat#564230; RRID:AB_2738684
CD27 O323 BV605	BioLegend	Cat#302829; RRID:AB_11204431
Streptavidin PE	BD Biosciences	Cat#554061, RRID:AB_10053328
Streptavidin APC	BD Biosciences	Cat#554067, RRID:AB_10050396
Peroxidase AffiniPure goat anti-human IgG, Fcγ fragment specific	Jackson ImmunoResearch	Cat#109-035-098; RRID: AB_2337586

(*Continued on next page*)

Continued

REAGENT or RESOURCE	SOURCE	IDENTIFIER
Biological samples		
Blood samples (peripheral blood mononuclear cells (PBMCs) and plasma samples) from COVID-19-vaccinated adult haematological malignancy patients and healthy control individuals	The Royal Melbourne Hospital, The Austin Hospital, St Vincent's Hospital, and The Peter McCallum Cancer Center	N/A
Chemicals, peptides, and recombinant proteins		
3,3′,5,5′-Tetramethylbenzidine (TMB) Liquid Substrate System for ELISA, peroxidase substrate	Sigma	Cat#T0440-1L
Alkaline phosphatase yellow (pNPP) liquid substrate for ELISA	Sigma	Cat#P7998-100ML
Pierce High Sensitivity Streptavidin-HRP	Thermo Fisher Scientific	Cat#21130
SARS-CoV-2 RBD protein	Amanat et al.,[40]	N/A
SARS-CoV-2 Spike protein	Juno et al.,[37]	N/A
SARS-CoV-2 peptides – A1/ORF1a$_{1637}$ TTDPSFLGRY; A1/S$_{865\text{-}873}$ LTDEMIAQY; A2/S269 YLQPRTFLL; A3/N$_{361}$ KTFPPTEPK; A3/S$_{378}$ KTFPPTEPK; A24/S$_{1208}$ QYIKWPWYI; B7/N$_{105\text{-}113}$ SPRWYFYYL; B15/S$_{919\text{-}927}$ NQKLIANQF; B35/S$_{321\text{-}329}$ QPTESIVRF; and DPB4/S$_{167}$ TFEYVSQPFLMDLE	GenScript	N/A
HLA-A*01:01/S$_{865}$ monomer (SARS-CoV-2, S$_{865}$, LTDEMIAQY)	Peptide sequence[30], monomer [Rossjohn Laboratory]	N/A
HLA-A*01:01/ORF1a$_{1637}$ monomer (SARS-CoV-2, ORF1a$_{1637}$, TTDPSFLGRY)	Peptide sequence[41], monomer[21]	N/A
HLA-A*03:01/S$_{378}$ monomer (SARS-CoV-2, S$_{378}$, KCYGVSPTK)	Peptide sequence[41], monomer [Rossjohn Laboratory]	N/A
HLA-A*03:01/N$_{361}$ monomer (SARS-CoV-2, N$_{361}$, KTFPPTEPK)	Peptide sequence[42], monomer[21]	N/A
HLA-B*07:02/N$_{105}$ monomer (SARS-CoV-2, N$_{105}$, SPRWYFYYL)	Peptide sequence[42], monomer[18]	N/A
HLA-B*15:01/S$_{919}$ monomer (SARS-CoV-2, S$_{919}$, NQKLIANQF)	Peptide sequence[23], monomer [Rossjohn Laboratory]	N/A
HLA-A*02:01/S$_{269}$ monomer (SARS-CoV-2, S$_{269}$, YLQPRTFLL)	Peptide sequence/monomer[19]	N/A
HLA-B*35:01/S$_{321}$ monomer (SARS-CoV-2, S$_{321}$, QPTESIVRF)	Peptide sequence[33], monomer [Rossjohn Laboratory]	N/A
HLA-A*24:02/S$_{1208}$ monomer (SARS-CoV-2, S$_{1208}$, QYIKWPWYI)	Peptide sequence[31], monomer[20]	N/A
HLA-DPA1*01:03/DPB1*04:01/S$_{167}$ monomer (SARS-CoV-2, S$_{167}$, TFEYVSQPFLMDLE)	Peptide sequence/monomer[22]	N/A
Software and algorithms		
R v4.2.1	R Core Team,[43]	https://cran.r-project.org
conga package	Schattgen et al.[44]	https://github.com/phbradley/conga
igraph R package v1.3.2	Csárdi and Nepusz[45]	https://igraph.org/r/
TCRdist pipeline	Dash et al.[46]	https://github.com/phbradley/tcr-dist
Gephi v0.9.7	Jacomy et al.[47]	https://gephi.org/
Corrplot v0.92	Wei and Simko[48]	https://github.com/taiyun/corrplot
rstatix pacakage v0.7.0	Kassambara[49]	https://CRAN.R-project.org/package=rstatix
EnhancedVolcano v1.14.0	Blighe et al.[50]	https://github.com/kevinblighe/EnhancedVolcano
FlowJo v10.5.3	FlowJo	https://www.flowjo.com
Prism v8.3.1 or v9.1.0	GraphPad	https://www.graphpad.com

(*Continued on next page*)

Continued

REAGENT or RESOURCE	SOURCE	IDENTIFIER
BD FACS Diva v8.0.1	BD Biosciences	https://www.bdbiosciences.com/en-us/instruments/research-instruments/research-software/flow-cytometry-acquisition/facsdiva-software
Other		
Anti-PE Micro-Beads	Miltenyi Biotec	Cat# 130-048-801, RRID:AB_244373
Anti-APC Micro-Beads	Miltenyi Biotec	Cat# 130-090-855, RRID:AB_244367

RESOURCE AVAILABILITY

Lead contact

Further information and requests for resources and reagents should be directed to and will be fulfilled by the lead contact, Katherine Kedzierska (kkedz@unimelb.edu.au).

Materials availability

This study did not generate new unique reagents.

Data and code availability

- The published article includes all datasets generated or analyzed during the study.
- This paper does not report original code.
- Any additional information required to reanalyze the data reported in this paper is available from the lead contact upon request.

EXPERIMENTAL MODEL AND SUBJECT DETAILS

Victorian blood cancer patients and healthy volunteers that were scheduled for the COVID-19 vaccine, as part of Australia's COVID-19 vaccine rollout in 2021, were recruited to the study. Patients with various haematological malignancies were enrolled at the Peter MacCallum Cancer Centre or St Vincent's Hospital following ethics approval by the Peter MacCallum Cancer Centre Human Research Ethics Committee (HREC/74271/PMCC-2021, HREC/74260/PMCC-2021). Healthy volunteers were enrolled at the Royal Melbourne Hospital or the Austin Hospital with approvals from Melbourne Health (HREC/68355/MH-2020) and Austin Health (HREC/73256/Austin-2021), respectively. Human ethics was also approved by the University of Melbourne HREC (21817, 21711, 21626, 21560, 13344). All participants provided written informed consent. Patient and healthy cohort demographics are summarised in Table S1. Clinical information and limited immune data have been described for a subset of CLL patients.[51]

Participants were vaccinated with 2 doses of the BNT162b2 Comirnaty (Pfizer) vaccine scheduled ~3 weeks apart or the ChAdOx1 (AstraZeneca) vaccine scheduled ~8–12 weeks apart. One patient also received 2 doses of the mRNA-1273 (Moderna) vaccine. Heparinised peripheral blood and serum were collected prior to vaccination (T1), ~1 week following the first dose (T2, optional bleed), just prior to the second dose (T3), ~1 week following the second dose (T4, optional bleed), and ~1 month (T5) following the second dose. Additionally, a subset of patients were bled prior to receiving a third dose of BNT162b2 Comirnaty or mRNA-1273 (T6), 1 month following the third dose (T7) and 3–4 months following the third dose (T8). Healthy vaccinated adults were recruited as controls. PBMCs were isolated by Ficoll-Paque separation for cellular assays, plasma was collected for measuring antibodies, serum for microneutralisation assays and DNA isolated from granulocytes for HLA typing by VTIS (Melbourne, Australia), essentially as described.[28]

The study was conducted in compliance with the conditions of the ethics committee approval, the NHMRC National Statement on ethical Conduct in Human Research (2007) and the Note for Guidance on Good Clinical Practice (CPMP/ICH-135/95).

METHOD DETAILS

Cellular activation in whole blood

The kinetics of ASCs and activation of Tfh/$CD8^+$/$CD4^+$ T cell subsets were measured at T1-T5 timepoints by directly staining whole blood with antibodies for flow cytometry, essentially as described.[25,28,52]

Assessment of SARS-CoV-2-specific antibodies and memory B cells

Spike and nucleocapsid antibodies were measured using Elecsys Anti-SARS-CoV-2 kit and Roche e601 analyser according to manufacturer's instructions. Plasma antibodies against wildtype SARS-CoV-2 RBD protein (vaccine strain) were assessed by IgG ELISA as previously described in detail.[18,40,53] MNT activity of serum samples (T1 and T5 only) was assessed as previously described with the wildtype and delta strains.[26,37,54] The sVNT assay was performed with wildtype and B.1.1.529 omicron (Genscript Z03730) strains essentially as described.[53] Spike-specific B cell responses from the vaccine strain were measured on thawed PBMCs or TAME-flow through fractions. Cells were stained with wildtype Spike recombinant probes conjugated to PE, fixed and acquired on a BD LSRII Fortessa, essentially as described.[18,37]

24-H stimulation with spike overlapping peptide pools

Thawed PBMCs were plated into a 96-well plate at 1e6 PBMCs/well. For AIM assay, cells were stimulated in complete-RPMI with 10 μg/ml SARS-CoV-2 Spike peptide pool (181 peptides, 0.06 μg/ml per peptide; BEI Resources, NIAID, NIH, SARS-Related Coronavirus 2 Spike (S) Glycoprotein, NR-52402) or DMSO (0.1%; Sigma), as a negative control, and cultured at 37°C/5% CO_2 for 24 h. Cells were washed and stained with CXCR5-BV421 (562747; BD Biosciences), CD3-BV510 (317332; BioLegend), CD8-BV605 (564116; BD Biosciences), CD4-BV650 (563875; BD Biosciences), CD25-BV711 (563159; BD Biosciences), CXCR3-BV786 (353738; BD Biosciences), CD137-APC (309810; BioLegend), CD27-AF700 (560611; BD Biosciences), CD14/CD19-APC-H7 (560180/560252; BD Biosciences), Live/Dead NIR (L34976; Invitrogen), CD69-PerCPCy5.5 (310925; BioLegend), CD134-PE (340420; BD Biosciences), CD95-PE-CF594 (562395; BD Biosciences), CD45RA-PeCy7 (337167; BD Biosciences) before fixing with 1% PFA.

For ICS, cells were stimulated in complete-RPMI with 100 μg/mL overlapping Spike peptide pool (181 peptides, 0.6 μg/ml per peptide; BEI Resources, NR-52402) or DMSO (1%), as a negative control, in combination with anti-CD28/CD49d (1:100, 347690; BD Biosciences) and 10U/ml IL-2 (11147528001; Roche), with Brefeldin A (½000 dilution; 555029; BD Biosciences) added after 6 h. Following further 18 h of the stimulation, cells were washed twice with MACS buffer (PBS/0.5% BSA, 2mM EDTA), then stained with surface antibodies: CD3-BV510 (317332; BioLegend), CD4-BV650 (563875; BD Biosciences), CD8-PerCPCy5.5 (565310; BD Biosciences) and Live/Dead NIR (L34976; Invitrogen) for 30 min on ice. Cells were washed twice, then fixed using the BD Cytofix/Cytoperm kit (554723; BD Biosciences) according to the manufacturer's instructions, washed twice and intracellularly stained with IFNγ-v450 (560371; BD Biosciences), MIP-1β-APC (560656; BD Biosciences) and TNFα-AF700 (557996; BD Biosciences) for 30 min on ice. Following two further washes, lymphocytes were resuspended in MACS buffer and acquisition was on an LSRII Fortessa. Data were analyzed using FlowJo v10. Values obtained for PBMCs cultured with DMSO under the same conditions (negative controls) were subtracted from peptide-stimulated values. As a negative control, PBMCs cultured with DMSO also had IL-2, thus this control accounts for any background cytokine production triggered by IL-2 by $CD4^+$ and $CD8^+$ T cells.

Spike and non-spike epitope-specific tetramer$^+$ T cell responses

HLA class I tetramers HLA-A*01:01/S_{865}[34] (LTDEMIAQY), HLA-A*01:01/ORF1a$_{1637}$[41] (TTDPSFLGRY), HLA-A*02:01/S_{269}[19] (YLQPRTFLL), HLA-A*03:01/S_{378}[41] (KCYGVSPTK), HLA-A*03:01/N_{361}[42] (KTFPPTEPK), HLA-A*24:02/S_{1208}[35] (QYIKWPWYI), HLA-B*07:02/N_{105}[42] (SPRWYFYYL), HLA-B*15:01/S_{919}[23] (NQKLIANQF) and HLA-B*35:01/S_{321}[33] (QPTESIVRF) were generated by Rossjohn laboratory and validated as previously described.[18–20] HLA class II tetramer HLA-DPA1*01:03/DPB1*04:01/S_{167} (TFEYVSQPFLMDLE) was generated by Rossjohn laboratory and validated as previously described.[22]

Cryopreserved PBMCs (5-10x10^6) underwent tetramer-associated magnetic enrichment (TAME) following staining with a class I and/or DP4 class II Spike tetramer on PE and/or another class I tetramer on APC as described.[18] Class I and class II tetramers on PE were exclusively stained on $CD8^+$ or $CD4^+$ T cells, respectively, with minimal to zero non-specific binding. Flow-through fractions were cryopreserved for Spike-specific B cell probe analysis, as previously described[21] which were negative for tetramer$^+$ cells. Samples were acquired on an LSRII Fortessa using the software BD FACS DIVA v8.0.1 and flow cytometry data were analyzed using FlowJo v10 software.

Enriched HLA-A*02:01/S_{269}, HLA-A*24:02/S_{1208} and HLA-DPB1*04:01/S_{167} tetramer$^+$ T cells were indexed single-cell sorted on a BD FACSAria III for TCR analysis essentially as described.[18,21] CDR3α and CDR3β regions from single cells were amplified using multiplex-nested RT-PCR[18,34] analyzed by IMGT/V-QUEST.

As in our study, we had a limited number of PBMCs from hematology patients (and healthy controls), our baseline T1 tetramer-positive T cell population correspond to a few events (<10 events) for some individuals. For transparency, we show any samples with <10 tetramer$^+$ events as open symbols. Only samples with more than 10 tetramer$^+$ events are included in the phenotypic analysis (Figures 4H and 4I).

QUANTIFICATION AND STATISTICAL ANALYSIS

TCRαβ statistical analysis

Single-chain alpha and beta TCR sequences were analyzed by TCRdist for modeling amino acid motifs, TCR landscapes, neighbor distance distribution and probabilities of generation (P_{gen}).[46] For comparisons, published TCR datasets from unvaccinated SARS-CoV-2-infected individuals in the blood were sourced from Rowntree et al.,[21] Nguyen et al.,[18] Rowntree

et al.[20] (HLA-A*02:01/S_{269}, HLA-A*24:02/S_{1208} and HLA-DPB1*04:01/S_{167}), Minervina et al.[23] (HLA-A*02:01/S_{269} and HLA-A*24:02/S_{1208}) and Mudd et al.[22] (HLA-DPB1*04:01/S_{167}). Published TCR datasets from COVID-19-vaccinated uninfected individuals were sourced from Minervina et al.[23] (HLA-A*02:01/S_{269} and HLA-A*24:02/S_{1208}). TCRdist[46] was used to calculate pairwise distances between clonotypes, sequence logos was created with *conga* python package[44] network was generated with igraph R package (v. 1.3.2)[45] and visualized with Gephi (v.0.9.7).[47]

STATISTICAL ANALYSIS

Statistical significance of nonparametric datasets (two-tailed) were determined using GraphPad Prism v9 software. Mann-Whitney U-test (unpaired) and Wilcoxin signed-rank test (paired) were used for comparisons between two groups. Kruskal-Wallis test (unmatched) with Dunn's multiple comparisons was used to compare more than two groups. Tukey's multiple comparison test compared row means between more than two groups, while Sidak's multiple comparison test compared column means between multiple groups. Correlation matrices were prepared in R using corrplot version 0.92.[48] Volcano plots were generated within healthy individuals and haematology patients, and in patients with differing B cell ranges by Wilcoxon Rank-Sum test with Benjamini-Hochberg adjustment for multiple comparisons, using the rstatix version 0.7.0 package[49] within R version 4.2.1,[43] and plotted using EnhancedVolcano version 1.14.0.[50] Volcano plots display log2(fold change) vs. -log10(unadjusted p value), with horizontal dashed line representing the adjusted p threshold. Parameters used for the volcano plots included sVNT, AIM, IgG RBD; log MNT (T5 only); B cell number and B cell probes (all participants and med-high B cell participants only).

Cell Reports Medicine, Volume *4*

Supplemental information

Robust SARS-CoV-2 T cell responses with common TCR$\alpha\beta$ motifs toward COVID-19 vaccines in patients with hematological malignancy impacting B cells

Thi H.O. Nguyen, Louise C. Rowntree, Lilith F. Allen, Brendon Y. Chua, Lukasz Kedzierski, Chhay Lim, Masa Lasica, G. Surekha Tennakoon, Natalie R. Saunders, Megan Crane, Lynette Chee, John F. Seymour, Mary Ann Anderson, Ashley Whitechurch, E. Bridie Clemens, Wuji Zhang, So Young Chang, Jennifer R. Habel, Xiaoxiao Jia, Hayley A. McQuilten, Anastasia A. Minervina, Mikhail V. Pogorelyy, Priyanka Chaurasia, Jan Petersen, Tejas Menon, Luca Hensen, Jessica A. Neil, Francesca L. Mordant, Hyon-Xhi Tan, Aira F. Cabug, Adam K. Wheatley, Stephen J. Kent, Kanta Subbarao, Theo Karapanagiotidis, Han Huang, Lynn K. Vo, Natalie L. Cain, Suellen Nicholson, Florian Krammer, Grace Gibney, Fiona James, Janine M. Trevillyan, Jason A. Trubiano, Jeni Mitchell, Britt Christensen, Katherine A. Bond, Deborah A. Williamson, Jamie Rossjohn, Jeremy Chase Crawford, Paul G. Thomas, Karin A. Thursky, Monica A. Slavin, Constantine S. Tam, Benjamin W. Teh, and Katherine Kedzierska

SUPPLEMENTAL INFORMATION

Robust T cell responses with common TCRαβ motifs towards COVID-19 vaccines in haematological malignancy patients with impacted B cell immunity

Thi H O Nguyen[1]*, Louise C Rowntree[1]*, Lilith F Allen[1]*, Brendon Y Chua[1,2], Lukasz Kedzierski[1,3], Chhay Lim[4], Masa Lasica[5,6], G Surekha Tennakoon[4], Natalie R Saunders[4], Megan Crane[4], Lynette Chee[7,8], John F Seymour[7,9], Mary Ann Anderson[7,9,10], Ashley Whitechurch[7], E Bridie Clemens[1], Wuji Zhang[1], So Young Chang[1], Jennifer R Habel[1], Xiaoxiao Jia[1], Hayley A McQuilten[1], Anastasia A Minervina[11], Mikhail V Pogorelyy[11], Priyanka Chaurasia[12], Jan Petersen[12], Tejas Menon[1], Luca Hensen[1], Jessica Neil[1], Francesca L Mordant[1], Hyon-Xhi Tan[1], Aira F Cabug, Adam K Wheatley[1], Stephen J Kent[1,13,14], Kanta Subbarao[15], Theo Karapanagiotidis[16], Han Huang[16], Lynn K Vo[16], Natalie L Cain[16], Suellen Nicholson[16], Florian Krammer[17], Grace Gibney[18], Fiona James[18], Janine M Trevillyan[18], Jason A Trubiano[4,8,19,20], Jeni Mitchell[21], Britt Christensen[8,21], Katherine A Bond[1,16,22], Deborah A Williamson[10,16,23], Jamie Rossjohn[12,24], Jeremy Chase Crawford[11], Paul G Thomas[11], Karin A Thursky[4,9,20], Monica A Slavin[4,9,20,23#], Constantine S Tam[7,8#], Benjamin W Teh[4,9,20#] and Katherine Kedzierska[1,2#]

Supplementary Tables

Table S1. Cohort demographics and clinical summary, refer to Figure 1.

	Healthy individuals	Haematology patients	BNT162b2, mRNA-1273	ChAdOx1
Number of individuals, *n*	58	95	25	70
Age, mean (range)	44 (20-80)	65 (19-91)	51 (19-80)	70 (51-91)
Female, *n* (%)	41 (71%)	28 (29%)	-	-
Vaccine (2 doses), *n* (%)			-	-
ChAdOx1 (AstraZeneca)	26 (45%)	70 (74%)	-	-
Age, mean (range)	51 (20-80)	70 (51-91)		
BNT162b2 Comirnaty (Pfizer)	32 (55%)	24 (25%)	-	-
Age, mean (range)	38 (23-60)	50 (19-80)		
mRNA-1273 (Moderna)	0	1 (1%)	-	-
Vaccine (3rd dose), *n* (%)			-	-
ChAdOx1 (AstraZeneca)	1 (2%)	5 (5%)	-	-
BNT162b2 Comirnaty (Pfizer)	20 (34%)	63 (66%)	-	-
mRNA-1273 (Moderna)	1 (2%)	10 (11%)	-	-
Novavax	1 (2%)	0 (0%)	-	-
Unknown due to lost follow-up	35 (60%)	17 (18%)	-	-
Cellular therapy, *n* (%)	-	33 (34%)	17 (68%)	16 (23%)
Allogeneic SCT		5 (5%)	4 (16%)	1 (1%)
Autograft	-	21(22%)	9 (36%)	12 (17%)
CAR T-cell	-	7 (7%)	4 (16%)	3 (5%)
Days post-cellular therapy, mean (range)	-	177 (45-393)	185 (45-393)	167 (73-337)
Malignancy/treatment, *n* (%)				
CLL/naive	-	14 (15%)	2 (8%)	12 (17%)
CLL/venetoclax	-	5 (5%)	1 (4%)	4 (6%)
CLL/zanubrutinib	-	25 (26%)	1 (4%)	24 (34%)
WM/naive	-	1 (1%)	0	1 (1%)
WM/zanubrutinib	-	10 (11%)	1 (4%)	9 (13%)
Myeloma	-	7 (7%)	3 (12%)	4 (6%)
Previous SARS-CoV-2 infection, *n*	1	0	0	0
SARS-CoV-2 infection during the study, *n*	8	12	5	7

Abbreviations: CAR T-cell, chimeric antigen receptor T-cell; CLL, chronic lymphocytic leukemia; SCT, stem cell transplantation; WM, Waldenstrom macroglobulinemia. Clinical information and limited immune data have been described for a subset of CLL patients.[41]

SUPPLEMENTARY FIGURES

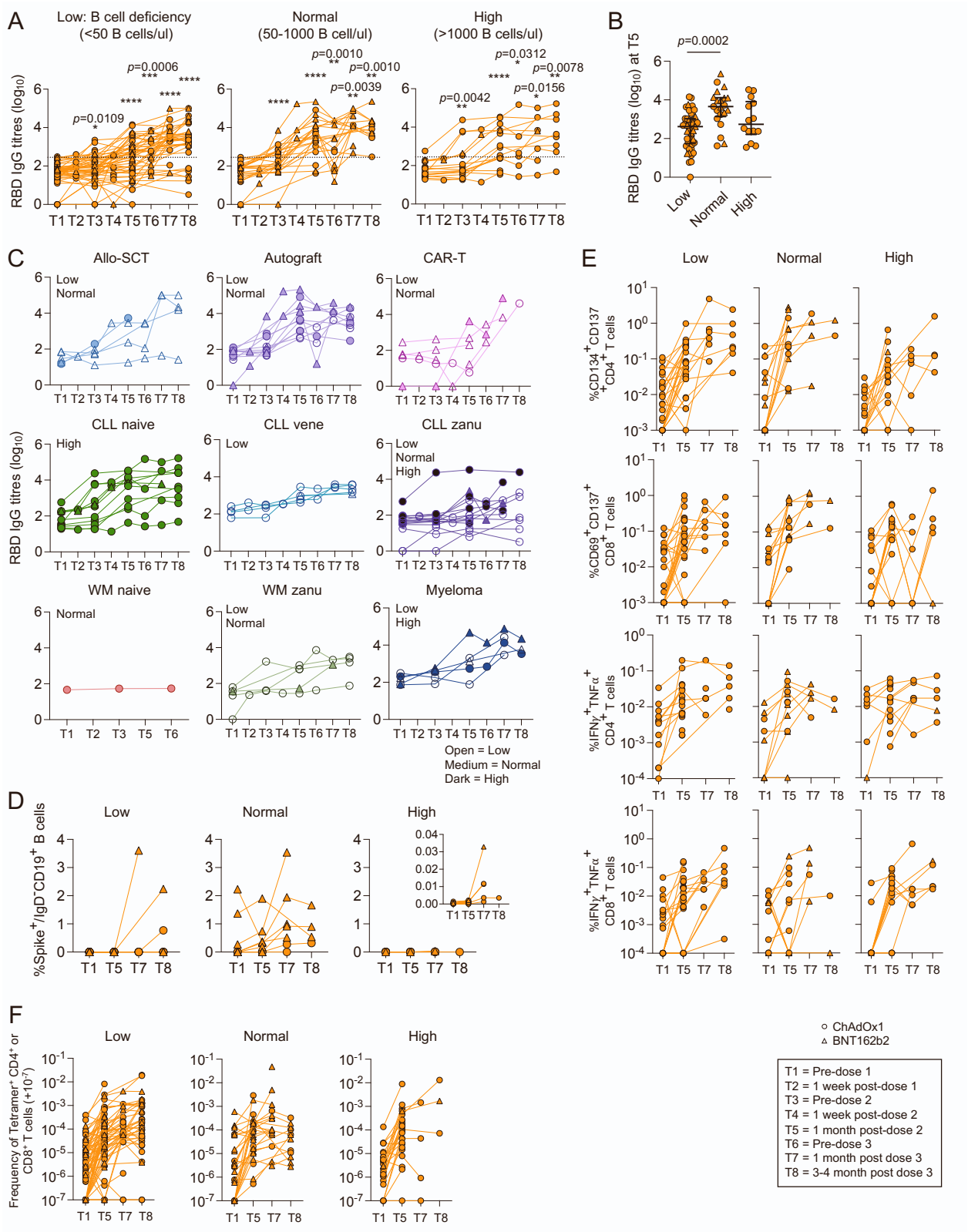

Figure S1. Haematology patients grouped by low, normal or high B cell numbers. End-point IgG titres of ancestral RBD antibodies (A) across sampling timepoints, (B) at T5, and (C) per malignancy and treatment group. (D) Spike-specific memory B cells in haematology patients grouped by low, normal or high B cell numbers. (E) AIM and ICS frequencies and (F) tetramer^{+} spike-specific CD4^{+} and CD8^{+} T cells grouped by low, normal or high B cell numbers. Due to limited sample availability, experiments were performed once for each sample. Related to Figure 1, 3, 4.

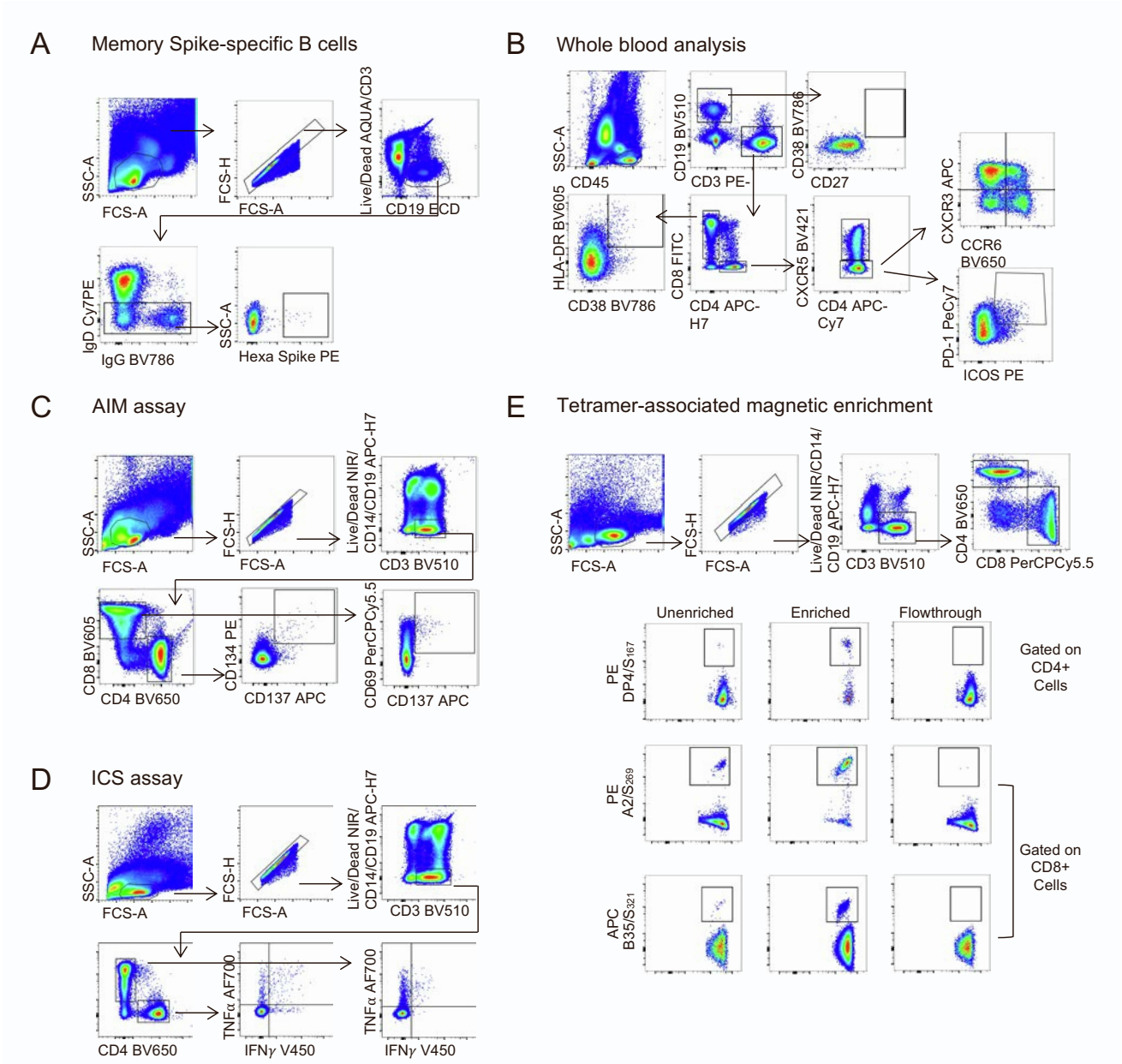

Figure S2. FACS gating strategies to measure cellular vaccine responses. Gating strategy for (A) memory spike-specific B cells, (B) whole blood analysis, (C) AIM and (D) ICS assay, and (E) TAME. Related to Figure 1, 2, 3 and 4.

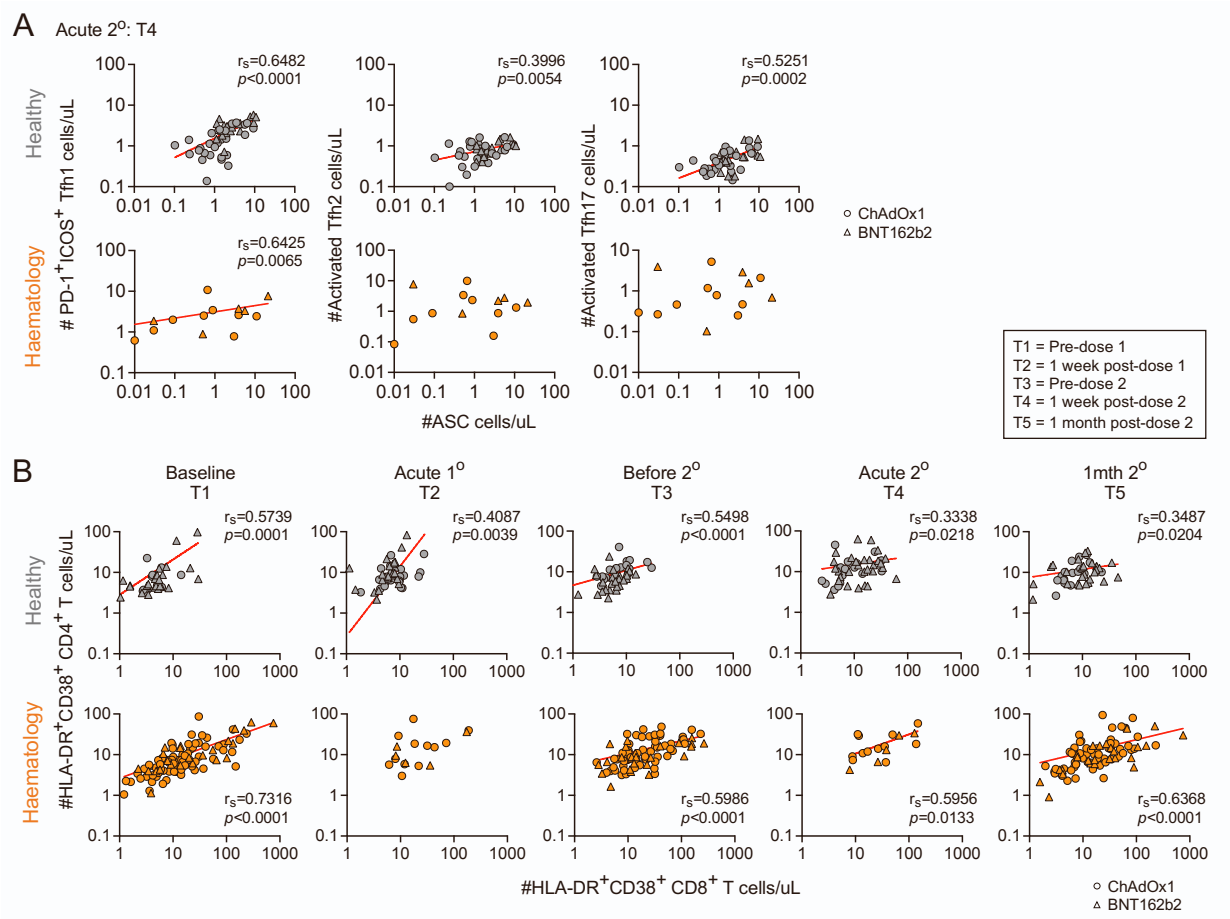

Figure S3. Correlations of whole blood subsets. (A) Spearman's correlation (r_s) of ASCs and Tfh1, Tfh2 and Tfh17 subsets at T4. (B) Spearman's correlation (r_s) of activated $CD4^+$ and $CD8^+$ T cells at T1-T5. Due to limited sample availability, experiments were performed once for each sample. Related to Figure 2.

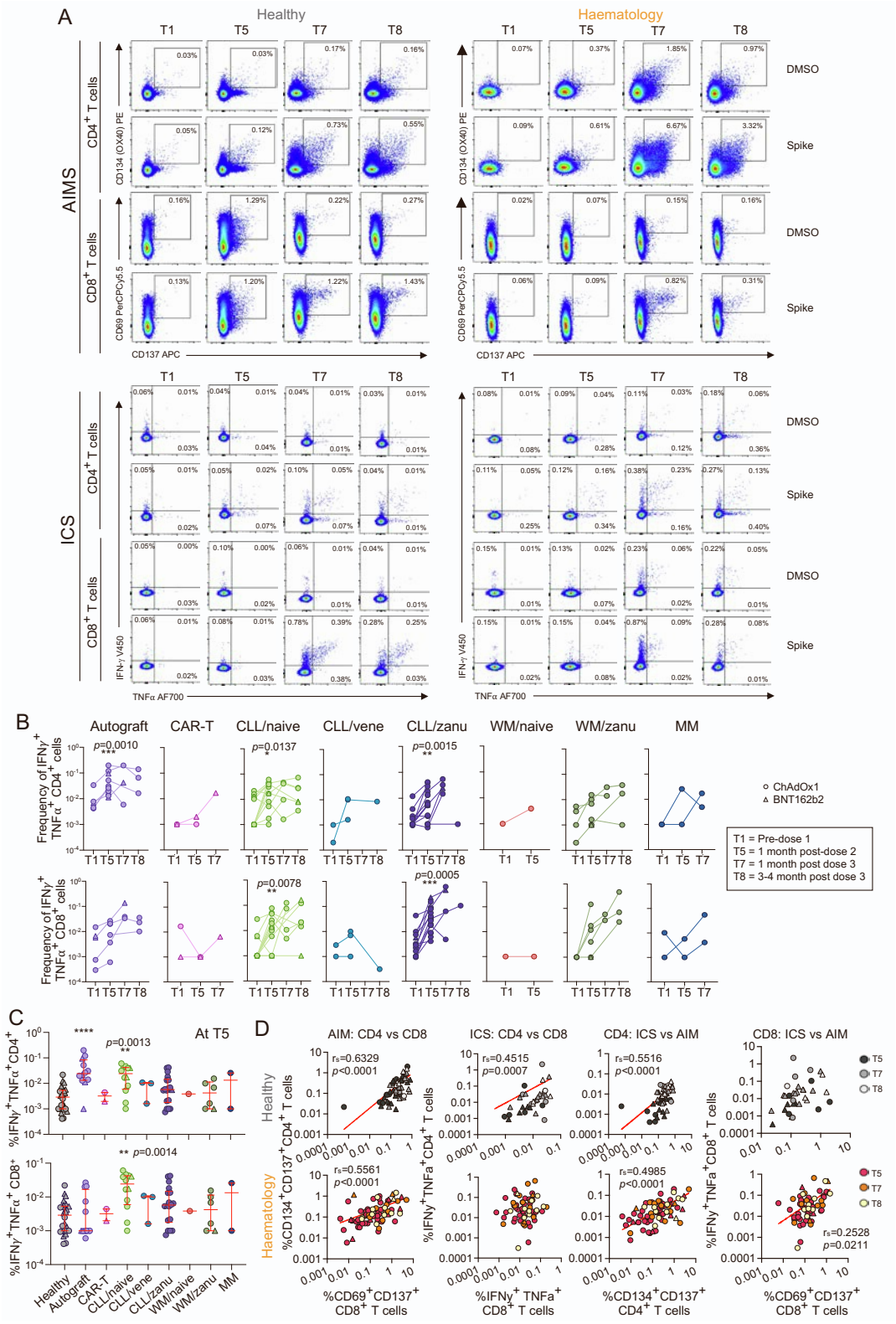

Figure S4. Functional spike-specific CD4$^+$ and CD8$^+$ T cell responses in haematology patients and healthy individuals. (A) Representative AIM and ICS FACS plots including DMSO controls. (B) ICS frequency per malignancy and treatment group at all timepoints measured and (C) at T5 where median and IQR are shown. Statistical significance determined by Dunn's multiple comparisons set on healthy versus all other disease groups. (D) Spearman correlations of CD4$^+$ and CD8$^+$ T cell responses via AIM and ICS assays. Statistical significance determined by Wilcoxon test for timepoint comparisons against T1 (floating values). Exact p values 0.0001<0.05 are shown except p<0.0001=****. Due to limited sample availability, experiments were performed once for each sample. Related to Figure 3.

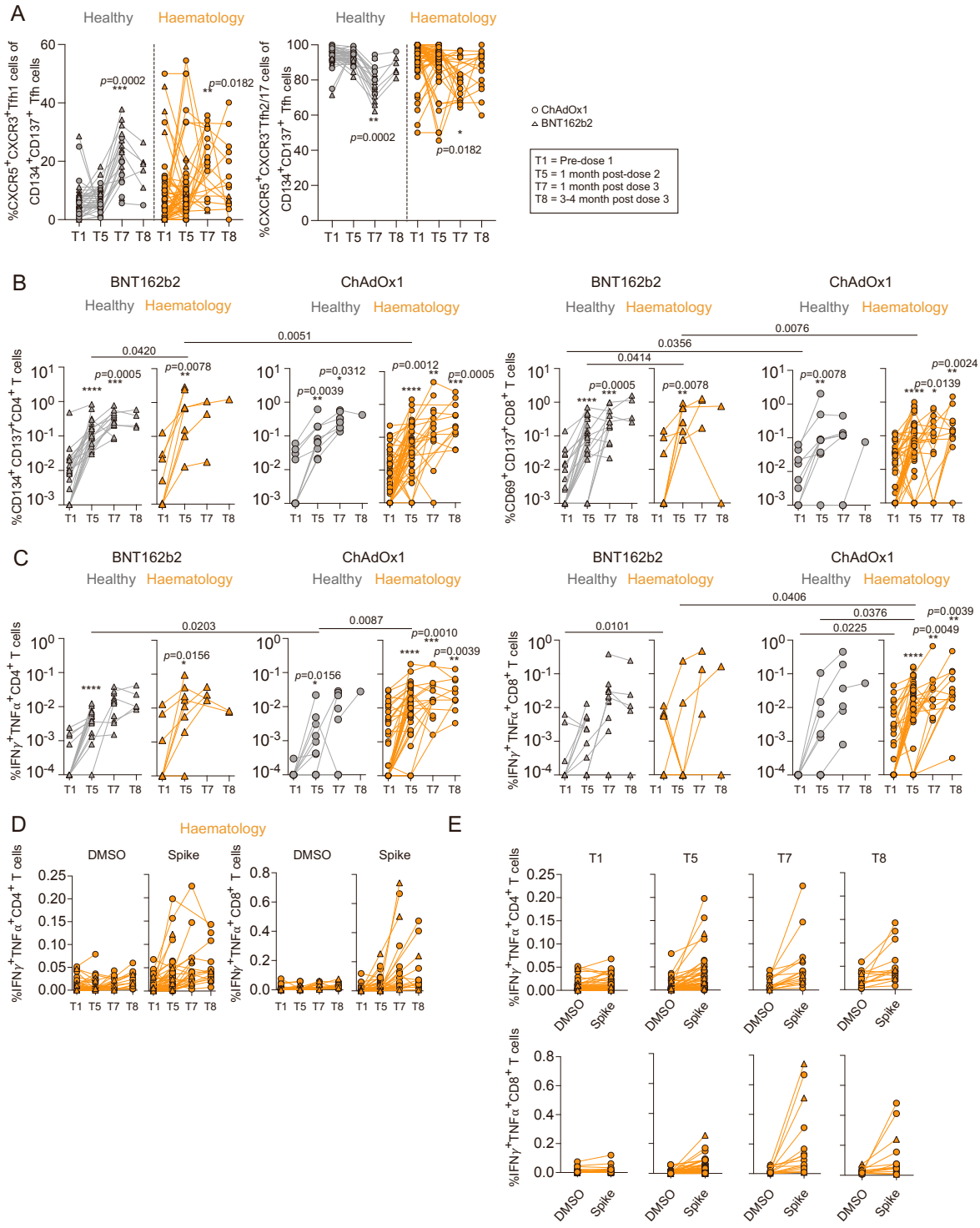

Figure S5. Spike-specific CD4$^+$ and CD8$^+$ T cell responses by vaccine type. (A) Frequency of Tfh1 and Tfh2/17 AIM$^+$ responses of total AIM$^+$ CXCR5$^+$CD4$^+$ Tfh cell response. (B) AIM and (C) ICS frequencies of CD4$^+$ and CD8$^+$ T cells in healthy and haematology per vaccine type. (D, E) Raw percentages of IFNγ$^+$TNF$^+$ in DMSO and spike ICS cultures. Statistical significance determined by Wilcoxon test for timepoint comparisons against T1 (floating values) or by Mann-Whitney for comparisons between healthy and patient timepoints or between vaccine type (connecting line). Exact p values 0.0001<0.05 are shown except p<0.0001=****. Due to limited sample availability, experiments were performed once for each sample. Related to Figure 3.

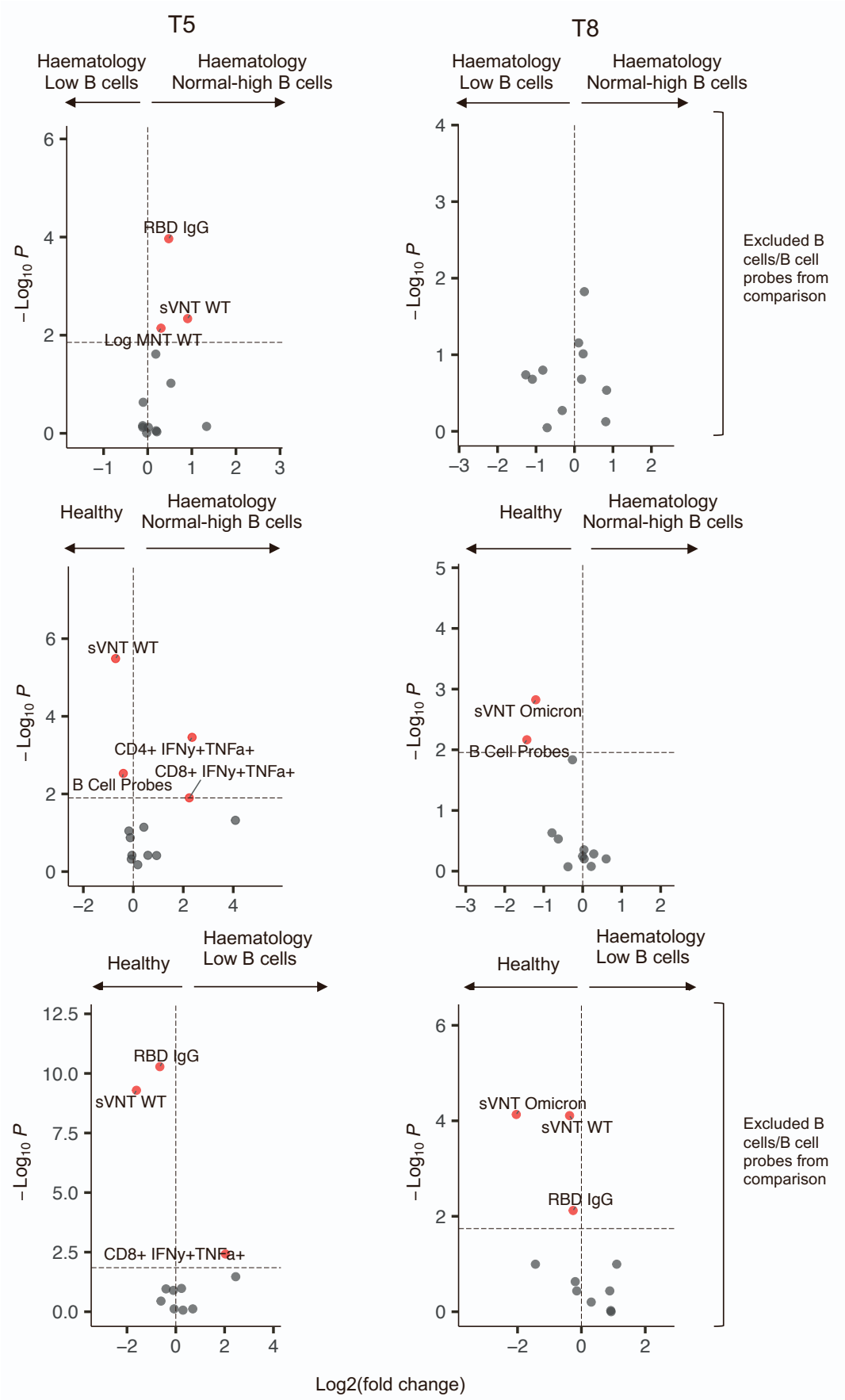

Figure S6. Volcano plots comparing healthy individuals and haematology patients. Related to Figure 3.

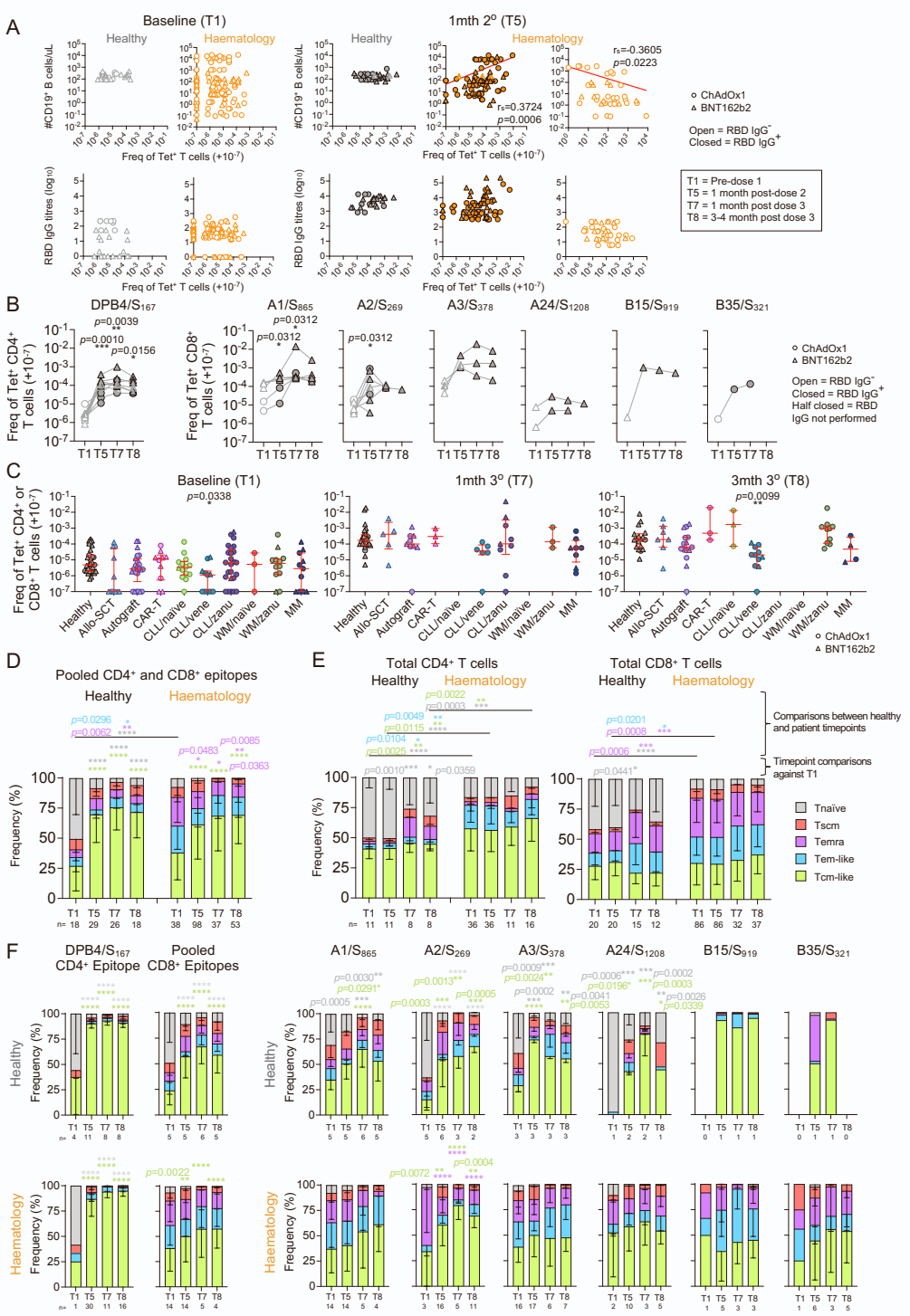

Figure S7. *Ex vivo* SARS-CoV-2-specific tetramer$^+$ T cell responses following COVID-19 vaccination. (A) Spearman's correlation (r_s) of tetramer frequencies versus B cell numbers and RBD IgG titres at T1 and T5. (B) Tetramer CD4$^+$ and CD8$^+$ T cell frequencies of healthy individuals per SARS-CoV-2 epitope. (C) Tetramer frequencies at T1, T7 and T8 where median and IQR are shown. (D) Phenotype profiles of pooled tetramer$^+$ cells, (E) total CD4$^+$ T cells and CD8$^+$ T cells and (F) per SARS-CoV-2 epitope. The frequency of tetramer$^+$ cells have been right-shifted by 10^{-7} (i.e. no detected tetramer$^+$ events displayed as 10^{-7}) to allow for visibility on the logarithmic y axis. Only samples with 10 or more tetramer$^+$ events are included in the phenotypic analysis (Figure D, E and F). Statistical significance determined by Wilcoxon test for timepoint comparisons against T1 ((B) floating values), Dunn's multiple comparisons set on healthy versus all other disease groups (c), Tukey's multiple comparison test (floating values are timepoint comparisons against T1; connecting line are comparisons between healthy and patient timepoints) (D,E), and Dunnett's multiple comparison test for timepoint comparisons against T1 (F). Exact p values 0.0001<0.05 are shown except p<0.0001=****. Due to limited sample availability, experiments were performed once for each sample. Related to Figure 4.

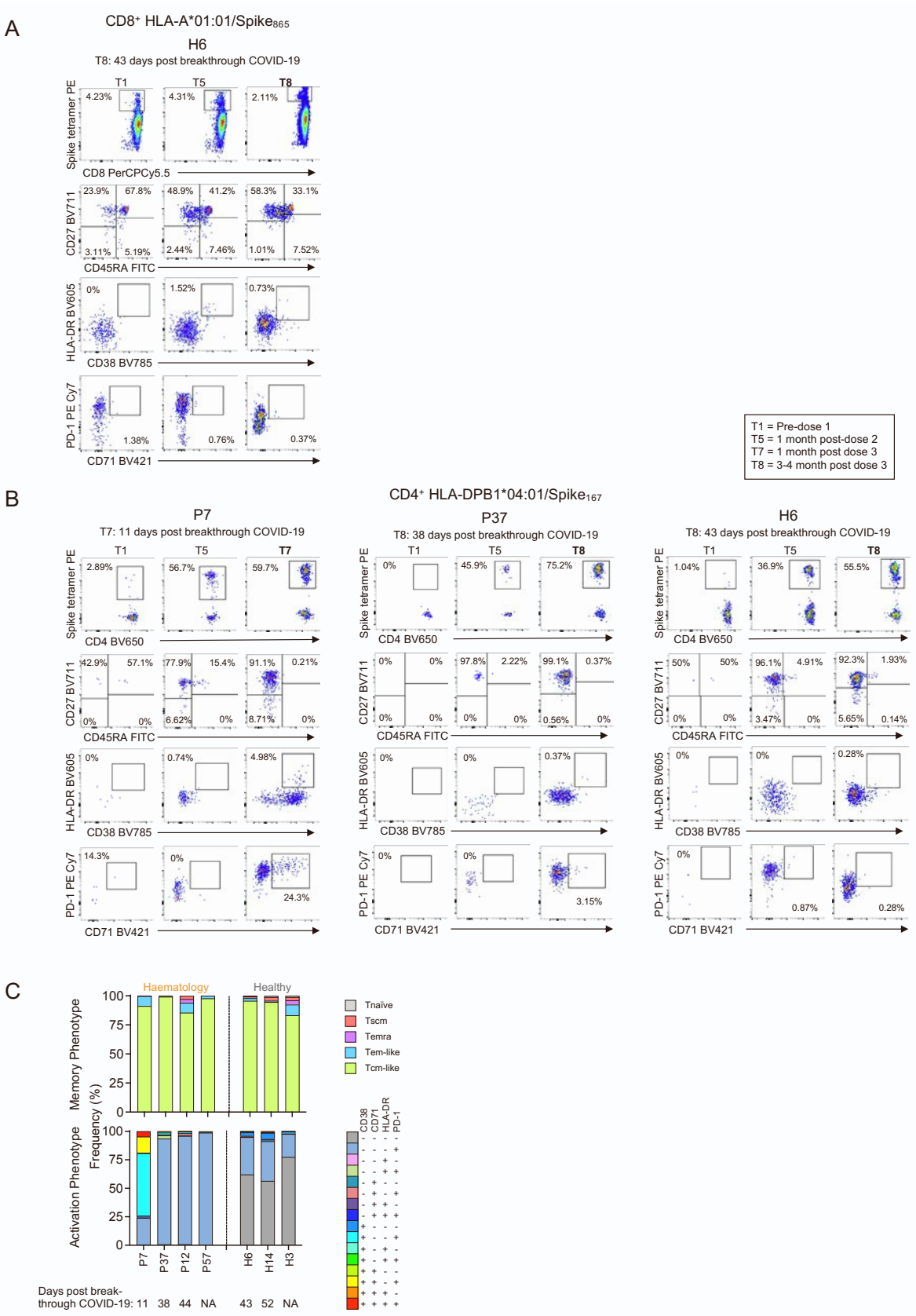

Figure S8. Vaccine responses in donors with breakthrough SARS-CoV-2 infections. Representative TAME enriched FACS plots gated on $CD8^+$ (A) and $CD4^+$ (B) T cells depicting tetramer, and memory and activation phenotypes. (C) Memory and activation phenotypes of DPB4/S_{167}-specfic $CD4^+$ T cells from individuals with breakthrough COVID-19. Due to limited sample availability, experiments were performed once for each sample. Related to Figure 5.

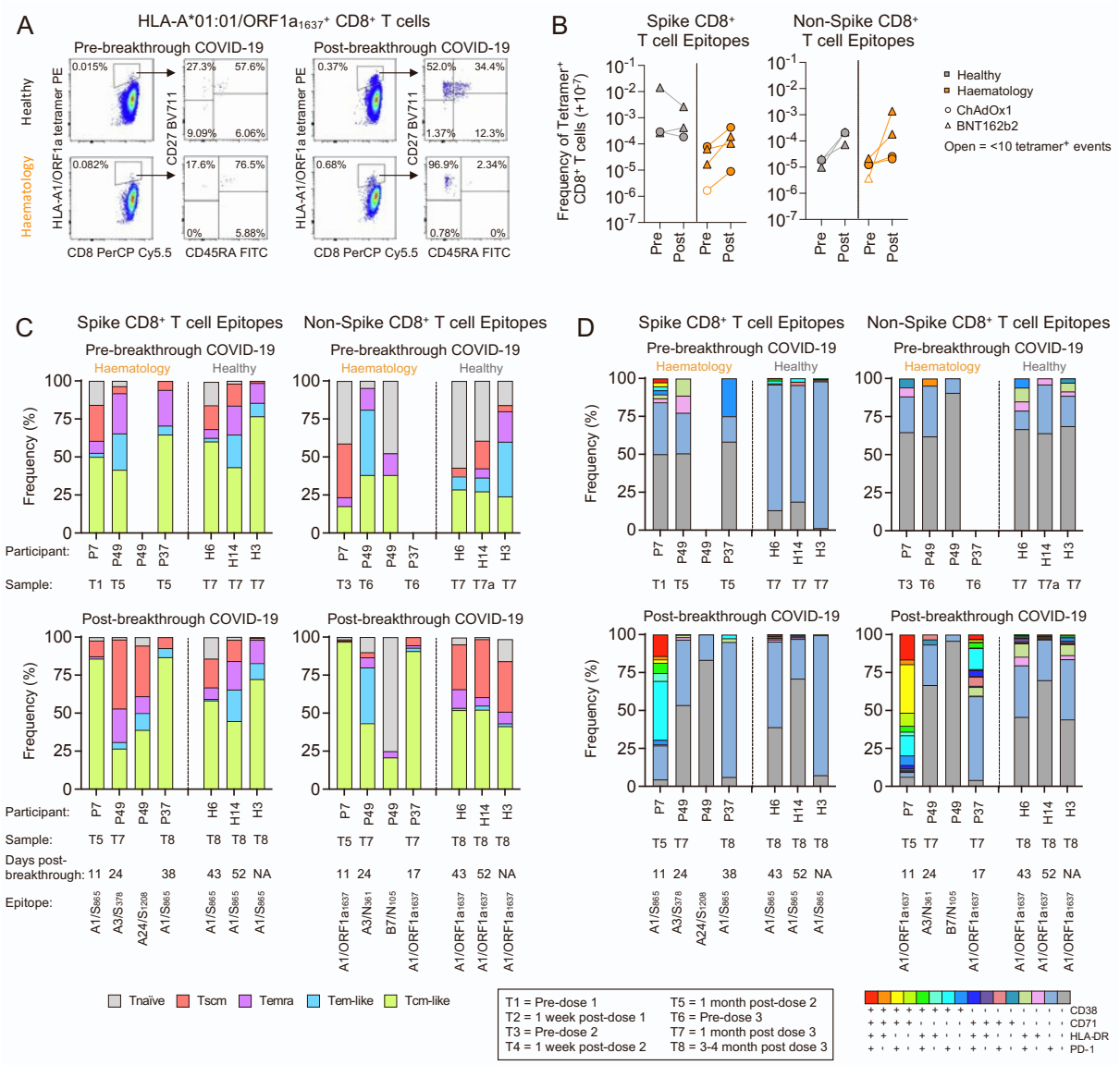

Figure S9. *Ex vivo* paired spike and non-spike-specific tetramer$^+$ CD8$^+$ T cell responses following breakthrough COVID-19. (A) Representative FACS plots of TAME-enriched non-spike-specific CD8$^+$ tetramer populations. (B) Paired tetramer CD8$^+$ T cell frequencies of healthy and haematology participants pre- and post-COVID-19 breakthrough. Any samples with <10 tetramer$^+$ events are shown as open symbols. (C) Memory and (D) activation phenotype profiles for spike and non-spike-specific CD8$^+$ T cells for individuals with breakthrough COVID-19. The frequency of tetramer$^+$ cells have been right-shifted by 10^{-7} (i.e. no detected tetramer$^+$ events displayed as 10^{-7}) to allow for visibility on the logarithmic y axis. Only samples with 10 or more tetramer$^+$ events are included in the phenotypic analysis (Figure C and D). Due to limited sample availability, experiments were performed once for each sample. Related to Figure 5.

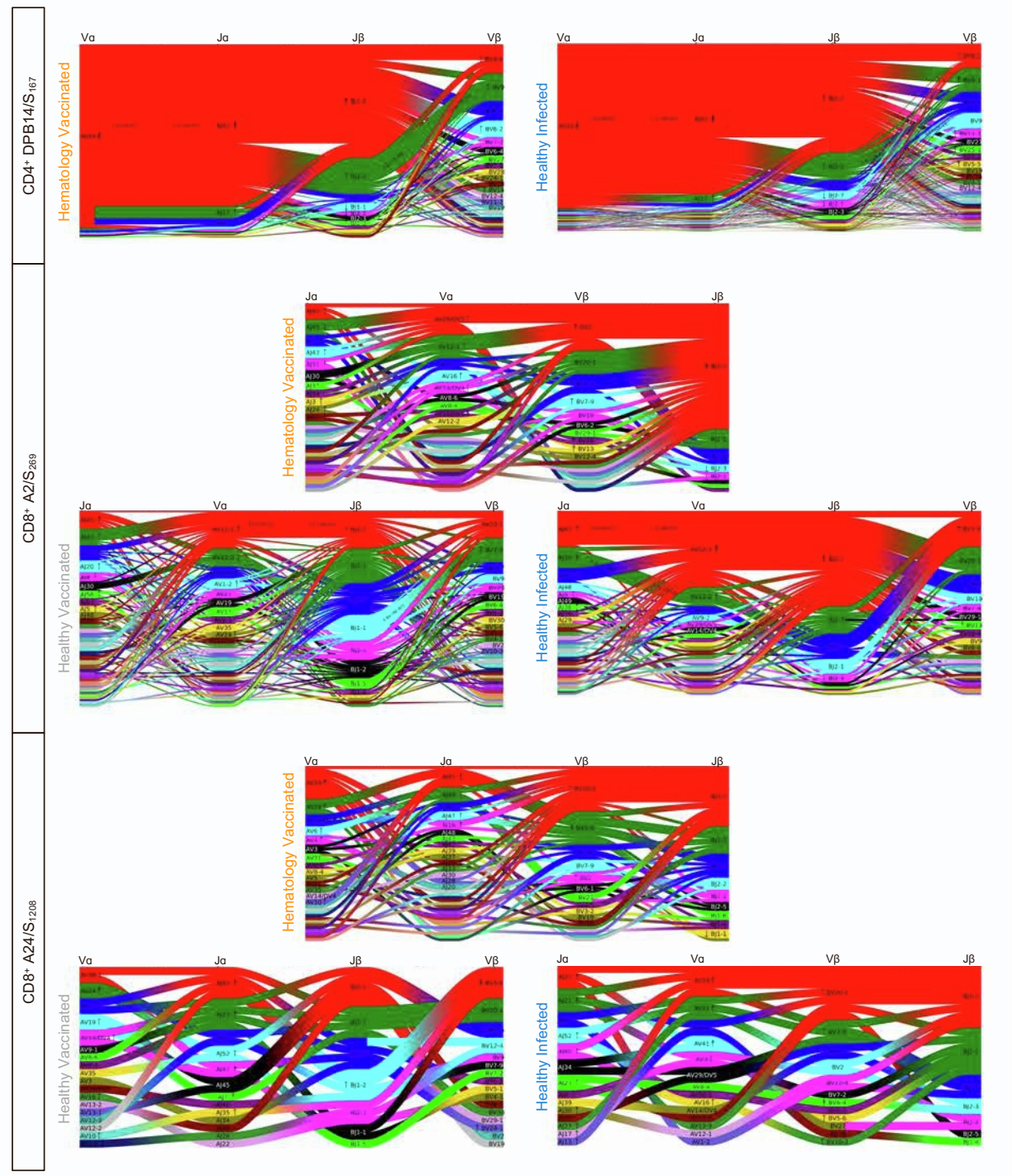

Figure S10. V and J gene segment usage and covariation in epitope-specific responses. Gene-gene pairing landscapes are depicted by curves between vertical gene segment stacks (thickness proportional to the number of TCRs with the gene pairing). Vertical arrows indicate the enrichment of gene segments relative to background frequencies, each arrowhead indicates a 2-fold enrichment. The clonally expanded TCRs were reduced to a single data point for this analysis. Genes are coloured based on frequency: red (most frequent), green (second most frequent), blue, cyan, magenta, and black, followed by assorted colours for rare frequencies. Related to Figure 6.

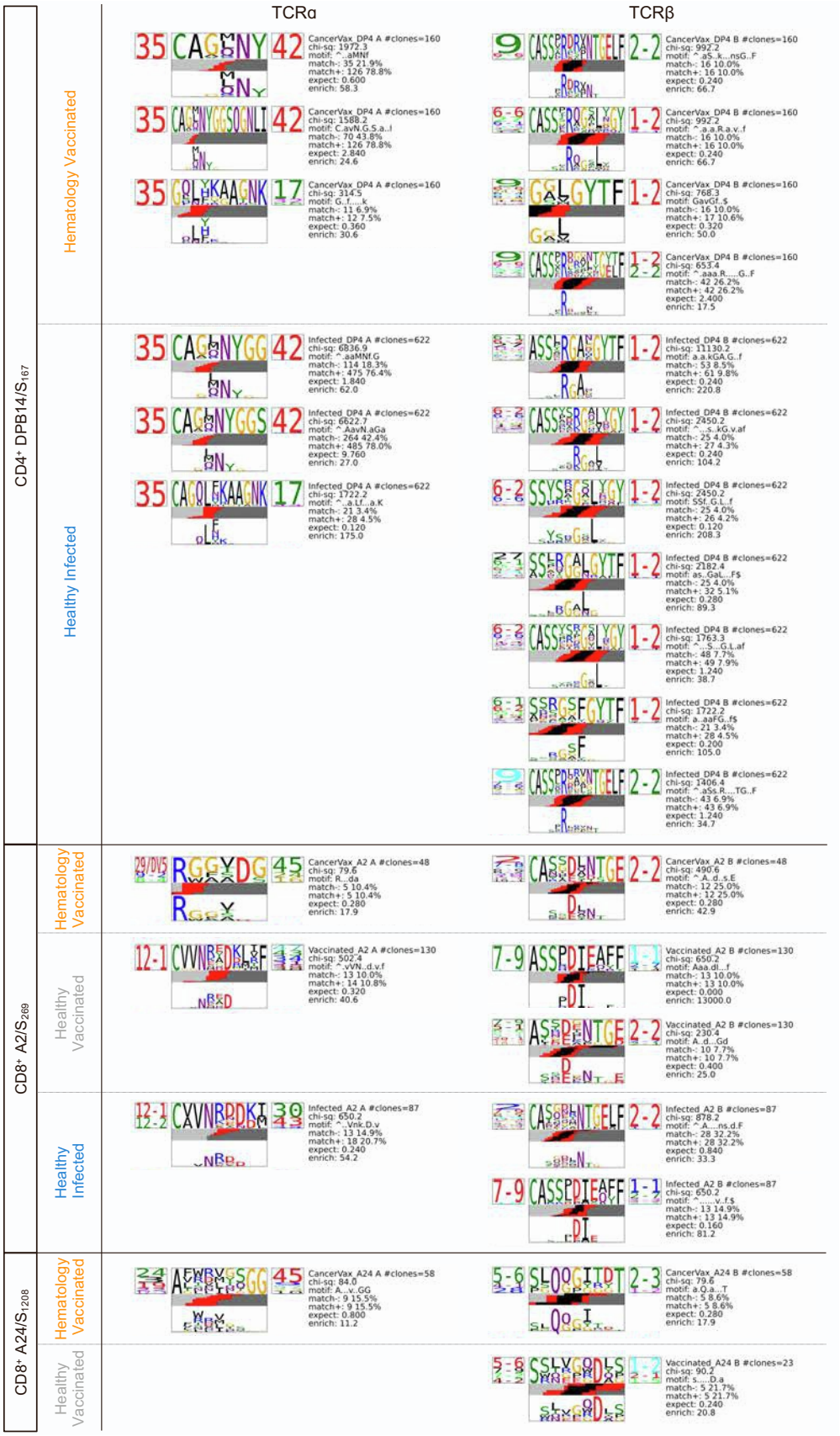

Figure S11. TCR logo representations of CDR3α and β sequence motifs for DPB4/S$_{167}$, A2/S$_{269}$ and A24/S$_{1208}$. Each TCR motif depicts the V (left side) and J (right side) gene frequencies, the CDR3 amino acid sequence (middle), and the inferred rearrangement structure (bottom bars coloured by source region; V-region, light grey; insertions, red; diversity (D)-region, black; and J-region dark grey). The motif scores with chi-squared values greater than 90 were considered highly significant. Related to Figure 6.

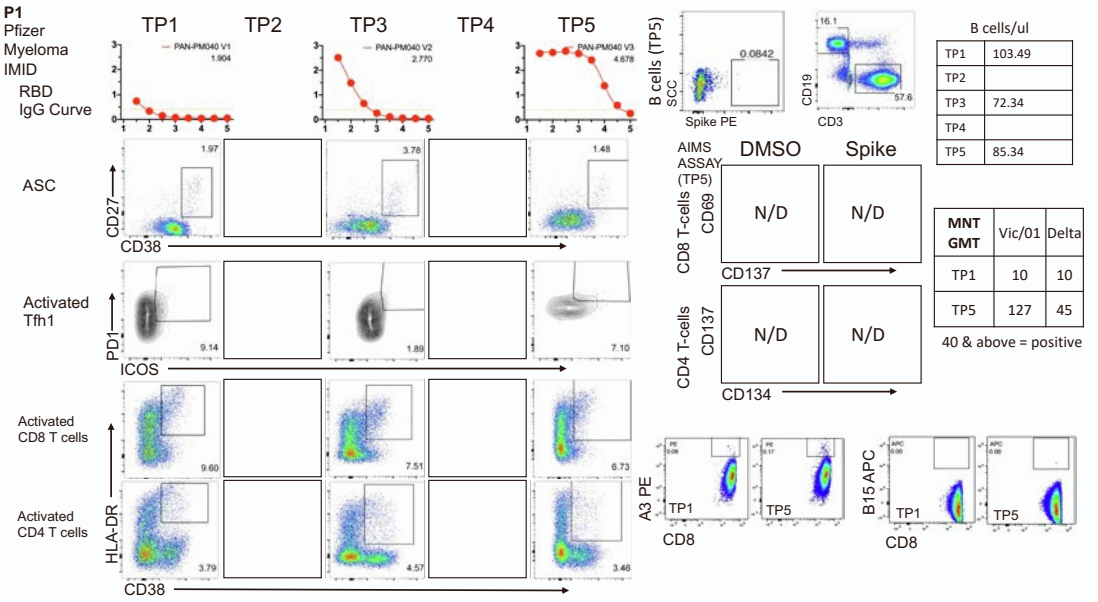
P1
Pfizer
Myeloma
IMID
RBD
IgG Curve
TP1
TP2
TP3
TP4
TP5
ASC
CD27
CD38
Activated
Tfh1
PD1
ICOS
Activated
CD8 T cells
Activated
CD4 T cells
HLA-DR
B cells (TP5)
SCC
Spike PE
CD19
CD3
AIMS
ASSAY
(TP5)
DMSO
Spike
CD8 T-cells
CD69
CD137
CD4 T-cells
N/D
CD134
A3 PE
B15 APC
CD8
B cells/ul
TP1 103.49
TP2
TP3 72.34
TP4
TP5 85.34
MNT GMT | Vic/01 | Delta
TP1 | 10 | 10
TP5 | 127 | 45
40 & above = positive

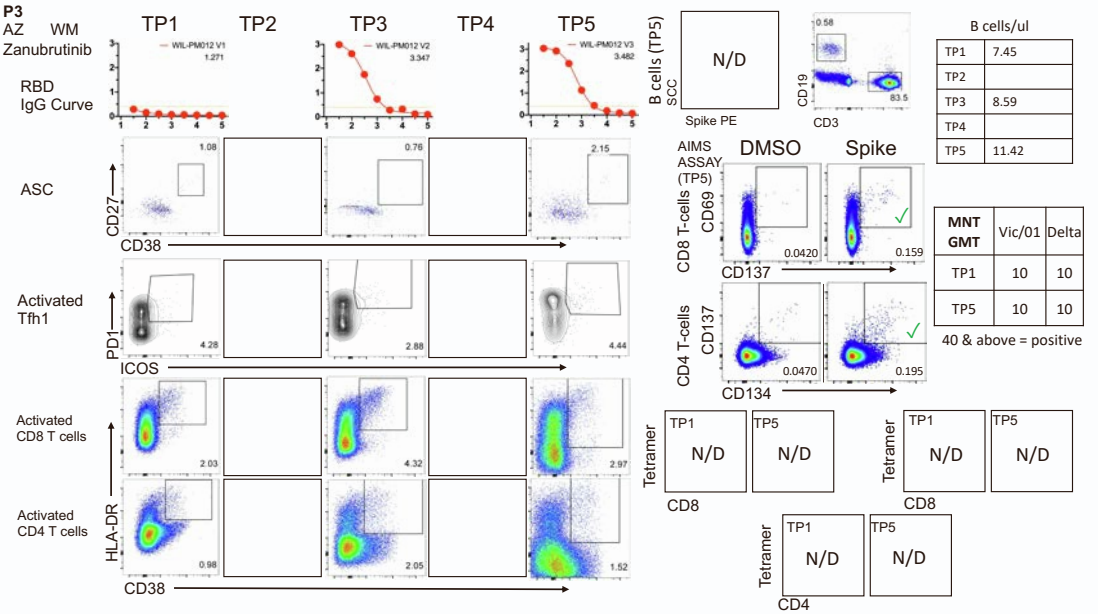
P3
AZ WM
Zanubrutinib
RBD
IgG Curve
TP1
TP2
TP3
TP4
TP5
ASC
CD27
CD38
Activated
Tfh1
PD1
ICOS
Activated
CD8 T cells
Activated
CD4 T cells
HLA-DR
B cells (TP5)
SCC
Spike PE
CD19
CD3
AIMS
ASSAY
(TP5)
DMSO
Spike
CD8 T-cells
CD69
CD137
CD4 T-cells
CD134
Tetramer
CD8
CD4
B cells/ul
TP1 7.45
TP2
TP3 8.59
TP4
TP5 11.42
MNT GMT | Vic/01 | Delta
TP1 | 10 | 10
TP5 | 10 | 10
40 & above = positive

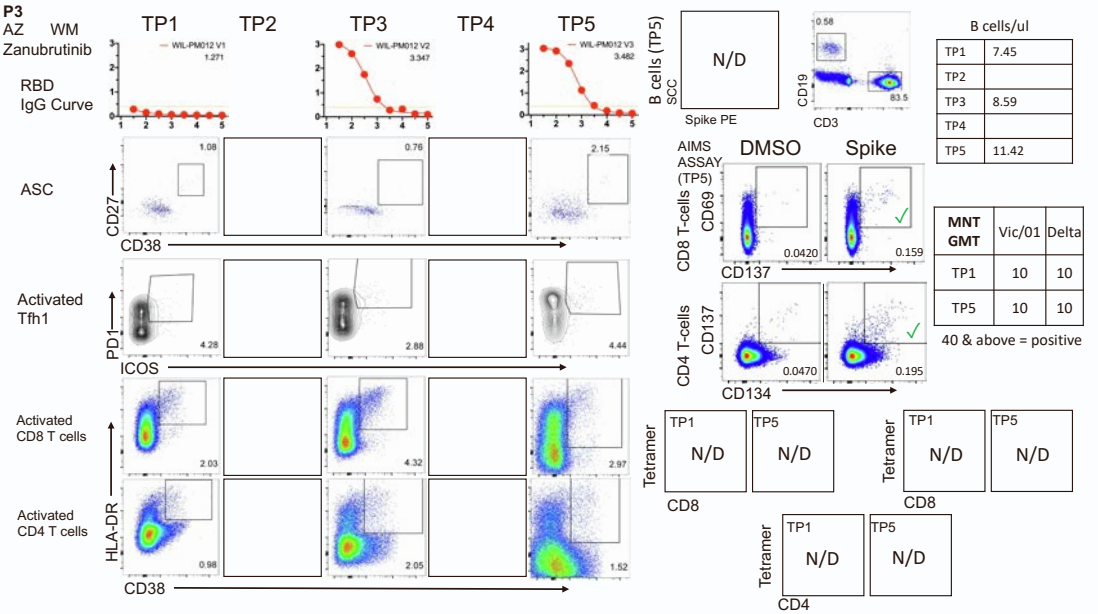
P3
AZ WM
Zanubrutinib
RBD
IgG Curve
TP1
TP2
TP3
TP4
TP5
ASC
CD27
CD38
Activated
Tfh1
PD1
ICOS
Activated
CD8 T cells
Activated
CD4 T cells
HLA-DR
B cells (TP5)
SCC
Spike PE
CD19
CD3
AIMS
ASSAY
(TP5)
DMSO
Spike
CD8 T-cells
CD69
CD137
CD4 T-cells
CD134
Tetramer
CD8
CD4
B cells/ul
TP1 7.45
TP2
TP3 8.59
TP4
TP5 11.42
MNT GMT | Vic/01 | Delta
TP1 | 10 | 10
TP5 | 10 | 10
40 & above = positive

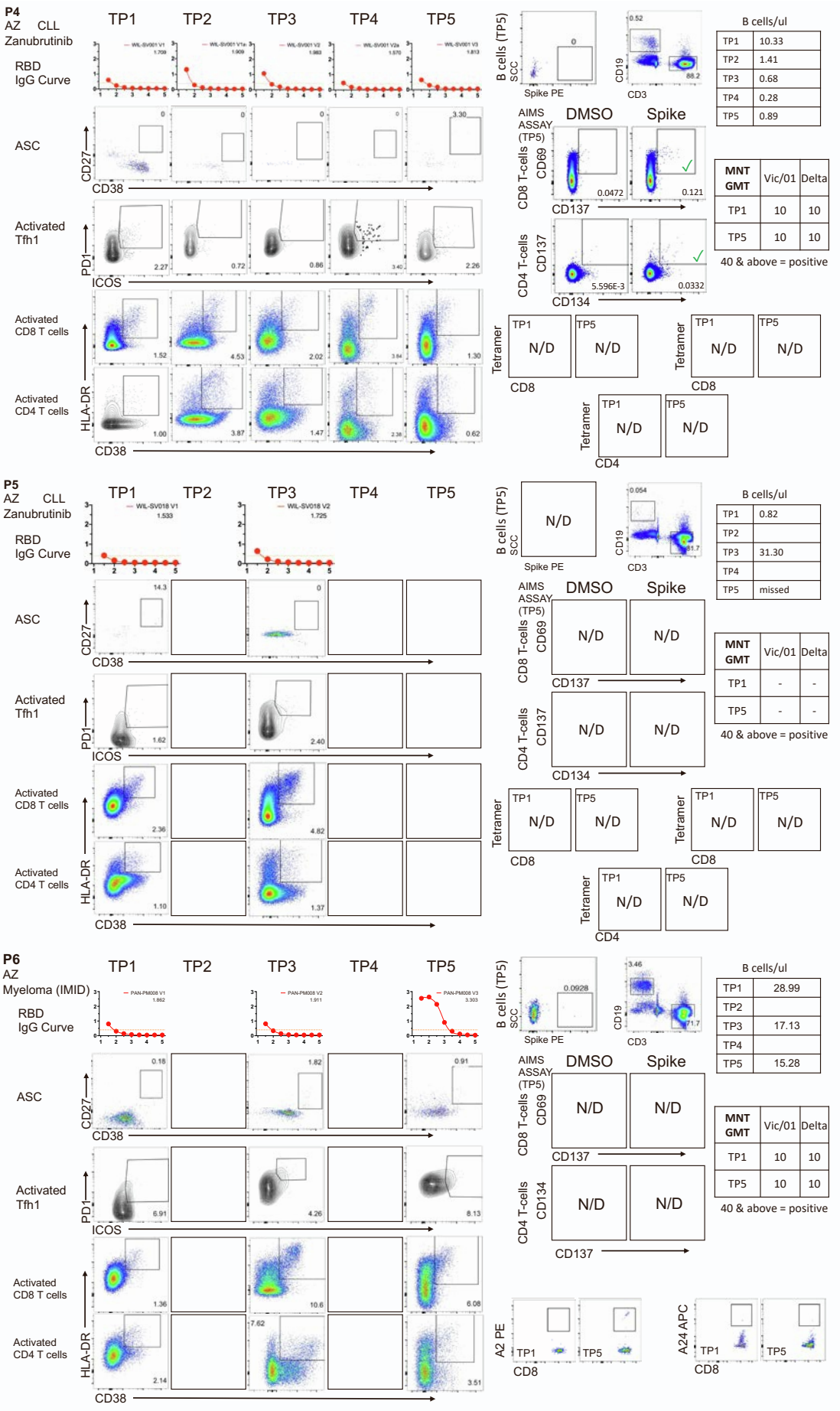
P4
AZ CLL
Zanubrutinib
TP1 TP2 TP3 TP4 TP5
RBD IgG Curve
ASC
CD27
CD38
Activated Tfh1
PD1
ICOS
Activated CD8 T cells
Activated CD4 T cells
HLA-DR
B cells (TP5)
SCC
Spike PE
CD19
CD3
B cells/ul
TP1 10.33
TP2 1.41
TP3 0.68
TP4 0.28
TP5 0.89
AIMS ASSAY (TP5)
DMSO
Spike
CD8 T-cells CD69
CD137
0.0472
0.121
CD4 T-cells CD137
CD134
5.596E-3
0.0332
MNT GMT | Vic/01 | Delta
TP1 | 10 | 10
TP5 | 10 | 10
40 & above = positive
Tetramer
TP1 N/D TP5 N/D
CD8
CD4
P5
AZ CLL
Zanubrutinib
TP1 TP2 TP3 TP4 TP5
RBD IgG Curve
B cells/ul
TP1 0.82
TP2
TP3 31.30
TP4
TP5 missed
N/D
MNT GMT | Vic/01 | Delta
TP1 | - | -
TP5 | - | -
40 & above = positive
P6
AZ
Myeloma (IMID)
TP1 TP2 TP3 TP4 TP5
RBD IgG Curve
B cells/ul
TP1 28.99
TP2
TP3 17.13
TP4
TP5 15.28
MNT GMT | Vic/01 | Delta
TP1 | 10 | 10
TP5 | 10 | 10
40 & above = positive
A2 PE
A24 APC
TP1
TP5
CD8

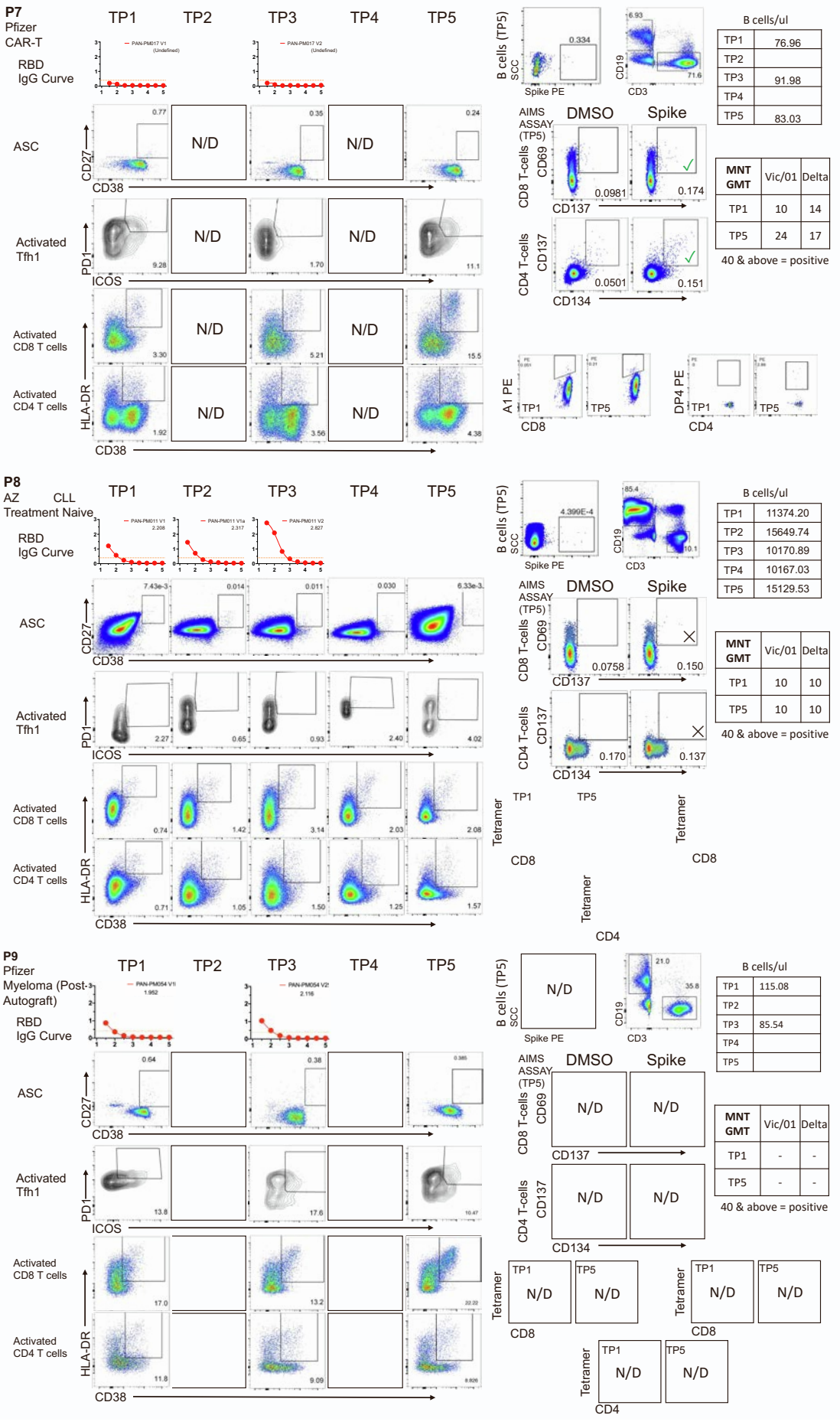
P7
Pfizer
CAR-T
TP1
TP2
TP3
TP4
TP5
RBD
IgG Curve
ASC
CD27
CD38
N/D
Activated
Tfh1
PD1
ICOS
Activated
CD8 T cells
Activated
CD4 T cells
HLA-DR
CD38
B cells (TP5)
SCC
Spike PE
CD19
CD3
B cells/ul
TP1 76.96
TP2
TP3 91.98
TP4
TP5 83.03
AIMS
ASSAY
(TP5)
DMSO
Spike
CD8 T-cells
CD69
CD137
CD4 T-cells
CD134
MNT GMT | Vic/01 | Delta
TP1 | 10 | 14
TP5 | 24 | 17
40 & above = positive
A1 PE
DP4 PE
CD8
CD4
P8
AZ CLL
Treatment Naive
TP1 TP2 TP3 TP4 TP5
RBD
IgG Curve
ASC
CD27
CD38
Activated
Tfh1
PD1
ICOS
Activated
CD8 T cells
Activated
CD4 T cells
HLA-DR
CD38
B cells (TP5)
SCC
Spike PE
CD19
CD3
B cells/ul
TP1 11374.20
TP2 15649.74
TP3 10170.89
TP4 10167.03
TP5 15129.53
AIMS
ASSAY
(TP5)
DMSO
Spike
CD8 T-cells
CD69
CD137
CD4 T-cells
CD134
MNT GMT | Vic/01 | Delta
TP1 | 10 | 10
TP5 | 10 | 10
40 & above = positive
TP1
TP5
Tetramer
CD8
CD4
P9
Pfizer
Myeloma (Post-Autograft)
TP1 TP2 TP3 TP4 TP5
RBD
IgG Curve
ASC
CD27
CD38
Activated
Tfh1
PD1
ICOS
Activated
CD8 T cells
Activated
CD4 T cells
HLA-DR
CD38
B cells (TP5)
SCC
Spike PE
CD19
CD3
N/D
B cells/ul
TP1 115.08
TP2
TP3 85.54
TP4
TP5
AIMS
ASSAY
(TP5)
DMSO
Spike
CD8 T-cells
CD69
CD137
CD4 T-cells
CD134
MNT GMT | Vic/01 | Delta
TP1 | - | -
TP5 | - | -
40 & above = positive
TP1
TP5
Tetramer
CD8
CD4

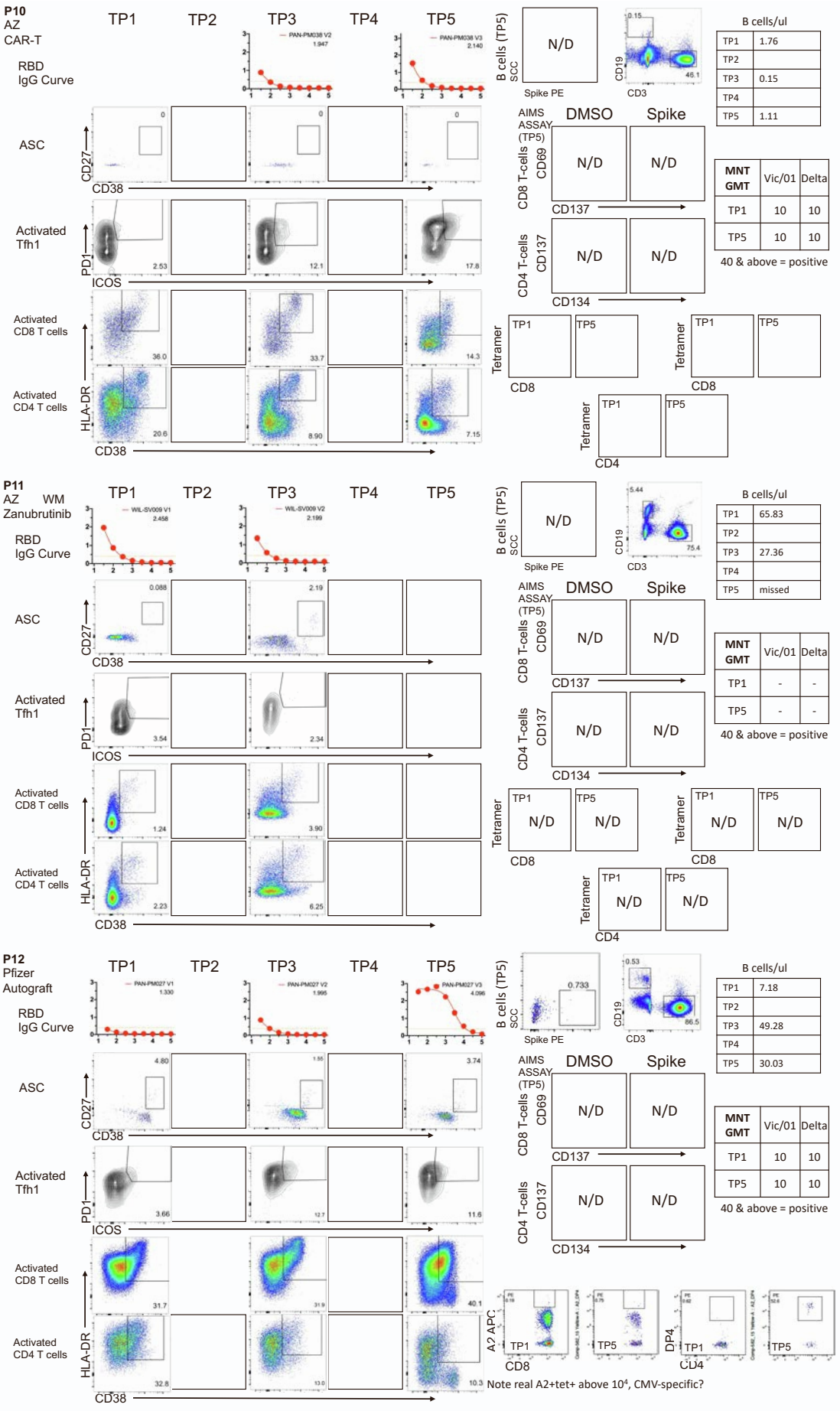
P10
AZ
CAR-T
TP1
TP2
TP3
TP4
TP5
RBD
IgG Curve
ASC
CD27
CD38
Activated
Tfh1
PD1
ICOS
Activated
CD8 T cells
Activated
CD4 T cells
HLA-DR
B cells (TP5)
SCC
Spike PE
CD19
CD3
N/D
B cells/ul
TP1 1.76
TP2
TP3 0.15
TP4
TP5 1.11
AIMS
ASSAY
(TP5)
DMSO
Spike
CD8 T-cells
CD69
CD137
CD4 T-cells
CD134
MNT GMT | Vic/01 | Delta
TP1 | 10 | 10
TP5 | 10 | 10
40 & above = positive
Tetramer
CD8
CD4
P11
AZ WM
Zanubrutinib
B cells/ul
TP1 65.83
TP2
TP3 27.36
TP4
TP5 missed
MNT GMT | Vic/01 | Delta
TP1 | - | -
TP5 | - | -
40 & above = positive
P12
Pfizer
Autograft
B cells/ul
TP1 7.18
TP2
TP3 49.28
TP4
TP5 30.03
MNT GMT | Vic/01 | Delta
TP1 | 10 | 10
TP5 | 10 | 10
40 & above = positive
A2 APC
DP4
Note real A2+tet+ above 10⁴, CMV-specific?

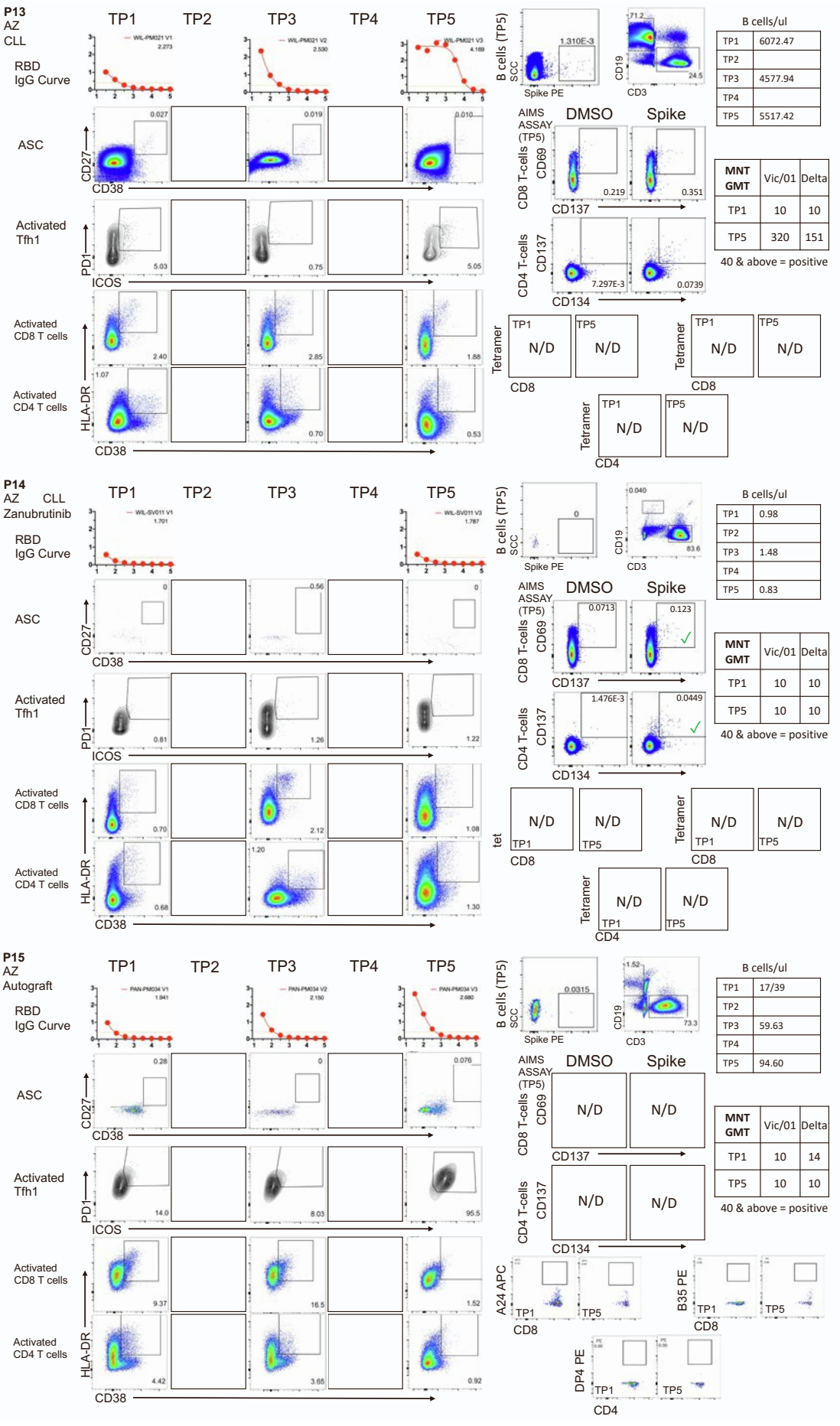
P13
AZ
CLL
RBD IgG Curve
TP1
TP2
TP3
TP4
TP5
ASC
CD27
CD38
Activated Tfh1
PD1
ICOS
Activated CD8 T cells
Activated CD4 T cells
HLA-DR
B cells (TP5)
SCC
Spike PE
CD19
CD3
B cells/ul
TP1 6072.47
TP2
TP3 4577.94
TP4
TP5 5517.42
AIMS ASSAY (TP5)
DMSO
Spike
CD8 T-cells CD69
CD137
CD4 T-cells CD137
CD134
MNT GMT | Vic/01 | Delta
TP1 | 10 | 10
TP5 | 320 | 151
40 & above = positive
Tetramer
CD8
CD4
N/D
P14
AZ CLL
Zanubrutinib
TP1 0.98
TP3 1.48
TP5 0.83
TP1 | 10 | 10
TP5 | 10 | 10
P15
AZ
Autograft
TP1 17/39
TP3 59.63
TP5 94.60
TP1 | 10 | 14
TP5 | 10 | 10
A24 APC
B35 PE
DP4 PE

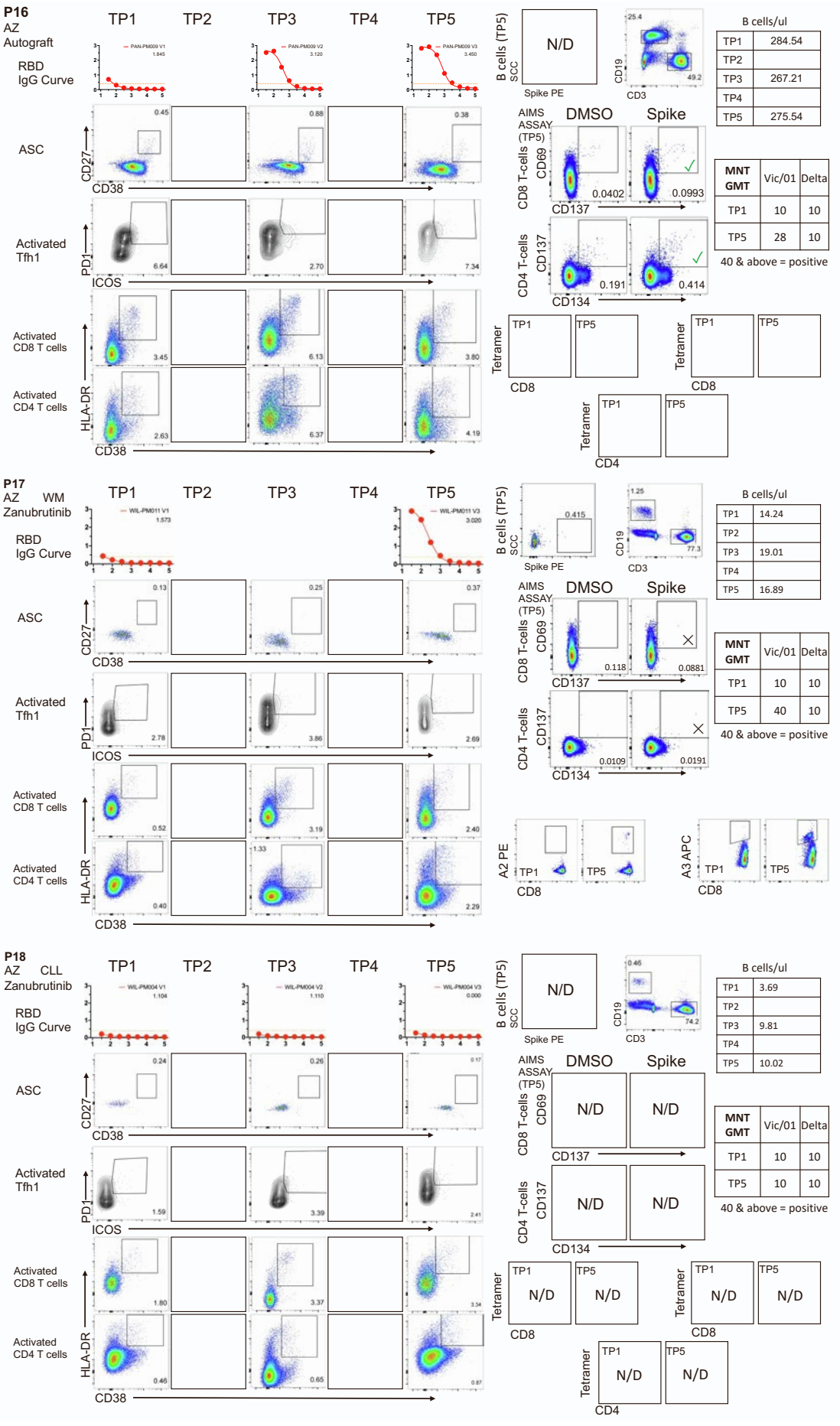
P16
AZ
Autograft
TP1
TP2
TP3
TP4
TP5
RBD
IgG Curve
ASC
CD27
CD38
Activated
Tfh1
PD1
ICOS
Activated
CD8 T cells
Activated
CD4 T cells
HLA-DR
CD38
B cells (TP5)
SCC
N/D
Spike PE
CD19
CD3
B cells/ul
TP1 284.54
TP2
TP3 267.21
TP4
TP5 275.54
AIMS
ASSAY
(TP5)
DMSO
Spike
CD8 T-cells
CD69
CD137
0.0402
0.0993
CD4 T-cells
CD137
CD134
0.191
0.414
MNT GMT | Vic/01 | Delta
TP1 | 10 | 10
TP5 | 28 | 10
40 & above = positive
Tetramer
TP1
TP5
CD8
CD4
P17
AZ WM
Zanubrutinib
0.415
1.25
77.3
14.24
19.01
16.89
0.118
0.0881
0.0109
0.0191
MNT GMT | Vic/01 | Delta
TP1 | 10 | 10
TP5 | 40 | 10
40 & above = positive
A2 PE
A3 APC
P18
AZ CLL
Zanubrutinib
0.46
74.2
3.69
9.81
10.02
MNT GMT | Vic/01 | Delta
TP1 | 10 | 10
TP5 | 10 | 10
40 & above = positive

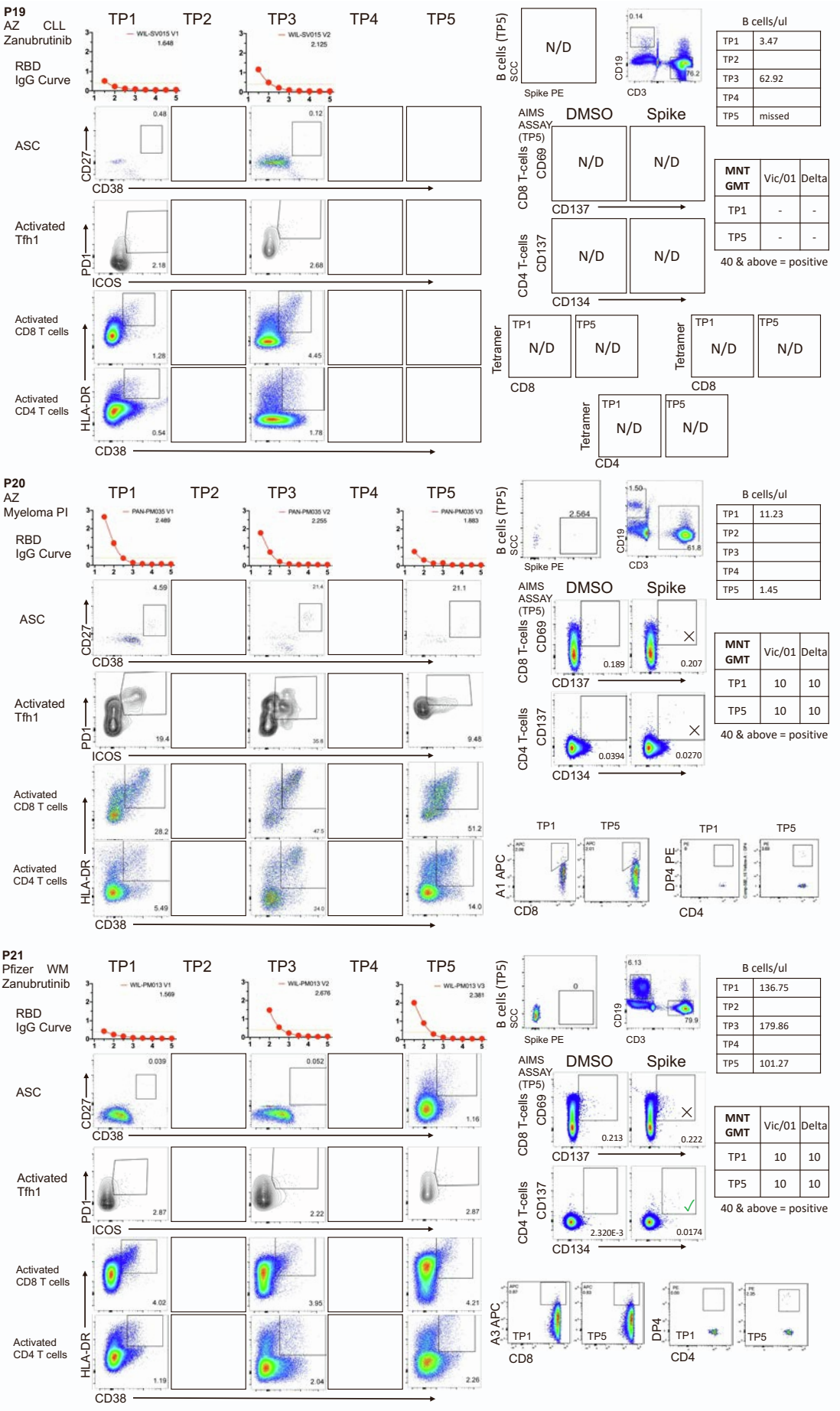
P19
AZ CLL
Zanubrutinib
TP1 TP2 TP3 TP4 TP5
RBD IgG Curve
ASC
CD27
CD38
Activated Tfh1
PD1
ICOS
Activated CD8 T cells
Activated CD4 T cells
HLA-DR
CD38
B cells (TP5)
SCC
Spike PE
CD19
CD3
N/D
AIMS ASSAY (TP5)
DMSO
Spike
CD8 T-cells CD69
CD137
CD4 T-cells CD137
CD134
Tetramer
CD8
CD4
B cells/ul
TP1 3.47
TP2
TP3 62.92
TP4
TP5 missed
MNT GMT | Vic/01 | Delta
TP1 - -
TP5 - -
40 & above = positive
P20
AZ
Myeloma PI
TP1 TP2 TP3 TP4 TP5
RBD IgG Curve
ASC
Activated Tfh1
Activated CD8 T cells
Activated CD4 T cells
CD38
B cells (TP5)
SCC
Spike PE
CD19
CD3
2.564
AIMS ASSAY (TP5)
DMSO
Spike
CD8 T-cells CD69
0.189
0.207
CD137
CD4 T-cells CD137
0.0394
0.0270
CD134
B cells/ul
TP1 11.23
TP2
TP3
TP4
TP5 1.45
MNT GMT | Vic/01 | Delta
TP1 10 10
TP5 10 10
40 & above = positive
A1 APC
DP4 PE
CD8
CD4
P21
Pfizer WM
Zanubrutinib
TP1 TP2 TP3 TP4 TP5
RBD IgG Curve
ASC
Activated Tfh1
Activated CD8 T cells
Activated CD4 T cells
CD38
B cells (TP5)
SCC
Spike PE
CD19
CD3
AIMS ASSAY (TP5)
DMSO
Spike
CD8 T-cells CD69
0.213
0.222
CD137
CD4 T-cells CD137
2.320E-3
0.0174
CD134
B cells/ul
TP1 136.75
TP2
TP3 179.86
TP4
TP5 101.27
MNT GMT | Vic/01 | Delta
TP1 10 10
TP5 10 10
40 & above = positive
A3 APC
DP4
CD8
CD4

P22
AZ
CLL

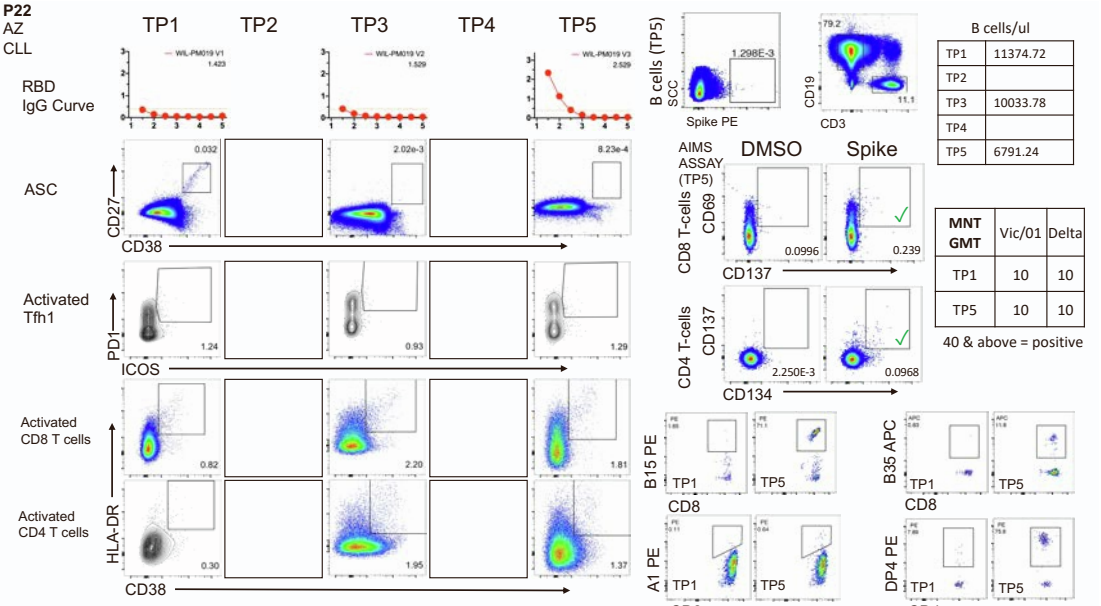

B cells/ul

TP1	11374.72
TP2	
TP3	10033.78
TP4	
TP5	6791.24

MNT GMT	Vic/01	Delta
TP1	10	10
TP5	10	10

40 & above = positive

P23
AZ CLL
Venetoclax

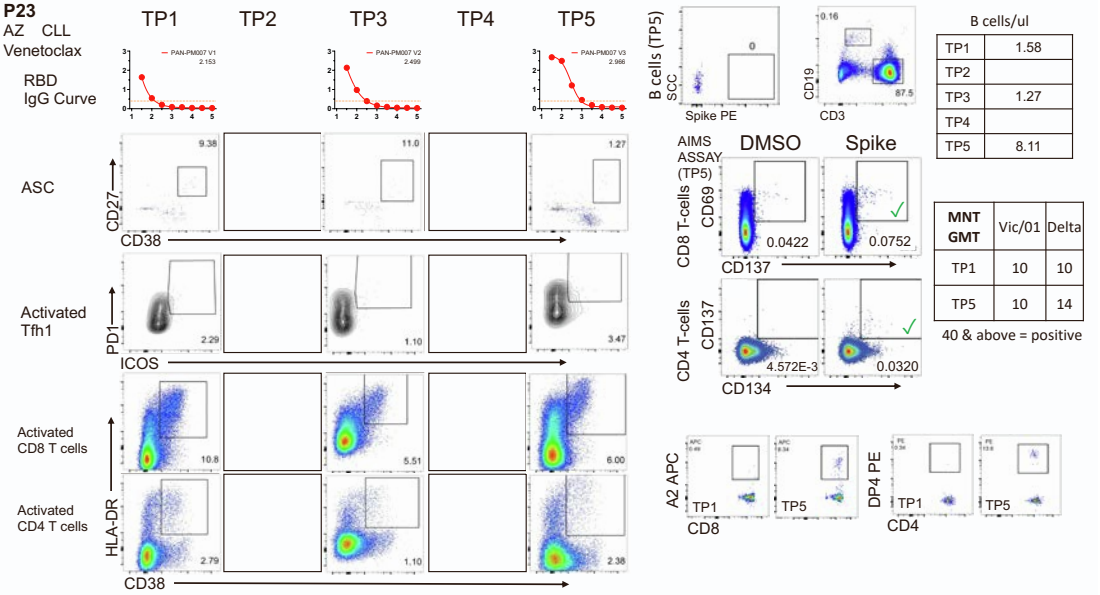

B cells/ul

TP1	1.58
TP2	
TP3	1.27
TP4	
TP5	8.11

MNT GMT	Vic/01	Delta
TP1	10	10
TP5	10	14

40 & above = positive

P24
Pfizer
CAR-T

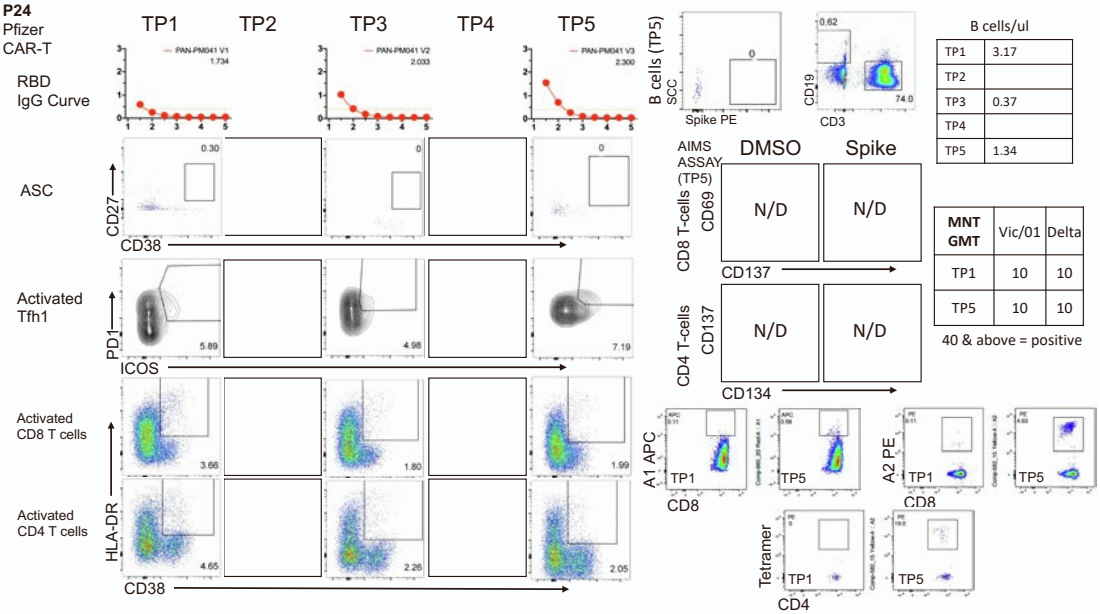

B cells/ul

TP1	3.17
TP2	
TP3	0.37
TP4	
TP5	1.34

MNT GMT	Vic/01	Delta
TP1	10	10
TP5	10	10

40 & above = positive

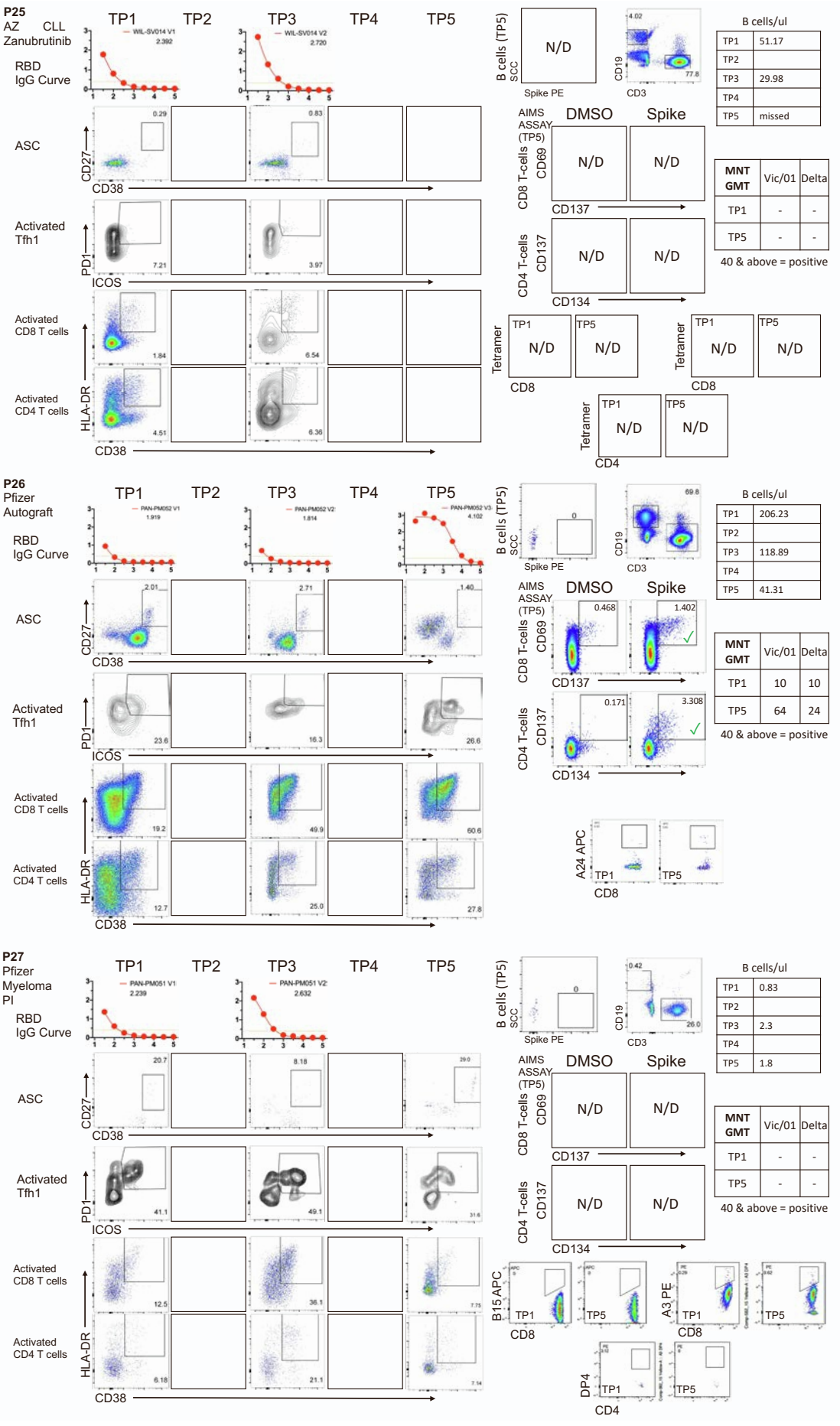
P25
AZ CLL
Zanubrutinib
RBD IgG Curve
ASC
Activated Tfh1
Activated CD8 T cells
Activated CD4 T cells
TP1 TP2 TP3 TP4 TP5
CD27
CD38
PD1
ICOS
HLA-DR
B cells (TP5)
SCC
Spike PE
CD19
CD3
N/D
B cells/ul
TP1 51.17
TP2
TP3 29.98
TP4
TP5 missed
AIMS ASSAY (TP5)
DMSO
Spike
CD8 T-cells CD69
CD137
CD4 T-cells CD137
CD134
MNT GMT | Vic/01 | Delta
TP1 - -
TP5 - -
40 & above = positive
Tetramer
CD8
CD4
P26
Pfizer
Autograft
RBD IgG Curve
ASC
Activated Tfh1
Activated CD8 T cells
Activated CD4 T cells
B cells/ul
TP1 206.23
TP2
TP3 118.89
TP4
TP5 41.31
0.468
1.402
0.171
3.308
MNT GMT | Vic/01 | Delta
TP1 10 10
TP5 64 24
40 & above = positive
A24 APC
P27
Pfizer
Myeloma
PI
RBD IgG Curve
ASC
Activated Tfh1
Activated CD8 T cells
Activated CD4 T cells
B cells/ul
TP1 0.83
TP2
TP3 2.3
TP4
TP5 1.8
MNT GMT | Vic/01 | Delta
TP1 - -
TP5 - -
40 & above = positive
B15 APC
A3 PE
DP4

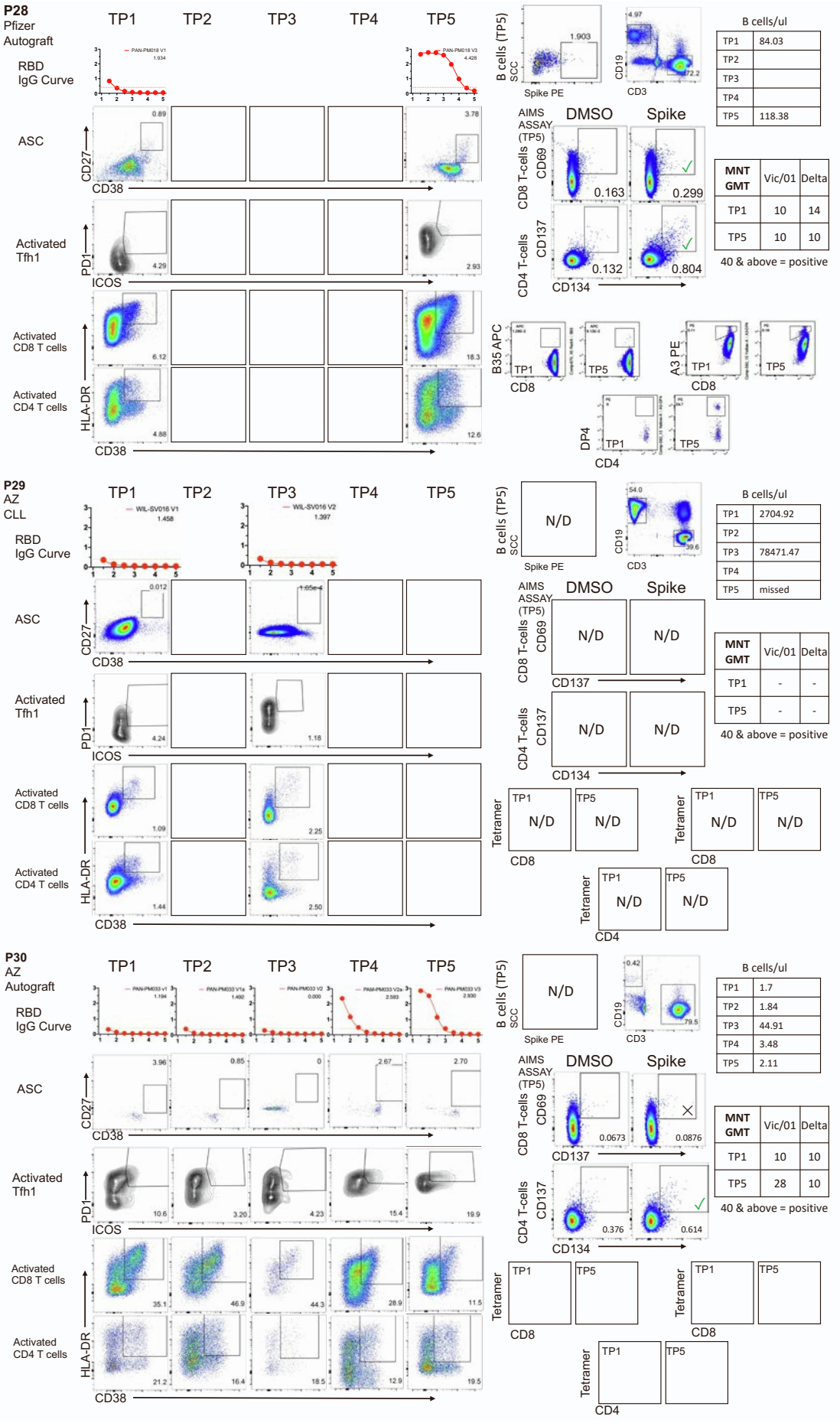
P28
Pfizer
Autograft
TP1
TP2
TP3
TP4
TP5
RBD
IgG Curve
ASC
CD27
CD38
Activated
Tfh1
PD1
ICOS
Activated
CD8 T cells
Activated
CD4 T cells
HLA-DR
B cells (TP5)
SCC
Spike PE
CD19
CD3
B cells/ul
TP1 84.03
TP2
TP3
TP4
TP5 118.38
AIMS
ASSAY
(TP5)
DMSO
Spike
CD8 T-cells
CD69
CD4 T-cells
CD137
CD134
MNT GMT Vic/01 Delta
TP1 10 14
TP5 10 10
40 & above = positive
B35 APC
A3 PE
CD8
DP4
CD4
P29
AZ
CLL
N/D
P30
AZ
Autograft
Tetramer

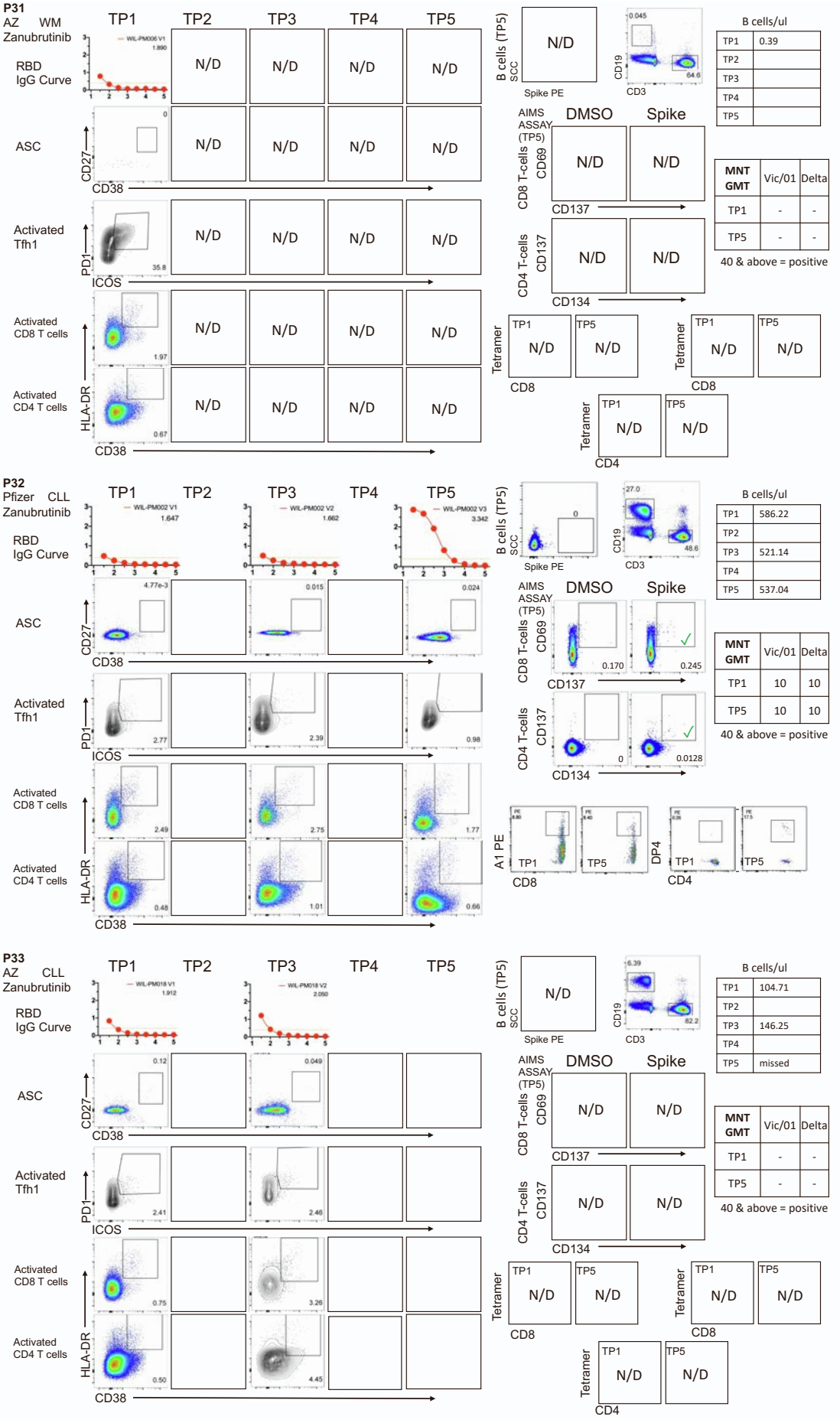
P31
AZ WM
Zanubrutinib
TP1 TP2 TP3 TP4 TP5
RBD IgG Curve
ASC
Activated Tfh1
Activated CD8 T cells
Activated CD4 T cells
CD27
CD38
PD1
ICOS
HLA-DR
N/D
B cells (TP5)
SCC
Spike PE
CD19
CD3
AIMS ASSAY (TP5)
DMSO
Spike
CD8 T-cells CD69
CD137
CD4 T-cells CD137
CD134
Tetramer
CD8
CD4
B cells/ul
TP1 0.39
TP2
TP3
TP4
TP5
MNT GMT | Vic/01 | Delta
TP1 - -
TP5 - -
40 & above = positive
P32
Pfizer CLL
Zanubrutinib
WIL-PM002 V1 1.647
WIL-PM002 V2 1.662
WIL-PM002 V3 3.342
TP1 586.22
TP2
TP3 521.14
TP4
TP5 537.04
TP1 10 10
TP5 10 10
A1 PE
DP4
P33
AZ CLL
Zanubrutinib
WIL-PM018 V1 1.912
WIL-PM018 V2 2.050
TP1 104.71
TP2
TP3 146.25
TP4
TP5 missed

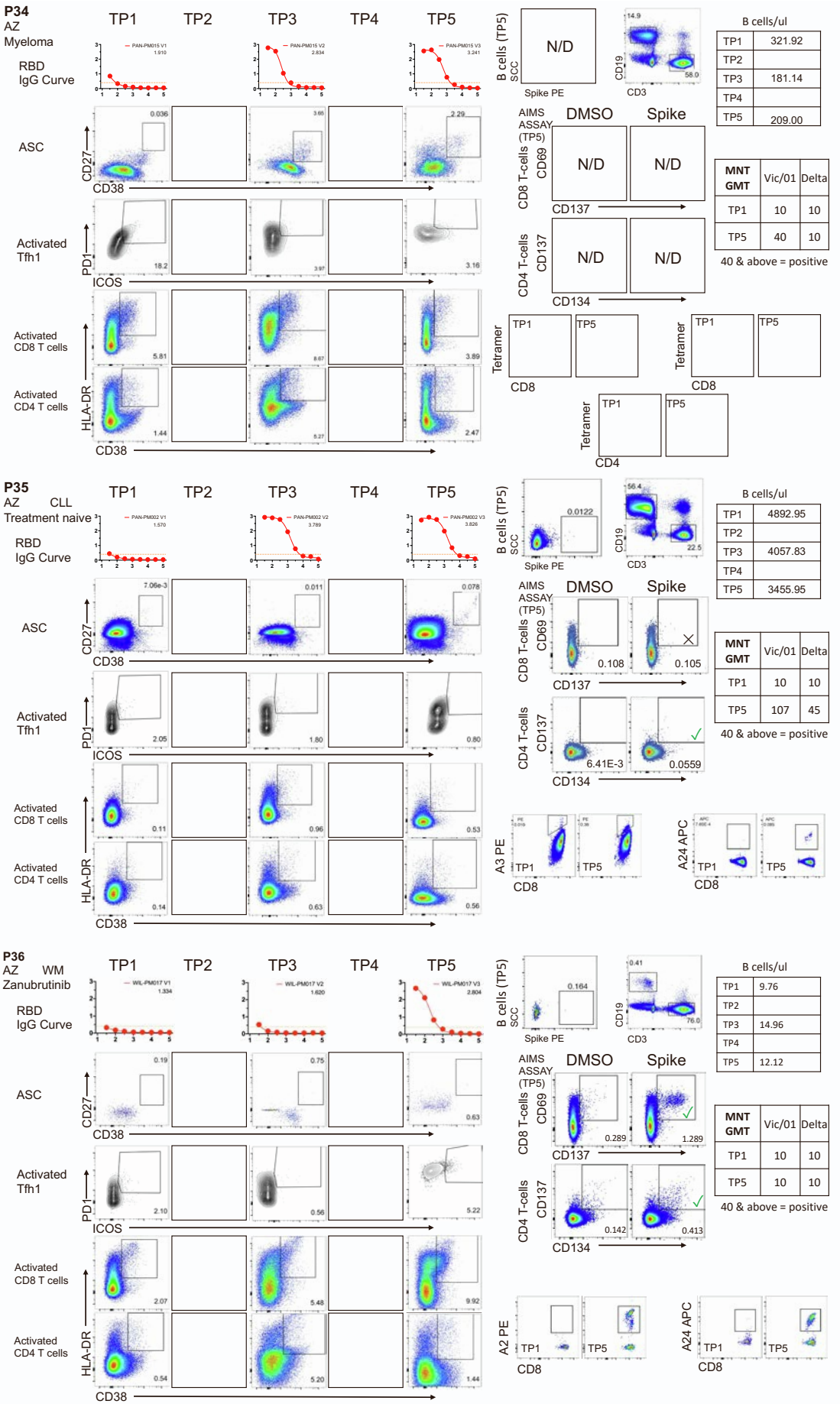
P34
AZ
Myeloma
TP1
TP2
TP3
TP4
TP5
RBD
IgG Curve
ASC
CD27
CD38
Activated
Tfh1
PD1
ICOS
Activated
CD8 T cells
Activated
CD4 T cells
HLA-DR
B cells (TP5)
SCC
Spike PE
CD19
CD3
N/D
AIMS
ASSAY
(TP5)
DMSO
Spike
CD8 T-cells
CD69
CD137
CD4 T-cells
CD134
Tetramer
CD8
CD4
B cells/ul
TP1 321.92
TP2
TP3 181.14
TP4
TP5 209.00
MNT GMT | Vic/01 | Delta
TP1 | 10 | 10
TP5 | 40 | 10
40 & above = positive
P35
AZ CLL
Treatment naive
B cells/ul
TP1 4892.95
TP2
TP3 4057.83
TP4
TP5 3455.95
MNT GMT | Vic/01 | Delta
TP1 | 10 | 10
TP5 | 107 | 45
40 & above = positive
A3 PE
A24 APC
P36
AZ WM
Zanubrutinib
B cells/ul
TP1 9.76
TP2
TP3 14.96
TP4
TP5 12.12
MNT GMT | Vic/01 | Delta
TP1 | 10 | 10
TP5 | 10 | 10
40 & above = positive
A2 PE
A24 APC

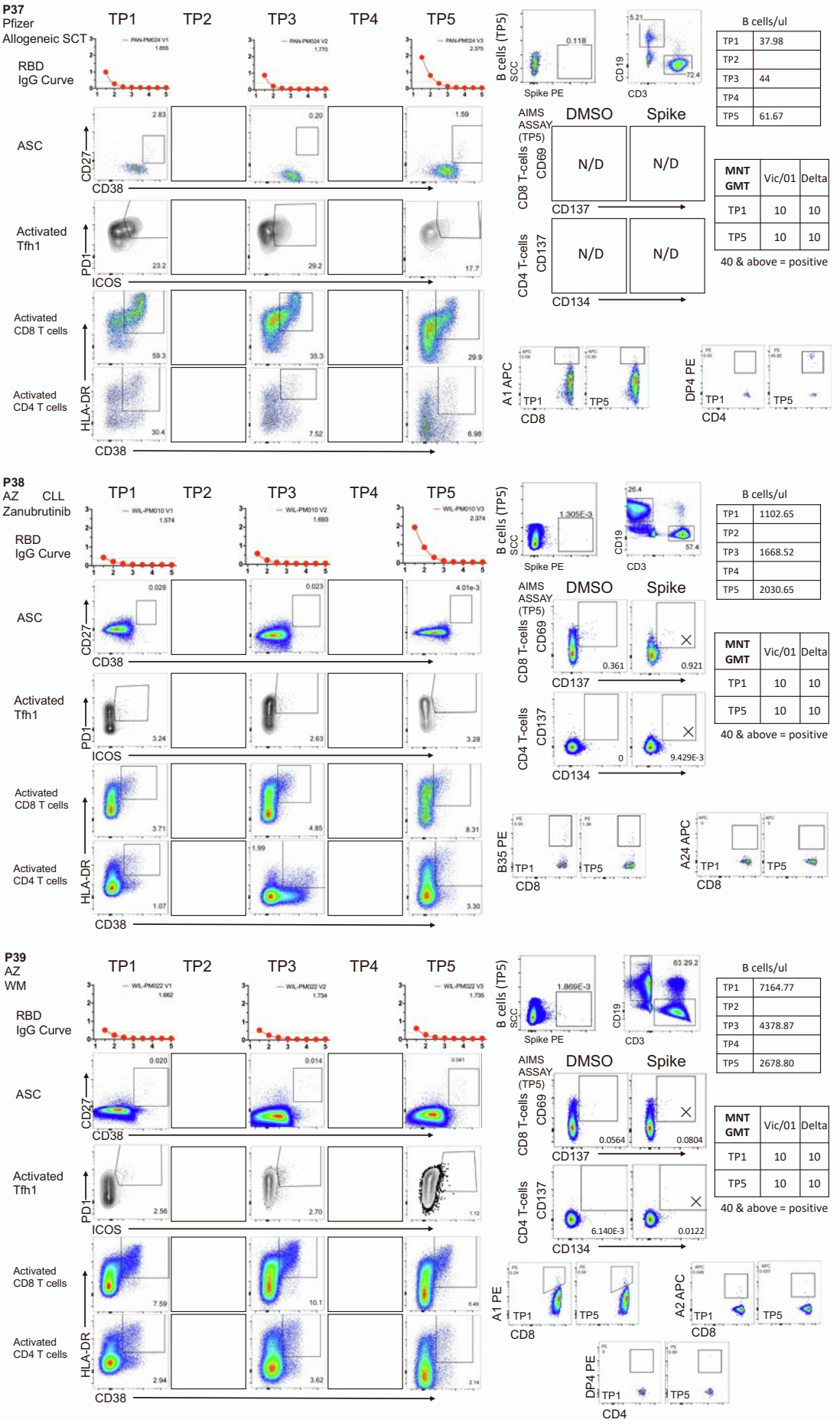
P37
Pfizer
Allogeneic SCT
TP1
TP2
TP3
TP4
TP5
RBD IgG Curve
ASC
CD27
CD38
Activated Tfh1
PD1
ICOS
Activated CD8 T cells
Activated CD4 T cells
HLA-DR
CD38
B cells (TP5)
SCC
Spike PE
CD19
CD3
AIMS ASSAY (TP5)
DMSO
Spike
CD8 T-cells
CD69
CD137
N/D
CD4 T-cells
CD134
A1 APC
DP4 PE
CD8
CD4
B cells/ul
TP1 37.98
TP2
TP3 44
TP4
TP5 61.67
MNT GMT | Vic/01 | Delta
TP1 10 10
TP5 10 10
40 & above = positive
P38
AZ CLL
Zanubrutinib
B cells/ul
TP1 1102.65
TP2
TP3 1668.52
TP4
TP5 2030.65
B35 PE
A24 APC
P39
AZ
WM
B cells/ul
TP1 7164.77
TP2
TP3 4378.87
TP4
TP5 2678.80
A1 PE
A2 APC

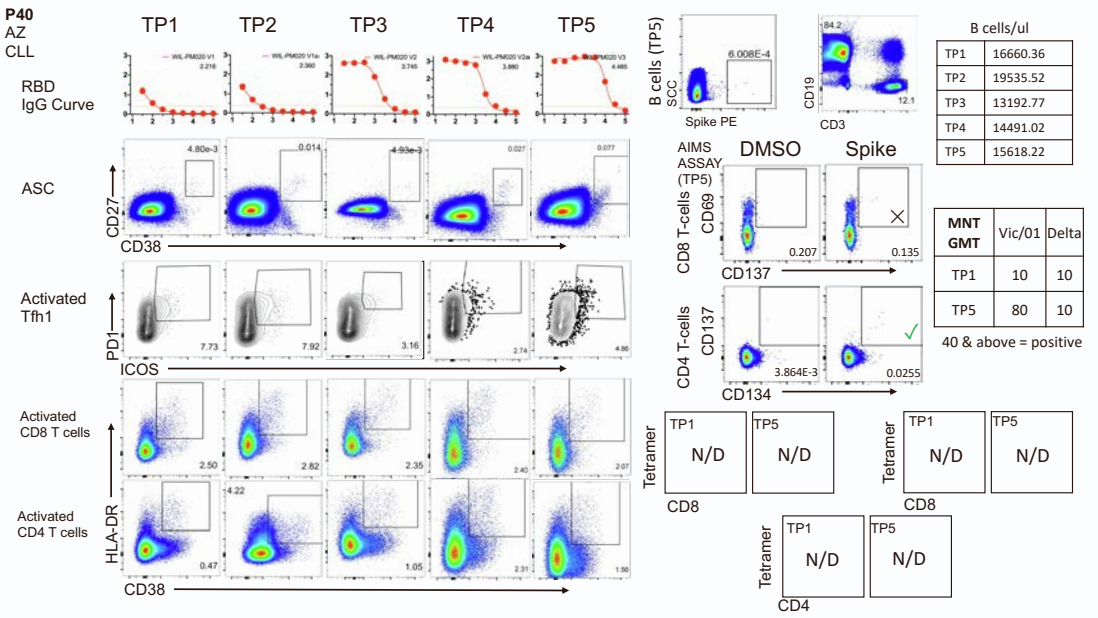

B cells/ul	
TP1	16660.36
TP2	19535.52
TP3	13192.77
TP4	14491.02
TP5	15618.22

MNT GMT	Vic/01	Delta
TP1	10	10
TP5	80	10

40 & above = positive

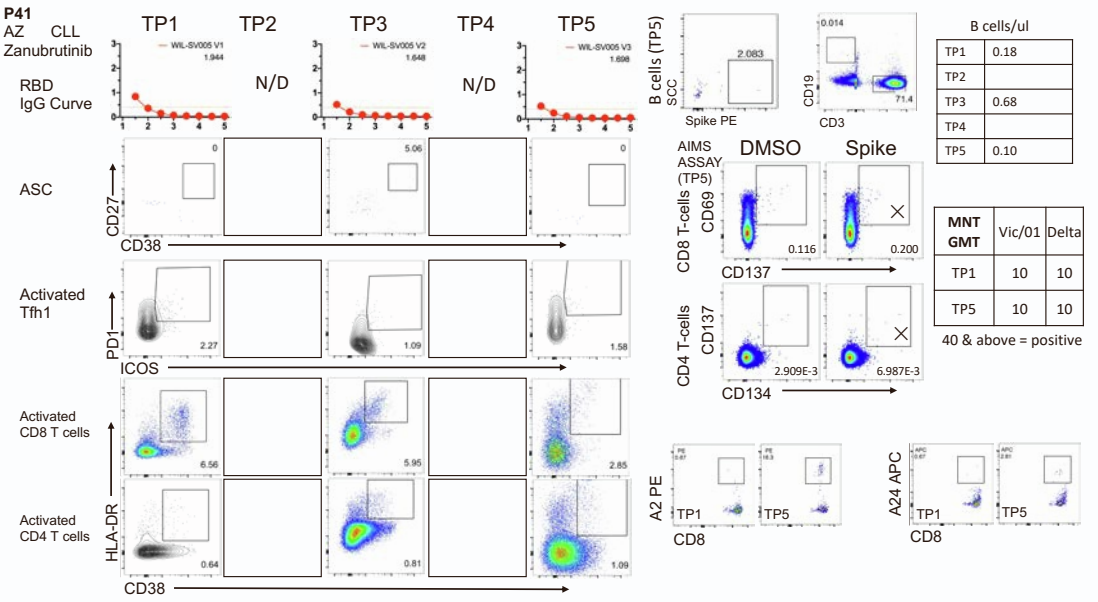

B cells/ul	
TP1	0.18
TP2	
TP3	0.68
TP4	
TP5	0.10

MNT GMT	Vic/01	Delta
TP1	10	10
TP5	10	10

40 & above = positive

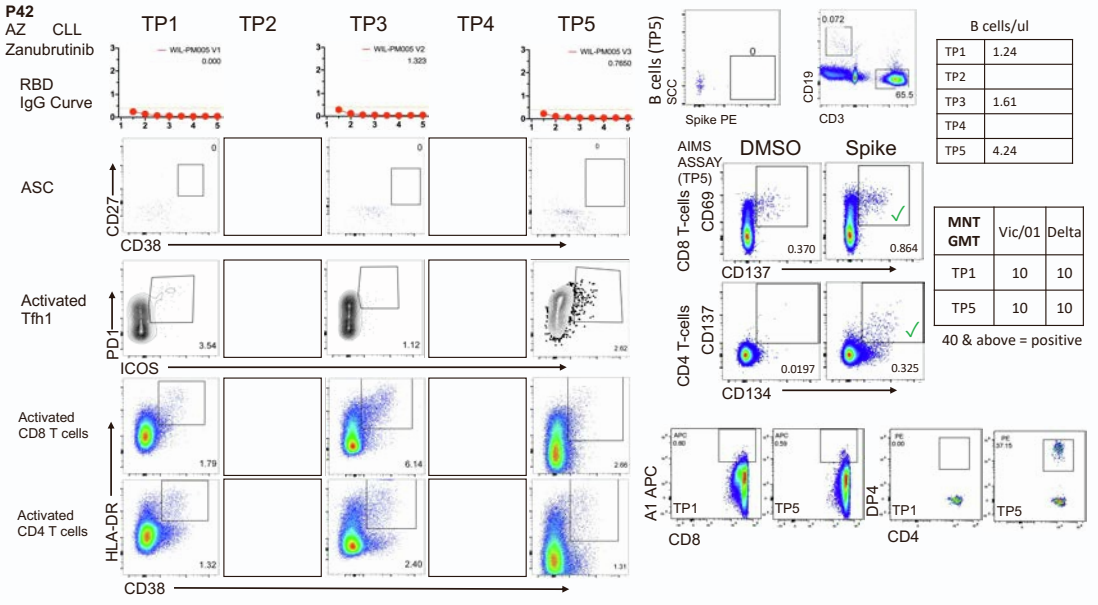

B cells/ul	
TP1	1.24
TP2	
TP3	1.61
TP4	
TP5	4.24

MNT GMT	Vic/01	Delta
TP1	10	10
TP5	10	10

40 & above = positive

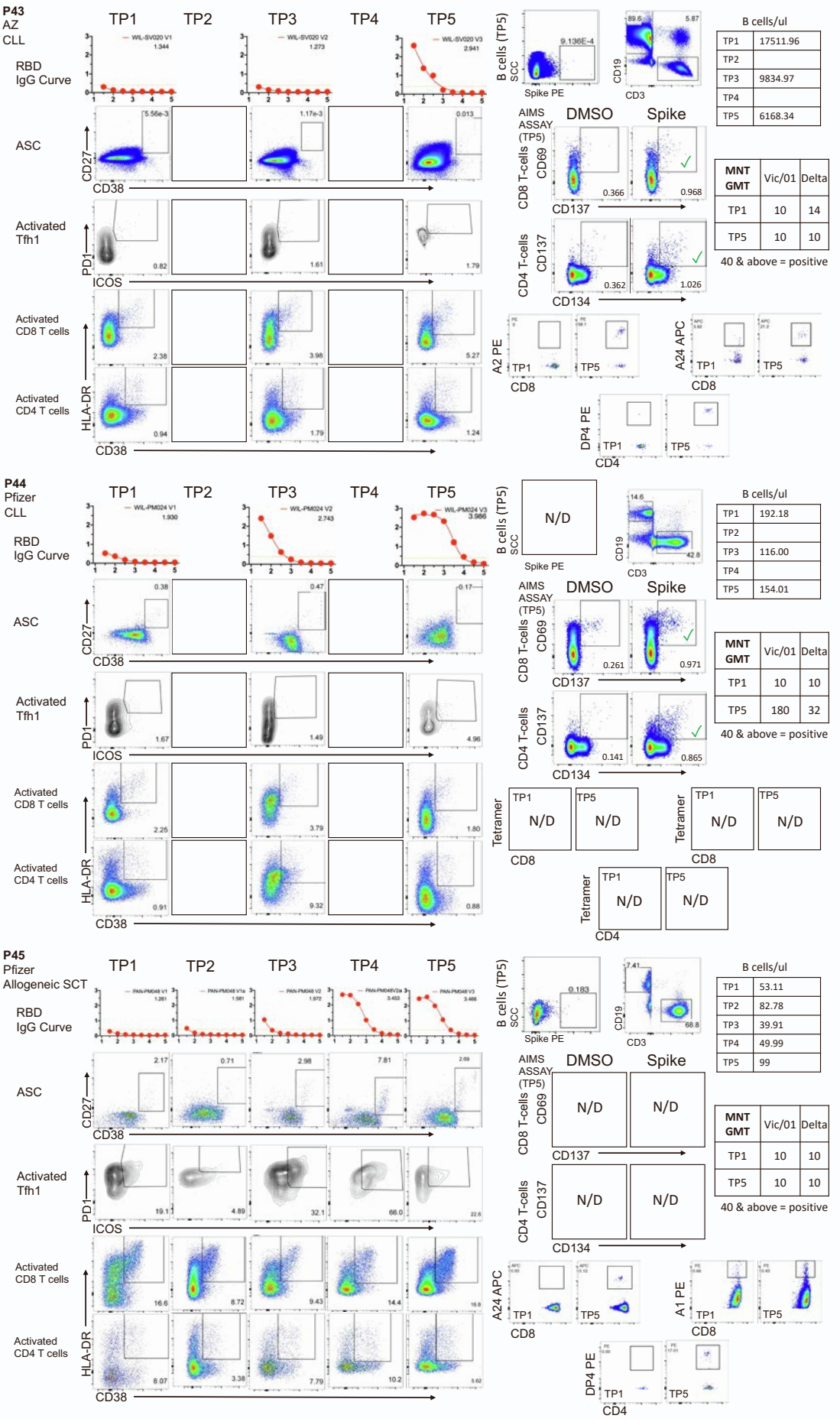
P43
AZ
CLL
RBD IgG Curve
ASC
Activated Tfh1
Activated CD8 T cells
Activated CD4 T cells
TP1
TP2
TP3
TP4
TP5
CD27
CD38
PD1
ICOS
HLA-DR
B cells (TP5)
SCC
Spike PE
CD19
CD3
AIMS ASSAY (TP5)
DMSO
Spike
CD8 T-cells
CD69
CD137
CD4 T-cells
CD134
A2 PE
A24 APC
CD8
DP4 PE
CD4
B cells/ul
TP1 17511.96
TP2
TP3 9834.97
TP4
TP5 6168.34
MNT GMT | Vic/01 | Delta
TP1 | 10 | 14
TP5 | 10 | 10
40 & above = positive
P44
Pfizer
CLL
N/D
TP1 192.18
TP2
TP3 116.00
TP4
TP5 154.01
TP1 | 10 | 10
TP5 | 180 | 32
Tetramer
P45
Pfizer
Allogeneic SCT
TP1 53.11
TP2 82.78
TP3 39.91
TP4 49.99
TP5 99
A1 PE
TP1 | 10 | 10
TP5 | 10 | 10

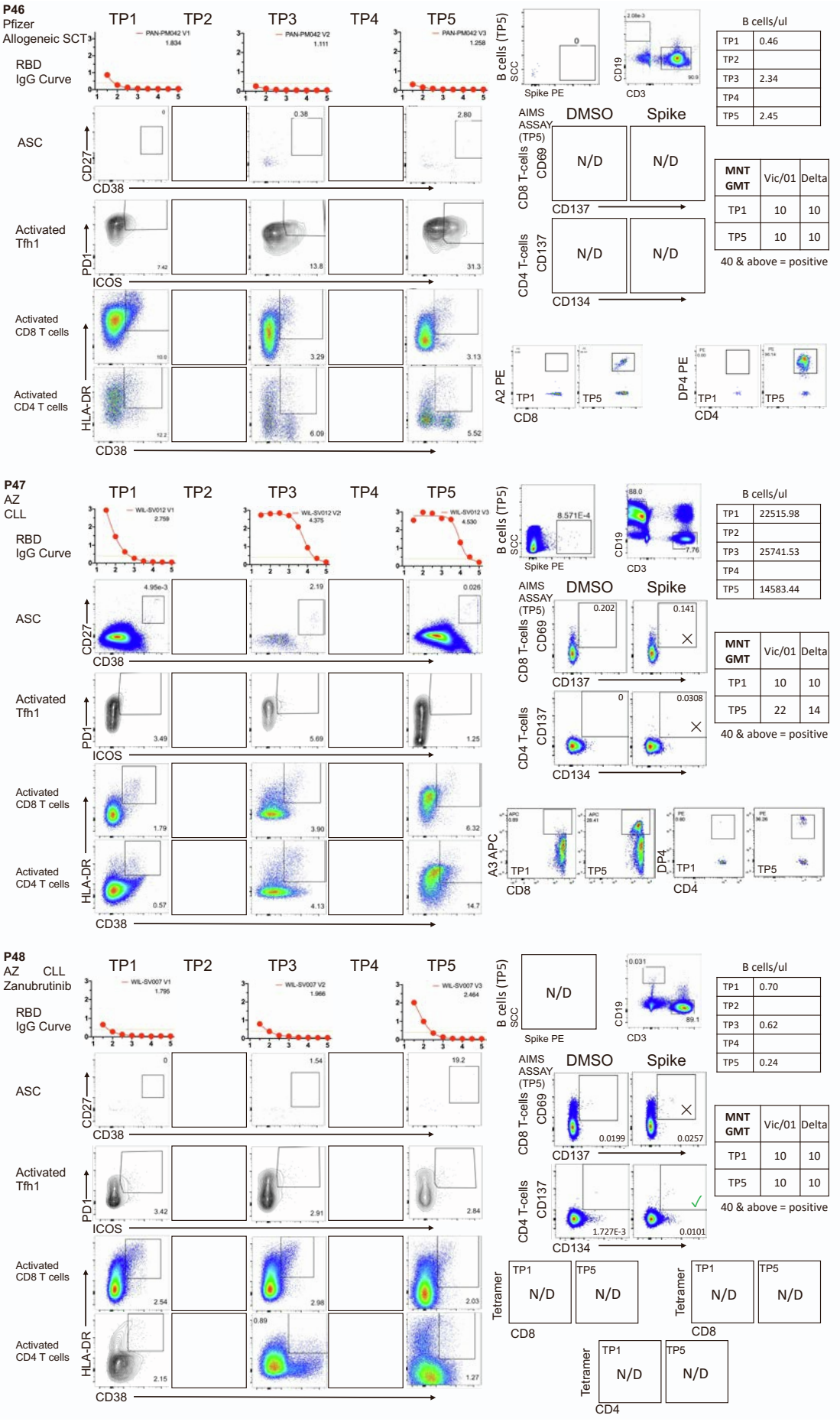
P46
Pfizer
Allogeneic SCT
TP1
TP2
TP3
TP4
TP5
RBD
IgG Curve
ASC
CD27
CD38
Activated
Tfh1
PD1
ICOS
Activated
CD8 T cells
Activated
CD4 T cells
HLA-DR
CD38
B cells (TP5)
SCC
Spike PE
CD19
CD3
AIMS
ASSAY
(TP5)
DMSO
Spike
CD8 T-cells
CD69
CD137
N/D
CD4 T-cells
CD134
B cells/ul
TP1 0.46
TP2
TP3 2.34
TP4
TP5 2.45
MNT GMT
Vic/01
Delta
TP1 10 10
TP5 10 10
40 & above = positive
A2 PE
CD8
DP4 PE
CD4
P47
AZ
CLL
0.571E-4
0.202
0.141
0.0308
TP1 22515.98
TP3 25741.53
TP5 14583.44
TP1 10 10
TP5 22 14
A3 APC
P48
AZ CLL
Zanubrutinib
TP1 0.70
TP3 0.62
TP5 0.24
0.0199
0.0257
1.727E-3
0.0101
Tetramer

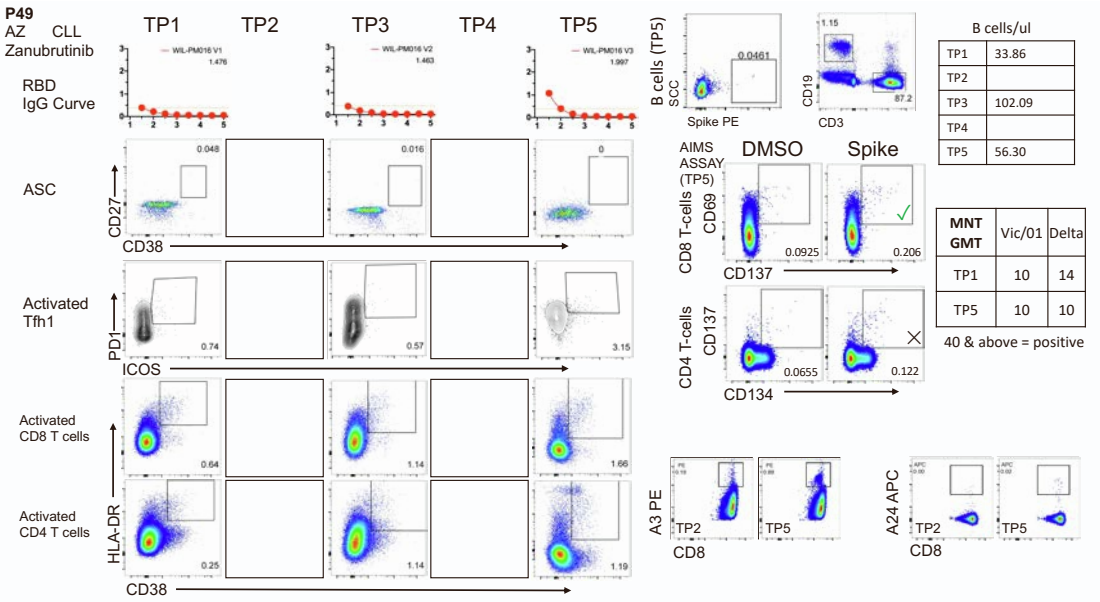

B cells/ul

TP1	33.86
TP2	
TP3	102.09
TP4	
TP5	56.30

MNT GMT	Vic/01	Delta
TP1	10	14
TP5	10	10

40 & above = positive

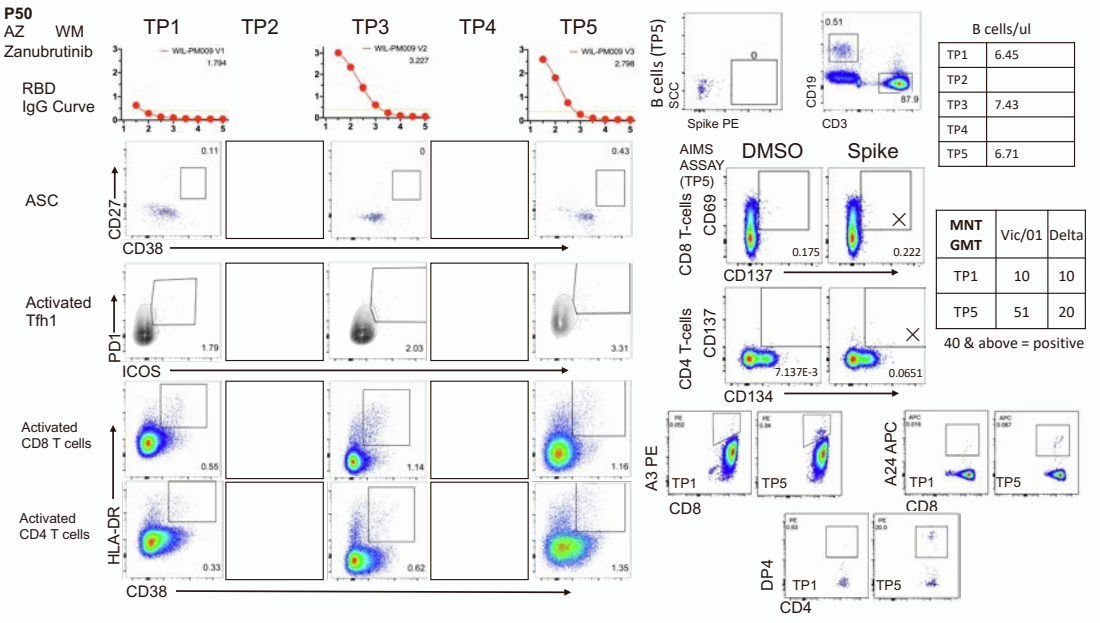

B cells/ul

TP1	6.45
TP2	
TP3	7.43
TP4	
TP5	6.71

MNT GMT	Vic/01	Delta
TP1	10	10
TP5	51	20

40 & above = positive

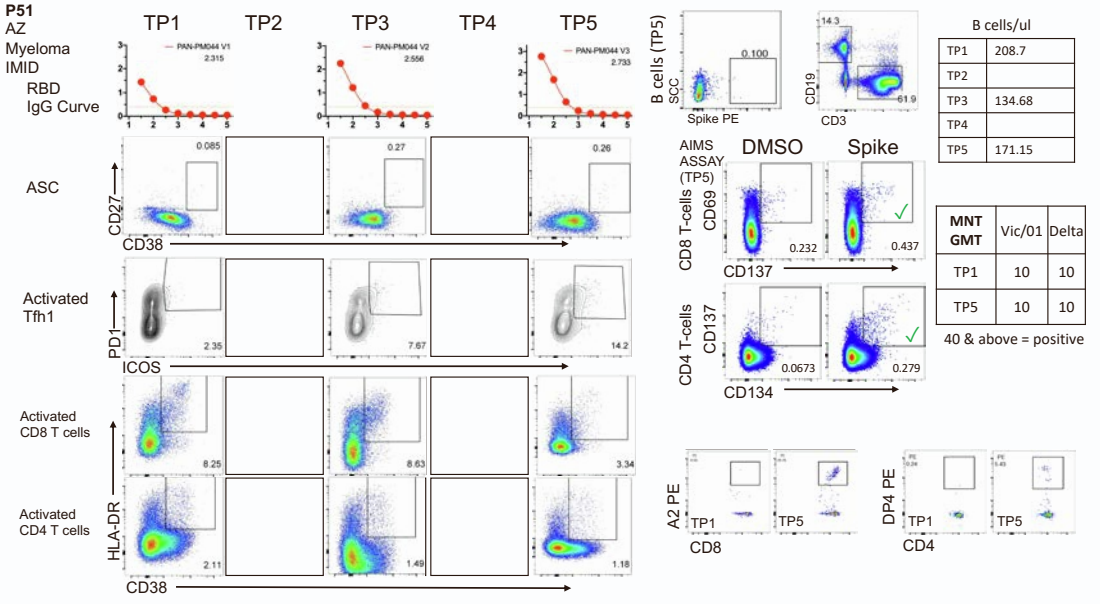

B cells/ul

TP1	208.7
TP2	
TP3	134.68
TP4	
TP5	171.15

MNT GMT	Vic/01	Delta
TP1	10	10
TP5	10	10

40 & above = positive

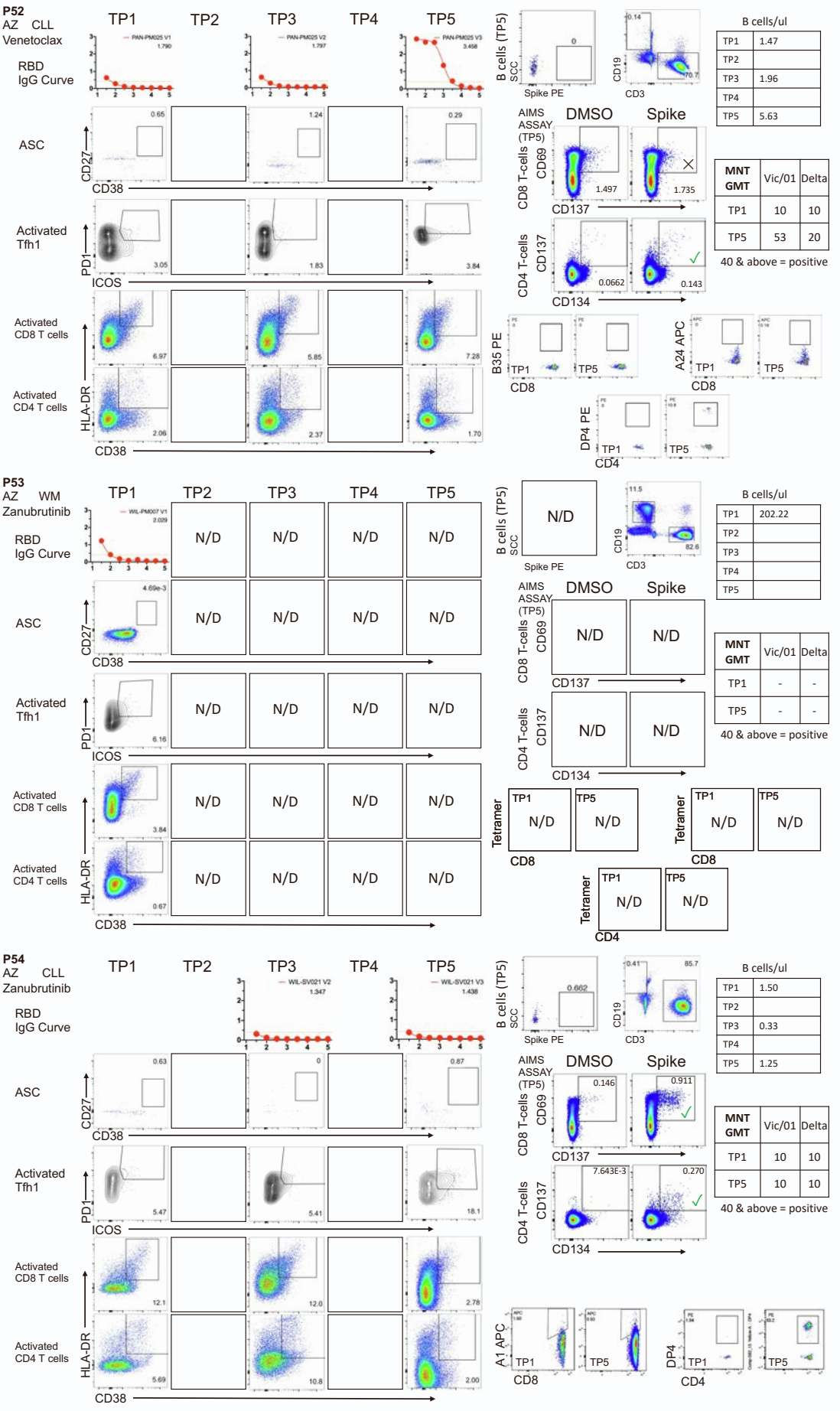
P52
AZ CLL
Venetoclax
TP1
TP2
TP3
TP4
TP5
RBD IgG Curve
ASC
CD27
CD38
Activated Tfh1
PD1
ICOS
Activated CD8 T cells
Activated CD4 T cells
HLA-DR
B cells (TP5)
SCC
Spike PE
CD19
CD3
B cells/ul
TP1 1.47
TP2
TP3 1.96
TP4
TP5 5.63
AIMS ASSAY (TP5)
DMSO
Spike
CD8 T-cells
CD69
CD137
CD4 T-cells
CD134
MNT GMT | Vic/01 | Delta
TP1 | 10 | 10
TP5 | 53 | 20
40 & above = positive
B35 PE
A24 APC
CD8
DP4 PE
CD4
P53
AZ WM
Zanubrutinib
N/D
Tetramer
P54
AZ CLL
Zanubrutinib
A1 APC
DP4

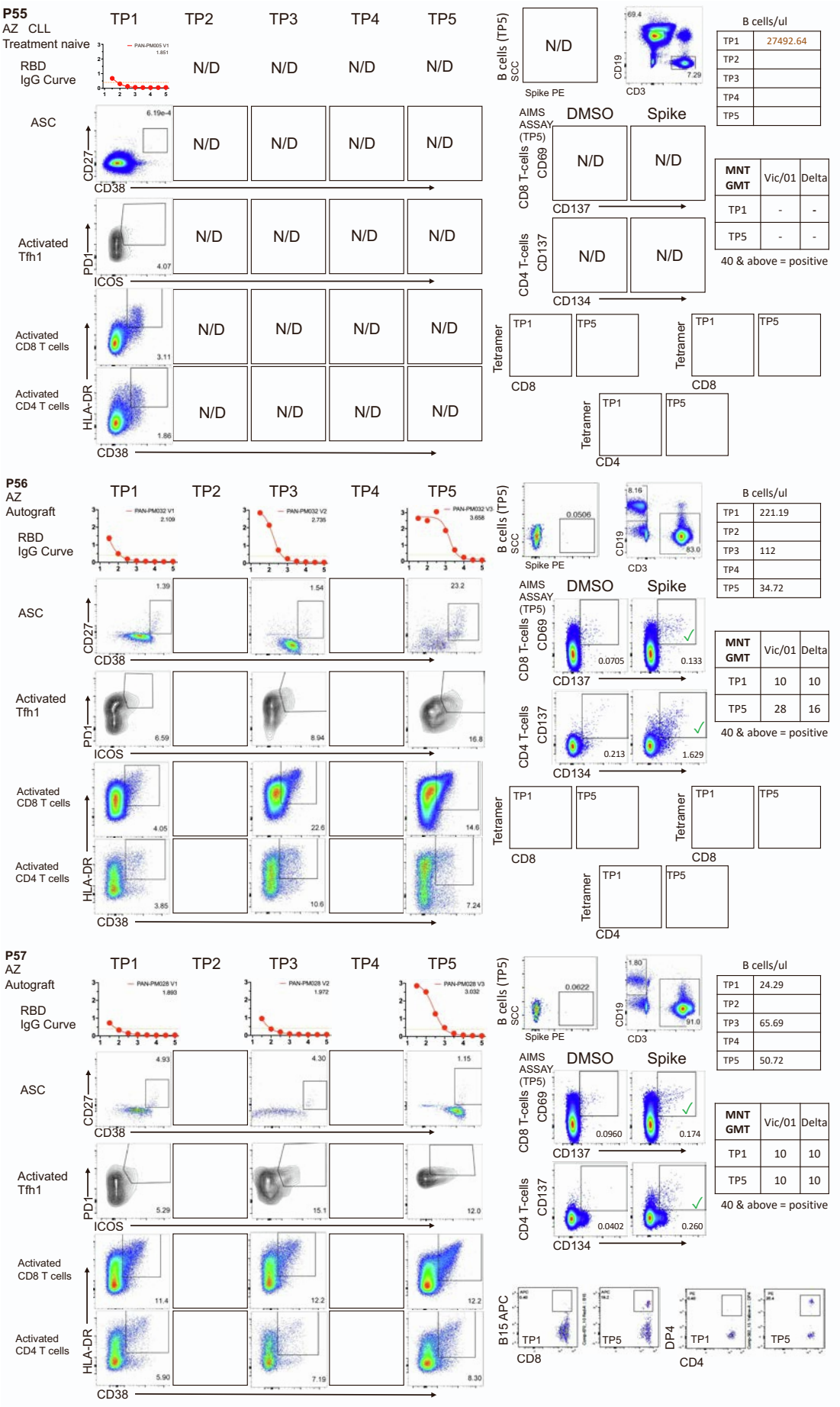
P55
AZ CLL
Treatment naive
TP1
TP2
TP3
TP4
TP5
RBD IgG Curve
ASC
Activated Tfh1
Activated CD8 T cells
Activated CD4 T cells
CD27
CD38
PD1
ICOS
HLA-DR
N/D
B cells (TP5)
SCC
Spike PE
CD19
CD3
AIMS ASSAY (TP5)
DMSO
Spike
CD8 T-cells
CD69
CD137
CD4 T-cells
CD134
Tetramer
CD8
CD4
B cells/ul
TP1 27492.64
TP2
TP3
TP4
TP5
MNT GMT
Vic/01
Delta
TP1 - -
TP5 - -
40 & above = positive
P56
AZ
Autograft
TP1 221.19
TP2
TP3 112
TP4
TP5 34.72
TP1 10 10
TP5 28 16
P57
AZ
Autograft
TP1 24.29
TP2
TP3 65.69
TP4
TP5 50.72
TP1 10 10
TP5 10 10
B15 APC
DP4

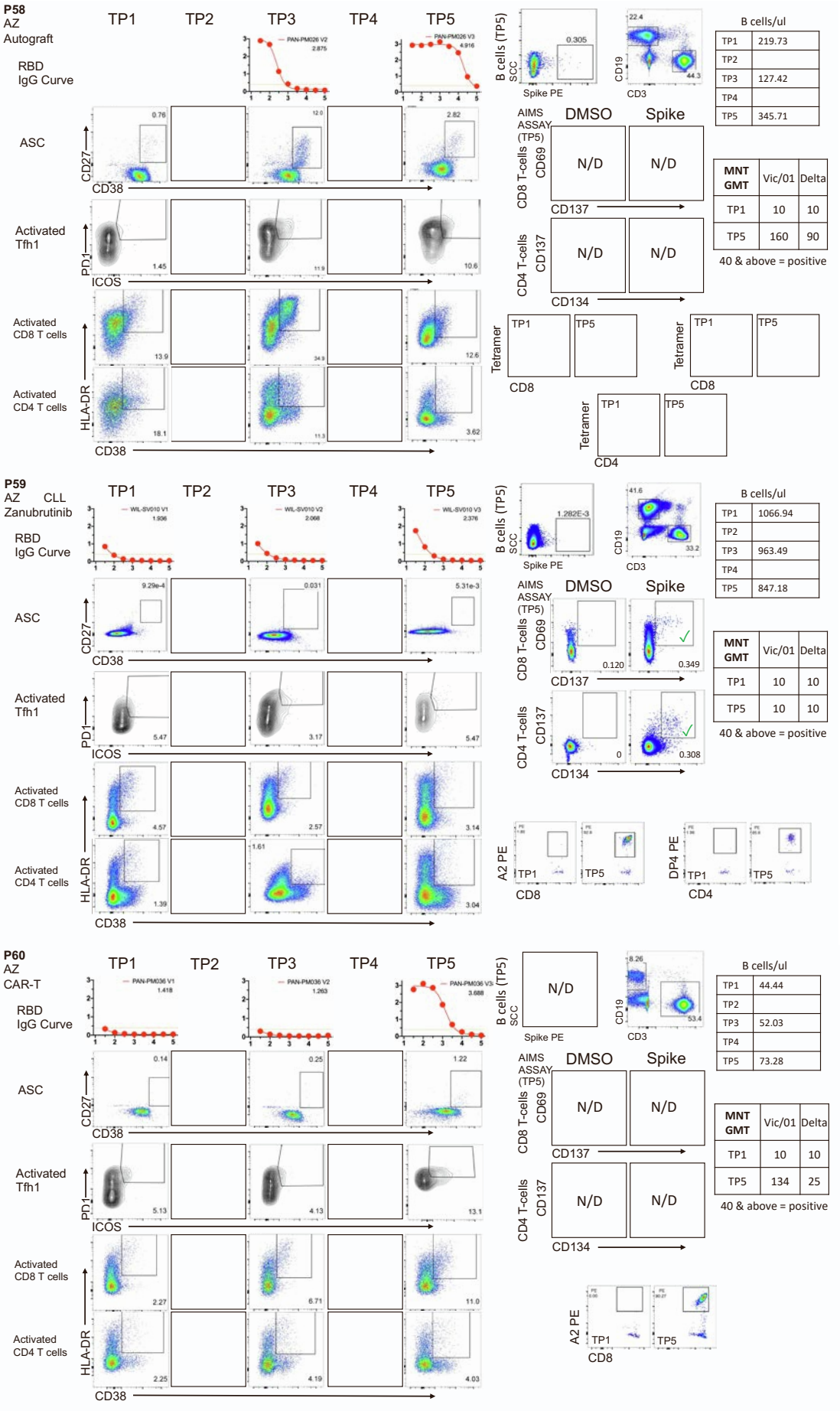
P58
AZ
Autograft
TP1
TP2
TP3
TP4
TP5
RBD
IgG Curve
ASC
CD27
CD38
Activated
Tfh1
PD1
ICOS
Activated
CD8 T cells
Activated
CD4 T cells
HLA-DR
B cells (TP5)
SCC
Spike PE
CD19
CD3
AIMS
ASSAY
(TP5)
DMSO
Spike
CD8 T-cells
CD69
CD137
CD4 T-cells
N/D
Tetramer
CD8
CD4
B cells/ul
TP1 219.73
TP2
TP3 127.42
TP4
TP5 345.71
MNT GMT | Vic/01 | Delta
TP1 | 10 | 10
TP5 | 160 | 90
40 & above = positive
P59
AZ CLL
Zanubrutinib
B cells/ul
TP1 1066.94
TP2
TP3 963.49
TP4
TP5 847.18
MNT GMT | Vic/01 | Delta
TP1 | 10 | 10
TP5 | 10 | 10
40 & above = positive
A2 PE
DP4 PE
P60
AZ
CAR-T
B cells/ul
TP1 44.44
TP2
TP3 52.03
TP4
TP5 73.28
MNT GMT | Vic/01 | Delta
TP1 | 10 | 10
TP5 | 134 | 25
40 & above = positive

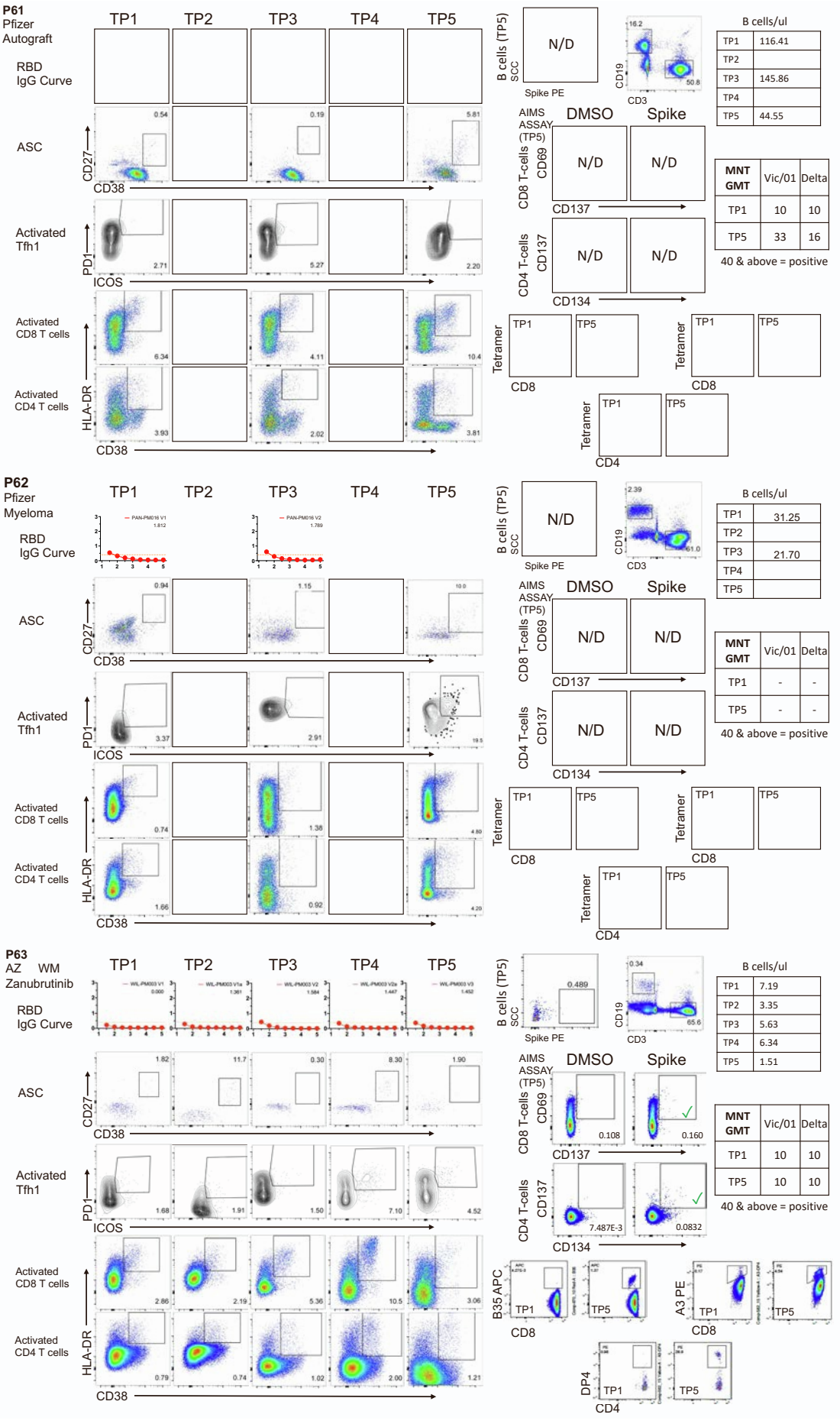
P61
Pfizer
Autograft
TP1
TP2
TP3
TP4
TP5
RBD
IgG Curve
ASC
CD27
CD38
Activated
Tfh1
PD1
ICOS
Activated
CD8 T cells
Activated
CD4 T cells
HLA-DR
CD38
B cells (TP5)
SCC
N/D
Spike PE
CD19
CD3
B cells/ul
TP1 116.41
TP2
TP3 145.86
TP4
TP5 44.55
AIMS
ASSAY
(TP5)
DMSO
Spike
CD8 T-cells
CD69
CD137
CD4 T-cells
CD137
CD134
MNT GMT Vic/01 Delta
TP1 10 10
TP5 33 16
40 & above = positive
Tetramer
CD8
CD4
P62
Pfizer
Myeloma
P63
AZ WM
Zanubrutinib
B35 APC
A3 PE
DP4

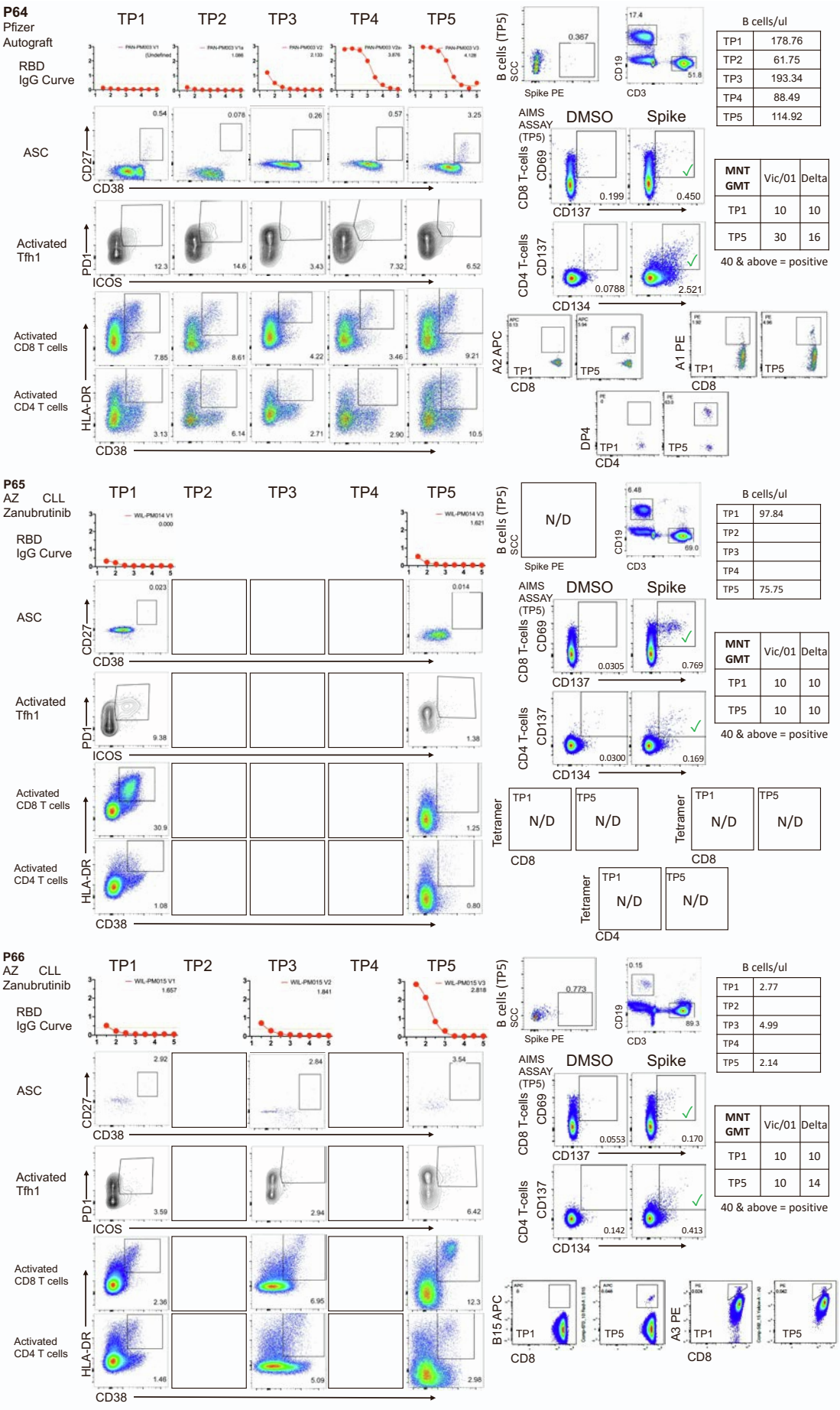
P64
Pfizer
Autograft
TP1
TP2
TP3
TP4
TP5
RBD
IgG Curve
ASC
CD27
CD38
Activated
Tfh1
PD1
ICOS
Activated
CD8 T cells
Activated
CD4 T cells
HLA-DR
B cells (TP5)
SCC
Spike PE
CD19
CD3
AIMS
ASSAY
(TP5)
DMSO
Spike
CD8 T-cells
CD69
CD137
CD4 T-cells
CD134
A2 APC
A1 PE
CD8
DP4
CD4
B cells/ul
TP1 178.76
TP2 61.75
TP3 193.34
TP4 88.49
TP5 114.92
MNT GMT | Vic/01 | Delta
TP1 | 10 | 10
TP5 | 30 | 16
40 & above = positive
P65
AZ CLL
Zanubrutinib
N/D
B cells/ul
TP1 97.84
TP2
TP3
TP4
TP5 75.75
MNT GMT | Vic/01 | Delta
TP1 | 10 | 10
TP5 | 10 | 10
40 & above = positive
Tetramer
P66
AZ CLL
Zanubrutinib
B cells/ul
TP1 2.77
TP2
TP3 4.99
TP4
TP5 2.14
MNT GMT | Vic/01 | Delta
TP1 | 10 | 10
TP5 | 10 | 14
40 & above = positive
B15 APC
A3 PE

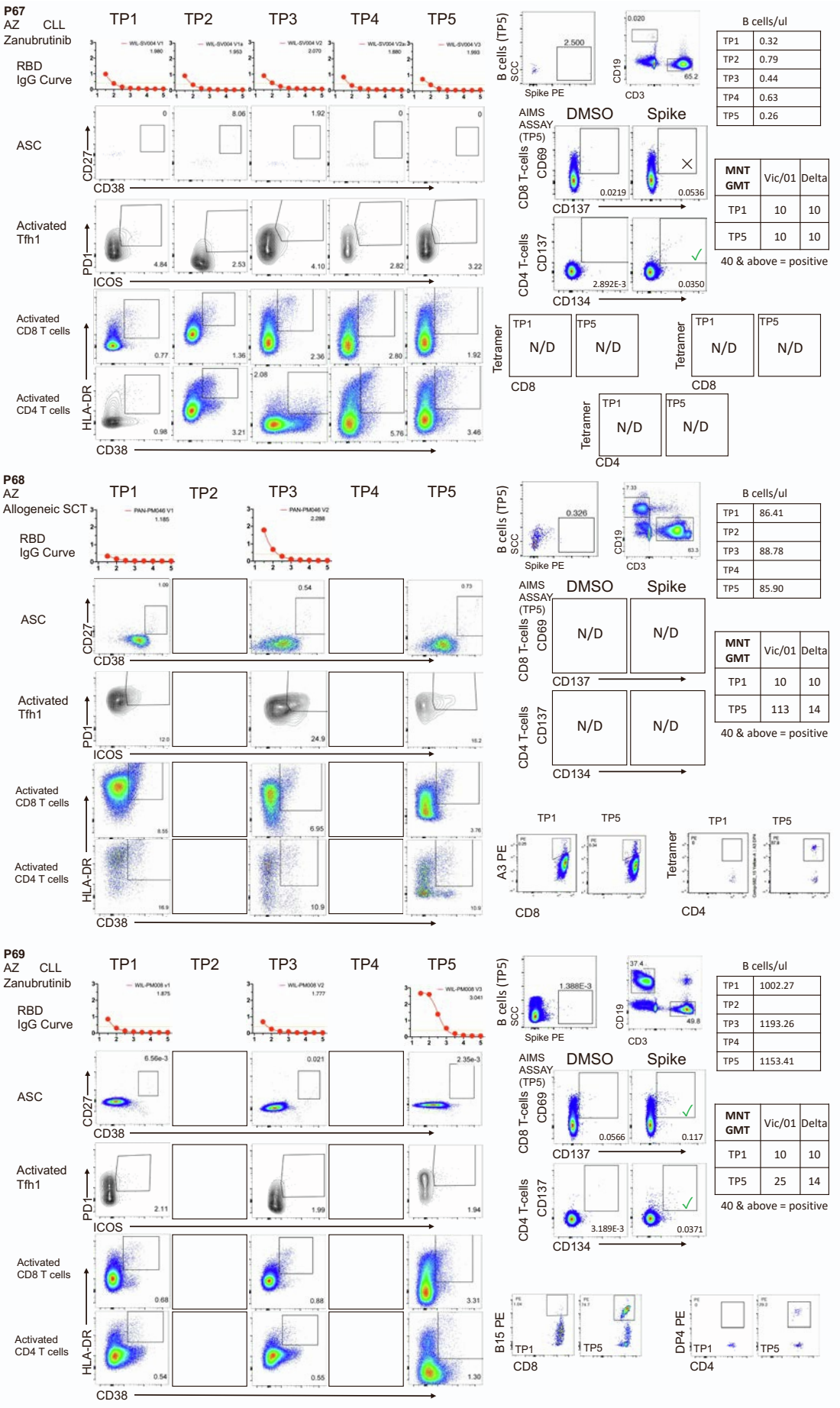
P67
AZ CLL
Zanubrutinib
TP1 TP2 TP3 TP4 TP5
RBD IgG Curve
ASC
CD27
CD38
Activated Tfh1
PD1
ICOS
Activated CD8 T cells
Activated CD4 T cells
HLA-DR
CD38
B cells (TP5)
SCC
Spike PE
CD19
CD3
AIMS ASSAY (TP5)
DMSO
Spike
CD8 T-cells CD69
CD137
CD4 T-cells CD137
CD134
Tetramer
CD8
CD4
N/D
B cells/ul
TP1 0.32
TP2 0.79
TP3 0.44
TP4 0.63
TP5 0.26
MNT GMT | Vic/01 | Delta
TP1 | 10 | 10
TP5 | 10 | 10
40 & above = positive
P68
AZ
Allogeneic SCT
TP1 TP2 TP3 TP4 TP5
RBD IgG Curve
ASC
Activated Tfh1
Activated CD8 T cells
Activated CD4 T cells
B cells/ul
TP1 86.41
TP2
TP3 88.78
TP4
TP5 85.90
MNT GMT | Vic/01 | Delta
TP1 | 10 | 10
TP5 | 113 | 14
40 & above = positive
A3 PE
P69
AZ CLL
Zanubrutinib
TP1 TP2 TP3 TP4 TP5
RBD IgG Curve
ASC
Activated Tfh1
Activated CD8 T cells
Activated CD4 T cells
B cells/ul
TP1 1002.27
TP2
TP3 1193.26
TP4
TP5 1153.41
MNT GMT | Vic/01 | Delta
TP1 | 10 | 10
TP5 | 25 | 14
40 & above = positive
B15 PE
DP4 PE

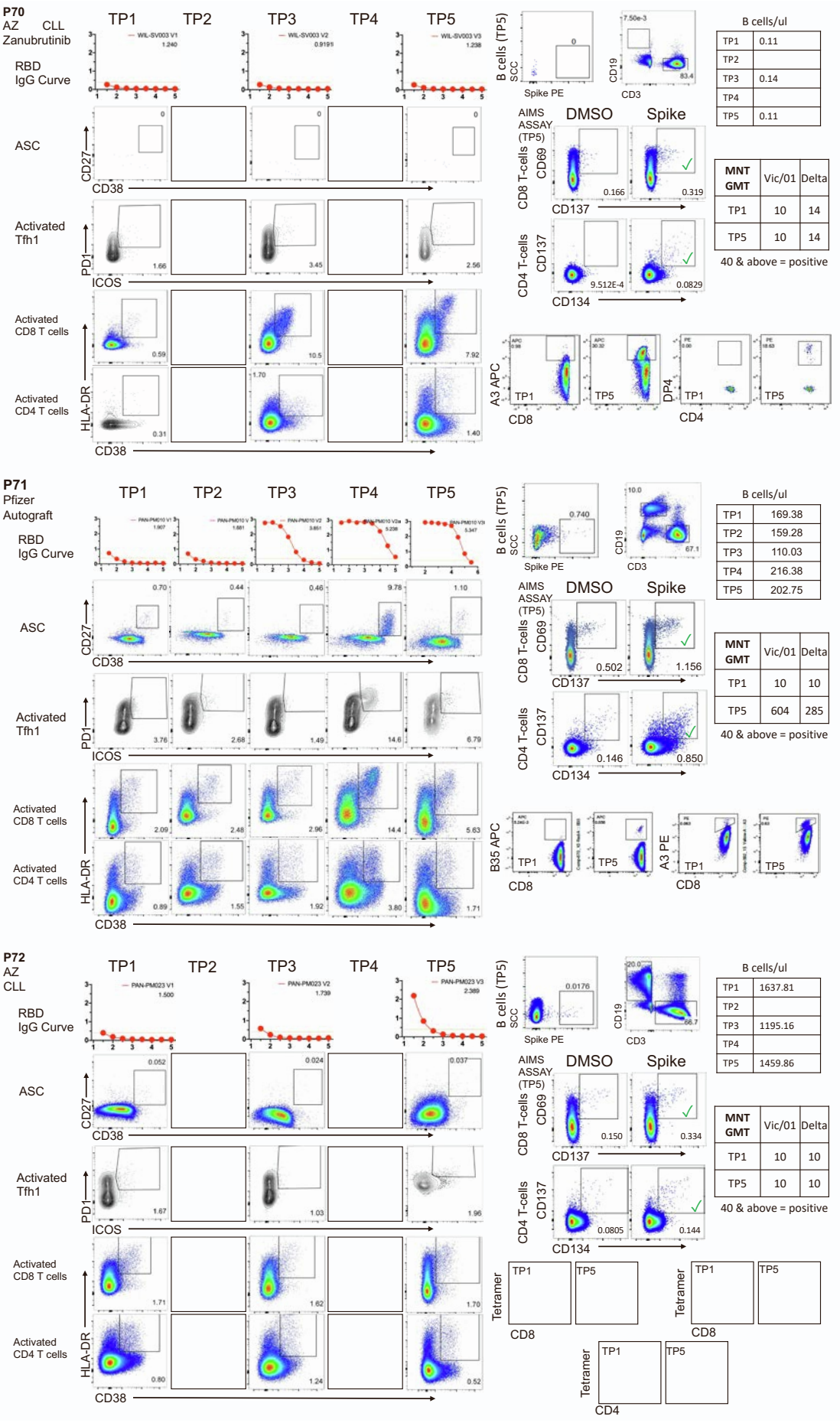
P70
AZ CLL
Zanubrutinib
TP1 TP2 TP3 TP4 TP5
RBD IgG Curve
ASC
CD27
CD38
Activated Tfh1
PD1
ICOS
Activated CD8 T cells
Activated CD4 T cells
HLA-DR
CD38
B cells (TP5)
SCC
Spike PE
CD19
CD3
AIMS ASSAY (TP5)
DMSO
Spike
CD8 T-cells
CD69
CD137
CD4 T-cells
CD137
CD134
A3 APC
TP1
TP5
CD8
DP4
CD4
B cells/ul
TP1 0.11
TP2
TP3 0.14
TP4
TP5 0.11
MNT GMT | Vic/01 | Delta
TP1 | 10 | 14
TP5 | 10 | 14
40 & above = positive
P71
Pfizer
Autograft
TP1 TP2 TP3 TP4 TP5
RBD IgG Curve
ASC
CD27
CD38
Activated Tfh1
PD1
ICOS
Activated CD8 T cells
Activated CD4 T cells
HLA-DR
CD38
B cells (TP5)
SCC
Spike PE
CD19
CD3
AIMS ASSAY (TP5)
DMSO
Spike
CD8 T-cells
CD69
CD137
CD4 T-cells
CD137
CD134
B35 APC
A3 PE
TP1
TP5
CD8
B cells/ul
TP1 169.38
TP2 159.28
TP3 110.03
TP4 216.38
TP5 202.75
MNT GMT | Vic/01 | Delta
TP1 | 10 | 10
TP5 | 604 | 285
40 & above = positive
P72
AZ
CLL
TP1 TP2 TP3 TP4 TP5
RBD IgG Curve
ASC
CD27
CD38
Activated Tfh1
PD1
ICOS
Activated CD8 T cells
Activated CD4 T cells
HLA-DR
CD38
B cells (TP5)
SCC
Spike PE
CD19
CD3
AIMS ASSAY (TP5)
DMSO
Spike
CD8 T-cells
CD69
CD137
CD4 T-cells
CD137
CD134
Tetramer
TP1
TP5
CD8
CD4
B cells/ul
TP1 1637.81
TP2
TP3 1195.16
TP4
TP5 1459.86
MNT GMT | Vic/01 | Delta
TP1 | 10 | 10
TP5 | 10 | 10
40 & above = positive

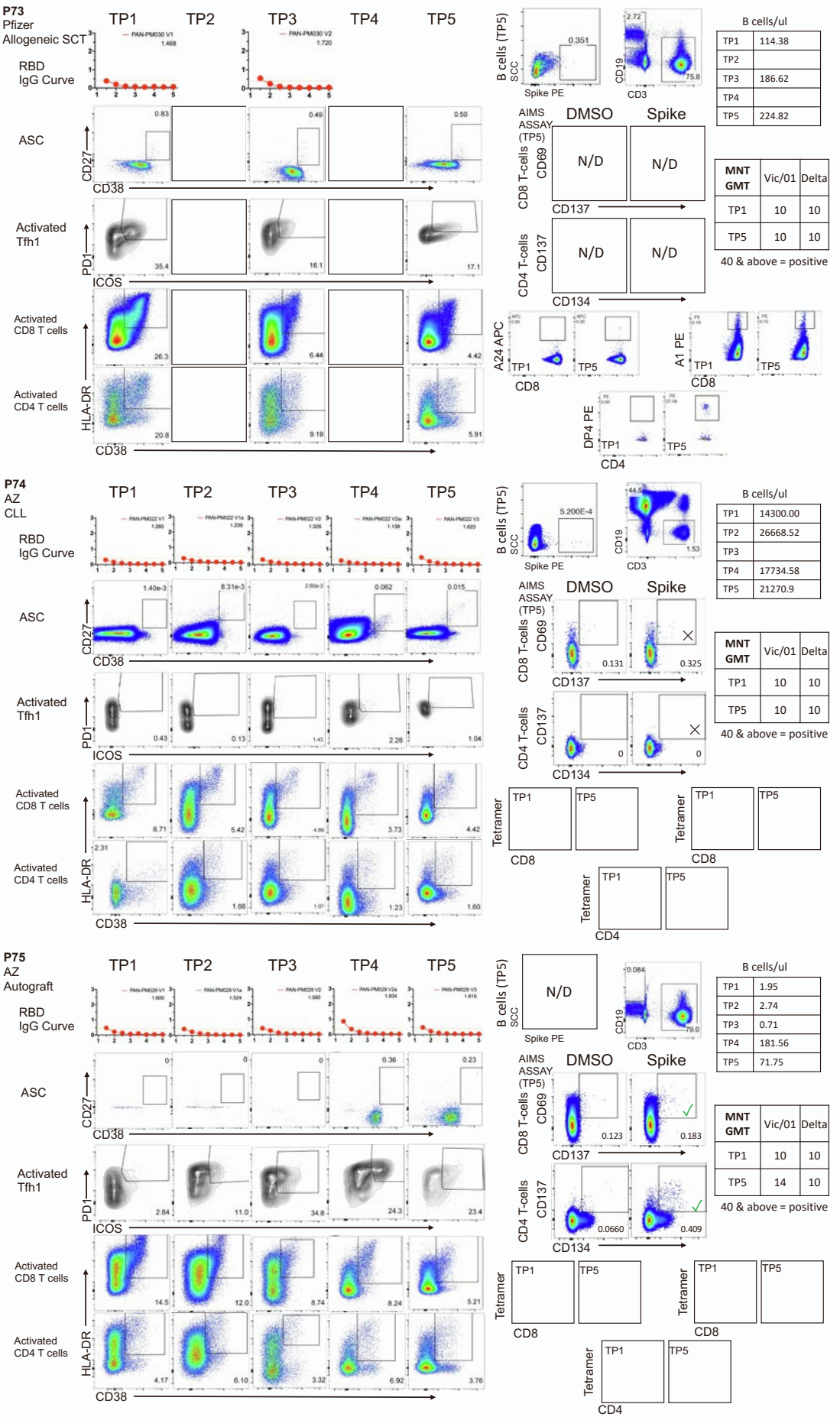
P73
Pfizer
Allogeneic SCT
TP1
TP2
TP3
TP4
TP5
RBD
IgG Curve
ASC
CD27
CD38
Activated
Tfh1
PD1
ICOS
Activated
CD8 T cells
Activated
CD4 T cells
HLA-DR
B cells (TP5)
SCC
Spike PE
CD19
CD3
B cells/ul
TP1 114.38
TP2
TP3 186.62
TP4
TP5 224.82
AIMS
ASSAY
(TP5)
DMSO
Spike
CD8 T-cells
CD69
CD137
N/D
CD4 T-cells
CD134
MNT GMT Vic/01 Delta
TP1 10 10
TP5 10 10
40 & above = positive
A24 APC
A1 PE
CD8
DP4 PE
CD4
P74
AZ
CLL
B cells/ul
TP1 14300.00
TP2 26668.52
TP3
TP4 17734.58
TP5 21270.9
Tetramer
P75
AZ
Autograft
B cells/ul
TP1 1.95
TP2 2.74
TP3 0.71
TP4 181.56
TP5 71.75

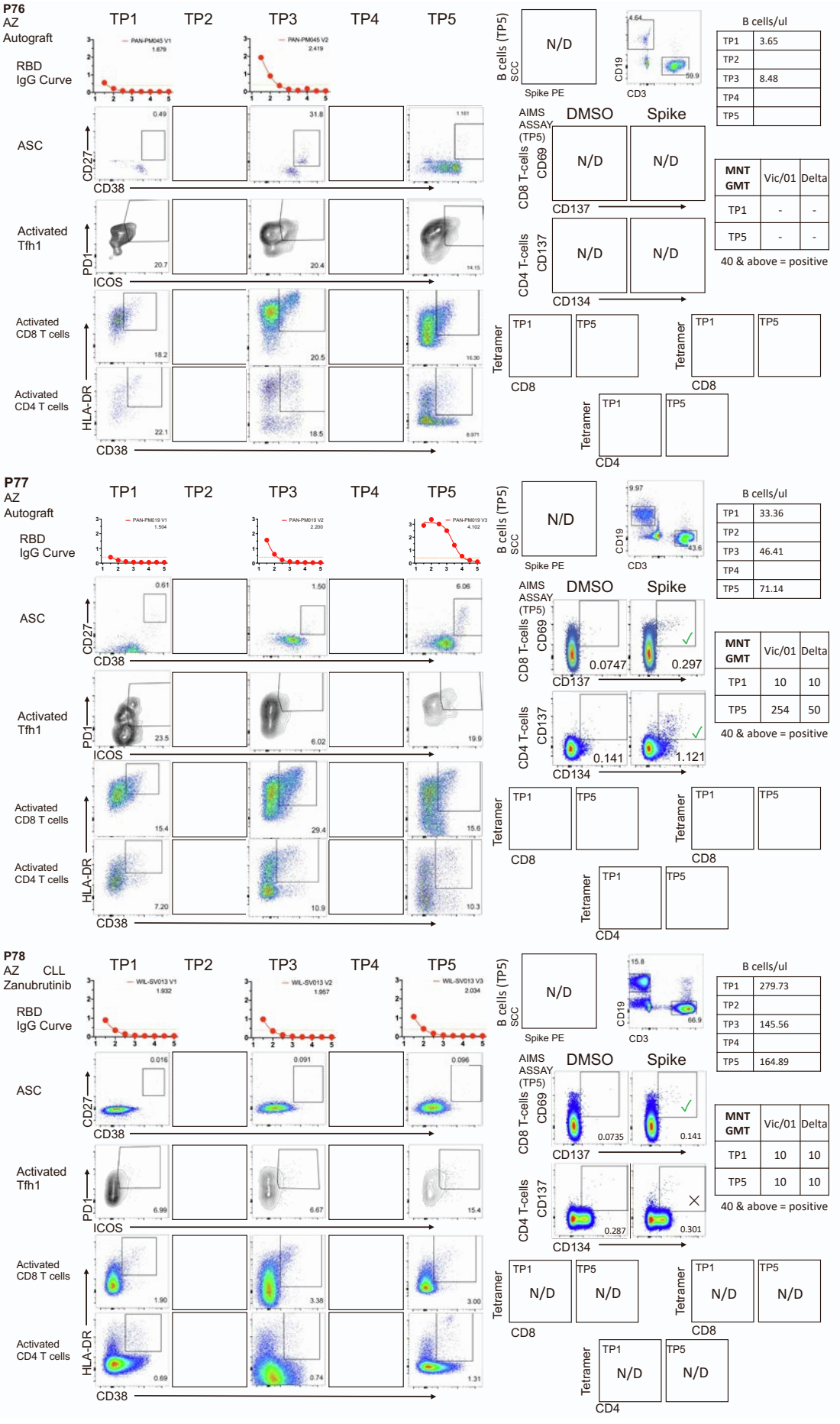
P76
AZ
Autograft
TP1
TP2
TP3
TP4
TP5
RBD
IgG Curve
ASC
CD27
CD38
Activated
Tfh1
PD1
ICOS
Activated
CD8 T cells
Activated
CD4 T cells
HLA-DR
B cells (TP5)
SCC
N/D
Spike PE
CD19
CD3
B cells/ul
TP1 3.65
TP2
TP3 8.48
TP4
TP5
AIMS
ASSAY
(TP5)
DMSO
Spike
CD8 T-cells
CD69
CD137
CD4 T-cells
CD134
MNT GMT | Vic/01 | Delta
TP1 - -
TP5 - -
40 & above = positive
Tetramer
CD8
CD4
P77
AZ
Autograft
0.0747
0.297
0.141
1.121
TP1 33.36
TP2
TP3 46.41
TP4
TP5 71.14
MNT GMT | Vic/01 | Delta
TP1 10 10
TP5 254 50
40 & above = positive
P78
AZ CLL
Zanubrutinib
0.0735
0.141
0.287
0.301
TP1 279.73
TP2
TP3 145.56
TP4
TP5 164.89
MNT GMT | Vic/01 | Delta
TP1 10 10
TP5 10 10
40 & above = positive

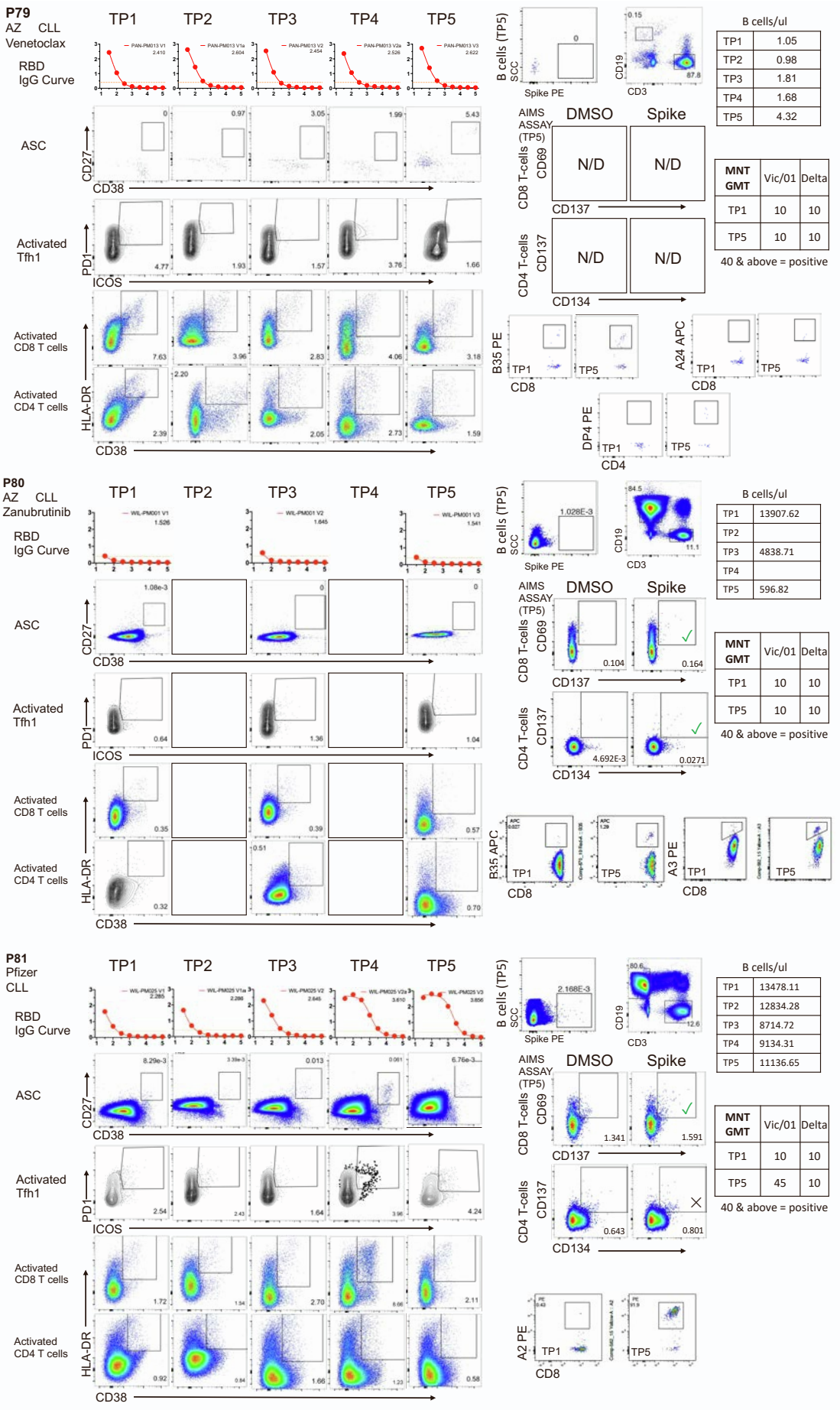
P79
AZ CLL
Venetoclax
TP1 TP2 TP3 TP4 TP5
RBD IgG Curve
ASC
CD27
CD38
Activated Tfh1
PD1
ICOS
Activated CD8 T cells
Activated CD4 T cells
HLA-DR
CD38
B cells (TP5)
SCC
Spike PE
CD19
CD3
B cells/ul
TP1 1.05
TP2 0.98
TP3 1.81
TP4 1.68
TP5 4.32
AIMS ASSAY (TP5)
DMSO
Spike
CD8 T-cells CD69
CD137
N/D
CD4 T-cells CD137
CD134
MNT GMT | Vic/01 | Delta
TP1 | 10 | 10
TP5 | 10 | 10
40 & above = positive
B35 PE
A24 APC
TP1
TP5
CD8
DP4 PE
CD4
P80
AZ CLL
Zanubrutinib
B cells/ul
TP1 13907.62
TP2
TP3 4838.71
TP4
TP5 596.82
MNT GMT | Vic/01 | Delta
TP1 | 10 | 10
TP5 | 10 | 10
40 & above = positive
B35 APC
A3 PE
P81
Pfizer
CLL
B cells/ul
TP1 13478.11
TP2 12834.28
TP3 8714.72
TP4 9134.31
TP5 11136.65
MNT GMT | Vic/01 | Delta
TP1 | 10 | 10
TP5 | 45 | 10
40 & above = positive
A2 PE

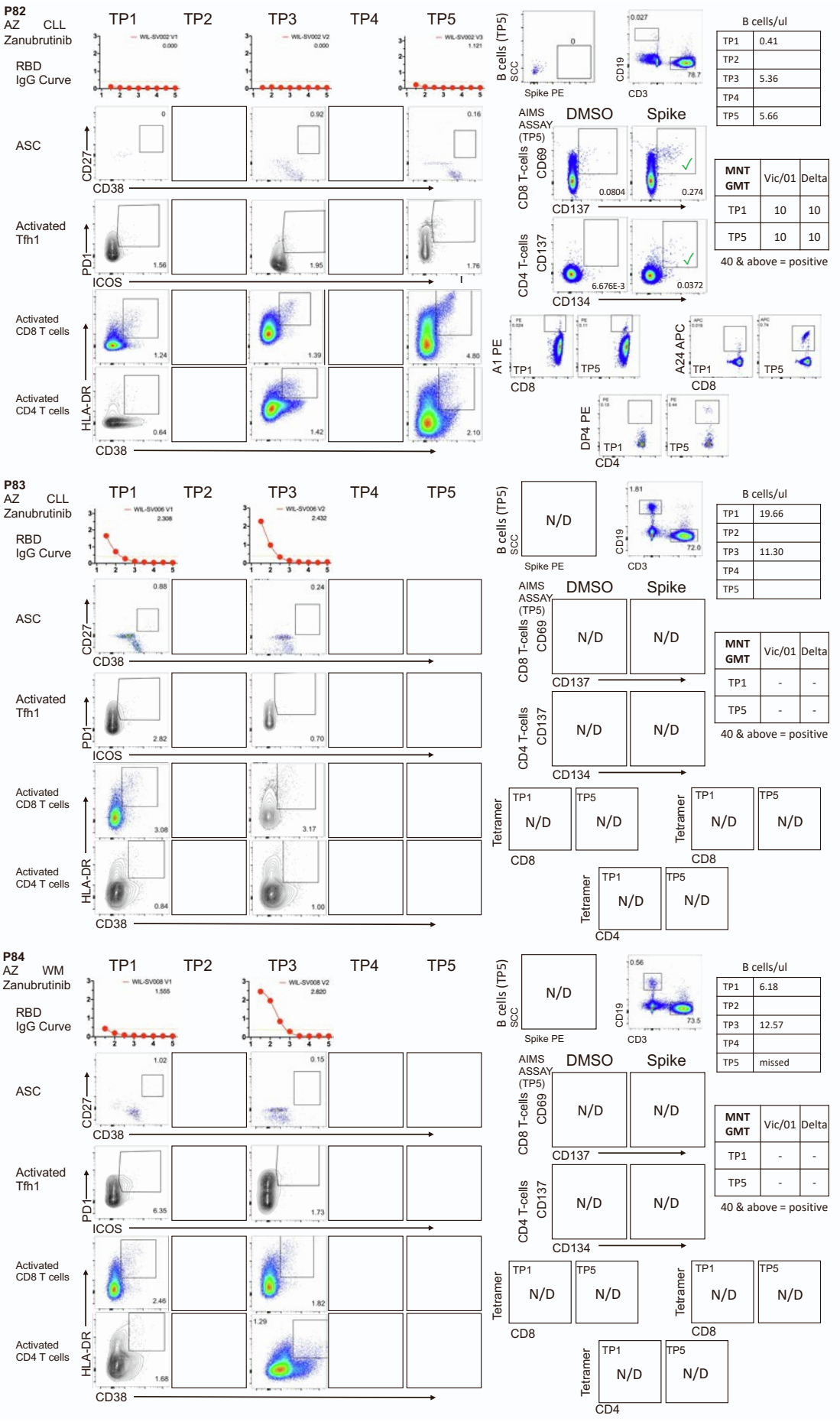
P82
AZ CLL
Zanubrutinib
RBD IgG Curve
TP1 TP2 TP3 TP4 TP5
ASC
CD27
CD38
Activated Tfh1
PD1
ICOS
Activated CD8 T cells
Activated CD4 T cells
HLA-DR
B cells (TP5)
SCC
Spike PE
CD19
CD3
B cells/ul
TP1 0.41
TP2
TP3 5.36
TP4
TP5 5.66
AIMS ASSAY (TP5)
DMSO
Spike
CD8 T-cells CD69
CD137
CD4 T-cells CD137
CD134
MNT GMT | Vic/01 | Delta
TP1 | 10 | 10
TP5 | 10 | 10
40 & above = positive
A1 PE
A24 APC
CD8
DP4 PE
CD4
P83
AZ CLL
Zanubrutinib
N/D
P84
AZ WM
Zanubrutinib
missed
Tetramer

P85
AZ
Autograft

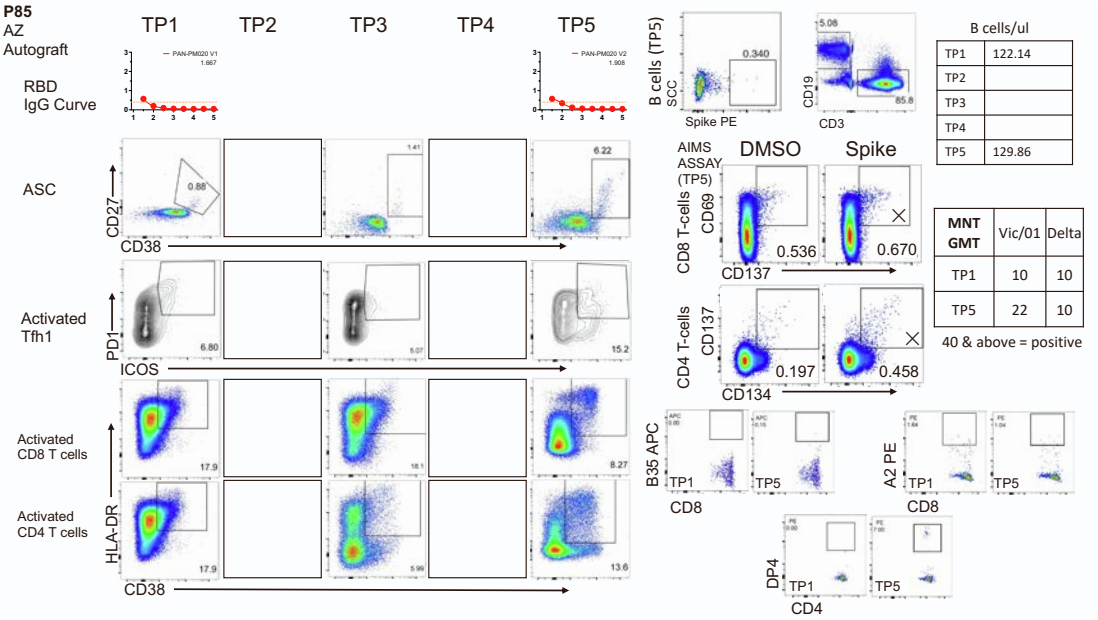

B cells/ul

TP1	122.14
TP2	
TP3	
TP4	
TP5	129.86

MNT GMT	Vic/01	Delta
TP1	10	10
TP5	22	10

40 & above = positive

P86
AZ
Autograft

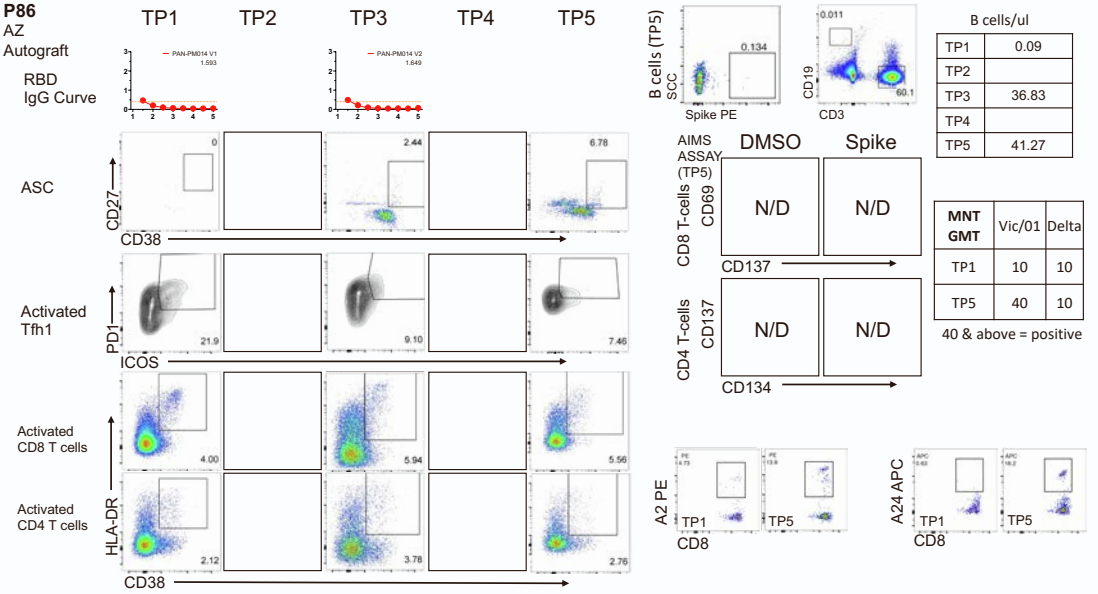

B cells/ul

TP1	0.09
TP2	
TP3	36.83
TP4	
TP5	41.27

MNT GMT	Vic/01	Delta
TP1	10	10
TP5	40	10

40 & above = positive

P87
AZ
CAR-T

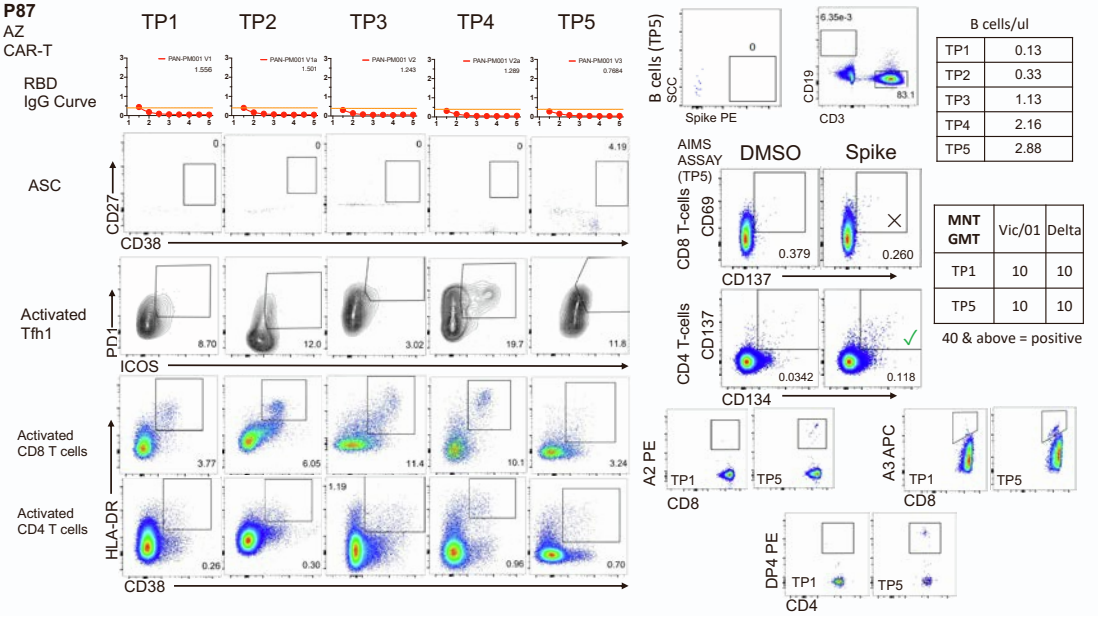

B cells/ul

TP1	0.13
TP2	0.33
TP3	1.13
TP4	2.16
TP5	2.88

MNT GMT	Vic/01	Delta
TP1	10	10
TP5	10	10

40 & above = positive

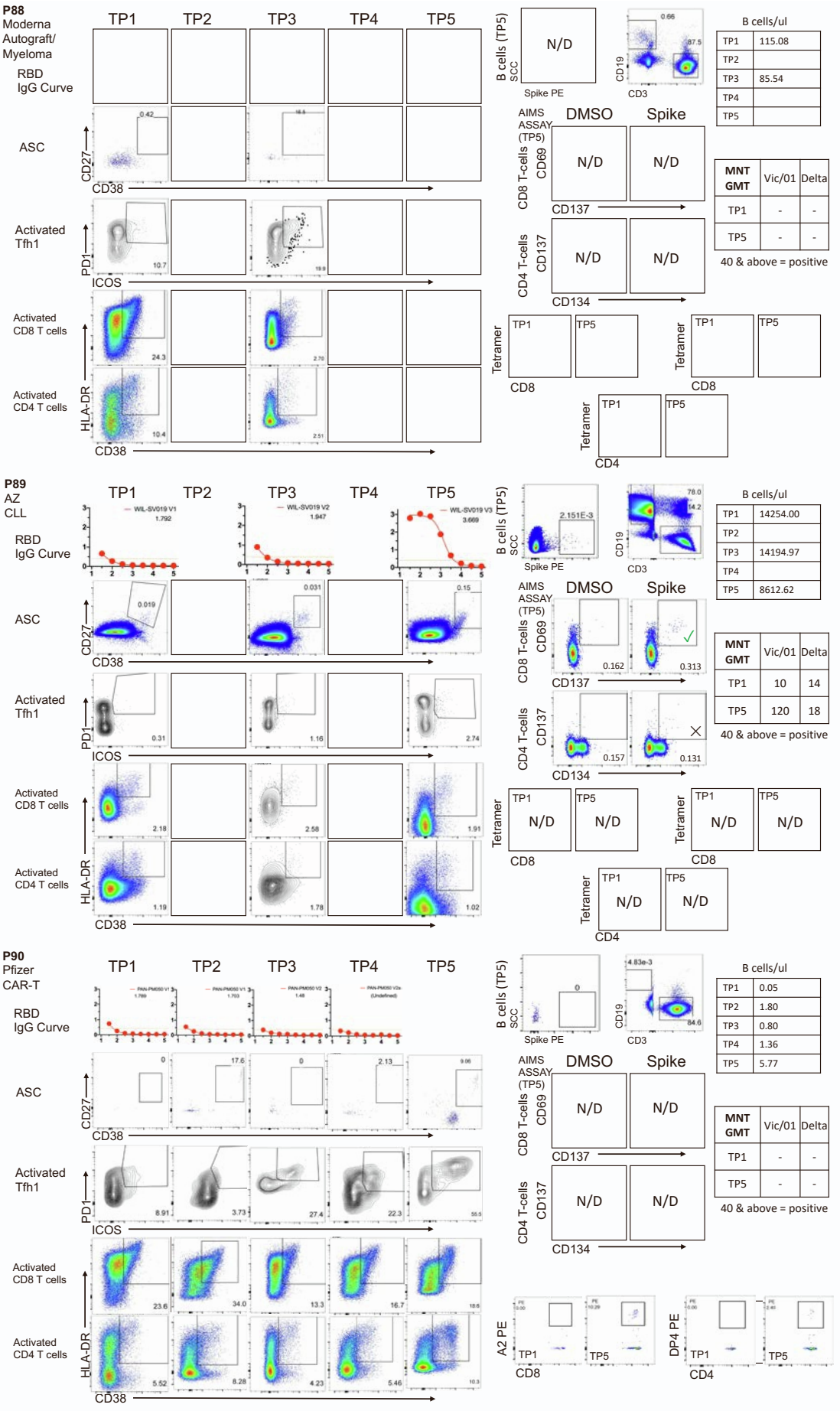
P88
Moderna
Autograft/
Myeloma
RBD
IgG Curve
ASC
Activated
Tfh1
Activated
CD8 T cells
Activated
CD4 T cells
TP1
TP2
TP3
TP4
TP5
CD27
CD38
PD1
ICOS
HLA-DR
B cells (TP5)
SCC
Spike PE
CD19
CD3
N/D
B cells/ul
TP1 115.08
TP2
TP3 85.54
TP4
TP5
AIMS
ASSAY
(TP5)
DMSO
Spike
CD8 T-cells
CD69
CD137
CD4 T-cells
CD134
MNT GMT | Vic/01 | Delta
TP1 - -
TP5 - -
40 & above = positive
Tetramer
CD8
CD4
P89
AZ
CLL
WIL-SV019 V1
WIL-SV019 V2
WIL-SV019 V3
2.151E-3
B cells/ul
TP1 14254.00
TP2
TP3 14194.97
TP4
TP5 8612.62
0.162
0.313
0.157
0.131
MNT GMT | Vic/01 | Delta
TP1 10 14
TP5 120 18
40 & above = positive
P90
Pfizer
CAR-T
4.83e-3
B cells/ul
TP1 0.05
TP2 1.80
TP3 0.80
TP4 1.36
TP5 5.77
MNT GMT | Vic/01 | Delta
TP1 - -
TP5 - -
40 & above = positive
A2 PE
DP4 PE

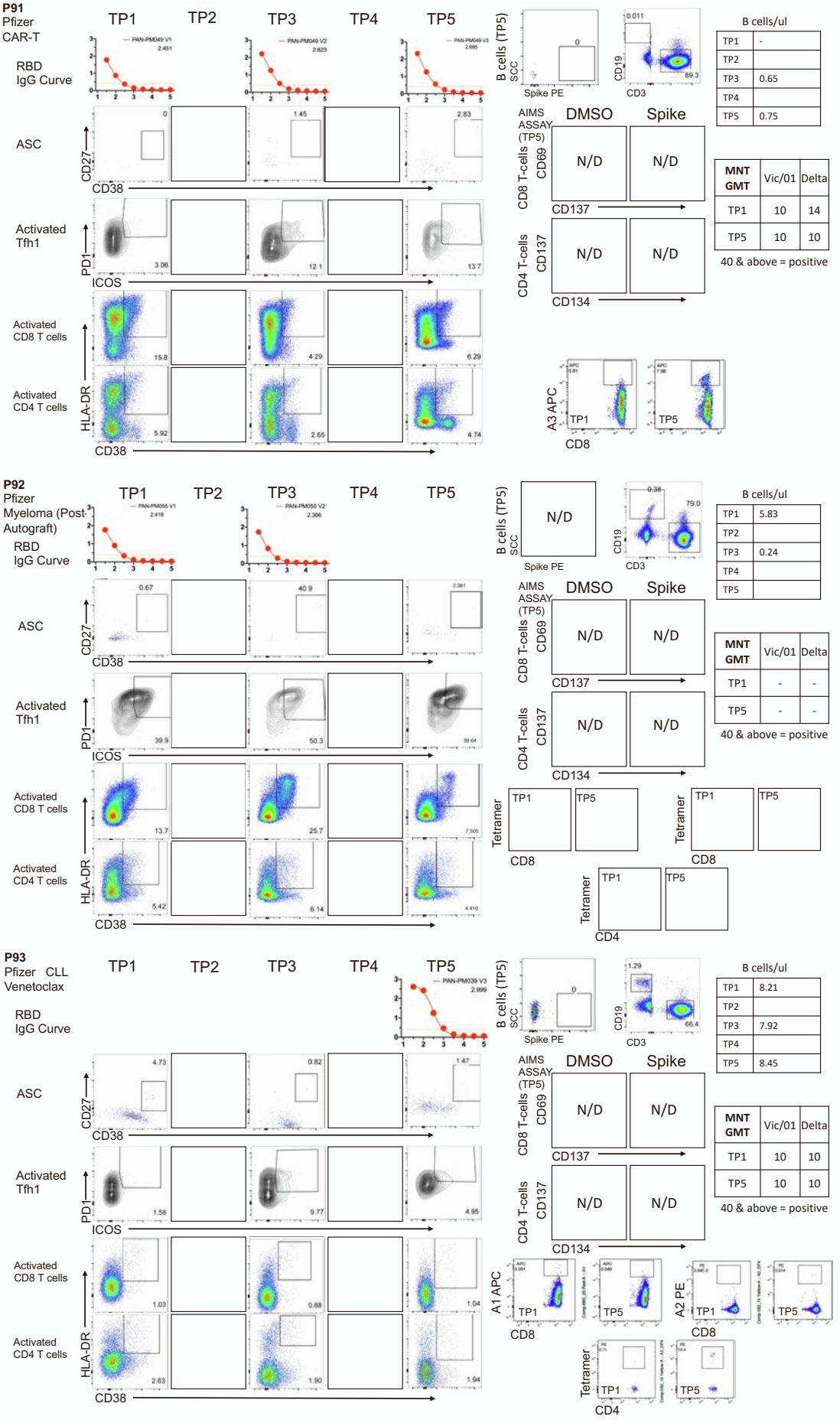
P91
Pfizer
CAR-T
TP1
TP2
TP3
TP4
TP5
RBD
IgG Curve
ASC
CD27
CD38
Activated
Tfh1
PD1
ICOS
Activated
CD8 T cells
Activated
CD4 T cells
HLA-DR
CD38
B cells (TP5)
SCC
Spike PE
CD19
CD3
B cells/ul
TP1 -
TP2
TP3 0.65
TP4
TP5 0.75
AIMS
ASSAY
(TP5)
DMSO
Spike
CD8 T-cells
CD69
N/D
CD137
CD4 T-cells
CD137
N/D
CD134
MNT GMT
Vic/01
Delta
TP1 10 14
TP5 10 10
40 & above = positive
A3 APC
TP1
TP5
CD8
P92
Pfizer
Myeloma (Post-Autograft)
RBD
IgG Curve
ASC
Activated
Tfh1
Activated
CD8 T cells
Activated
CD4 T cells
CD38
B cells (TP5)
SCC
Spike PE
CD19
CD3
B cells/ul
TP1 5.83
TP2
TP3 0.24
TP4
TP5
AIMS
ASSAY
(TP5)
DMSO
Spike
CD8 T-cells
CD69
N/D
CD137
CD4 T-cells
CD137
N/D
CD134
MNT GMT
Vic/01
Delta
TP1 - -
TP5 - -
40 & above = positive
Tetramer
TP1
TP5
CD8
CD4
P93
Pfizer CLL
Venetoclax
RBD
IgG Curve
ASC
Activated
Tfh1
Activated
CD8 T cells
Activated
CD4 T cells
CD38
B cells (TP5)
SCC
Spike PE
CD19
CD3
B cells/ul
TP1 8.21
TP2
TP3 7.92
TP4
TP5 8.45
AIMS
ASSAY
(TP5)
DMSO
Spike
CD8 T-cells
CD69
N/D
CD137
CD4 T-cells
CD137
N/D
CD134
MNT GMT
Vic/01
Delta
TP1 10 10
TP5 10 10
40 & above = positive
A1 APC
A2 PE
TP1
TP5
CD8
CD4
Tetramer

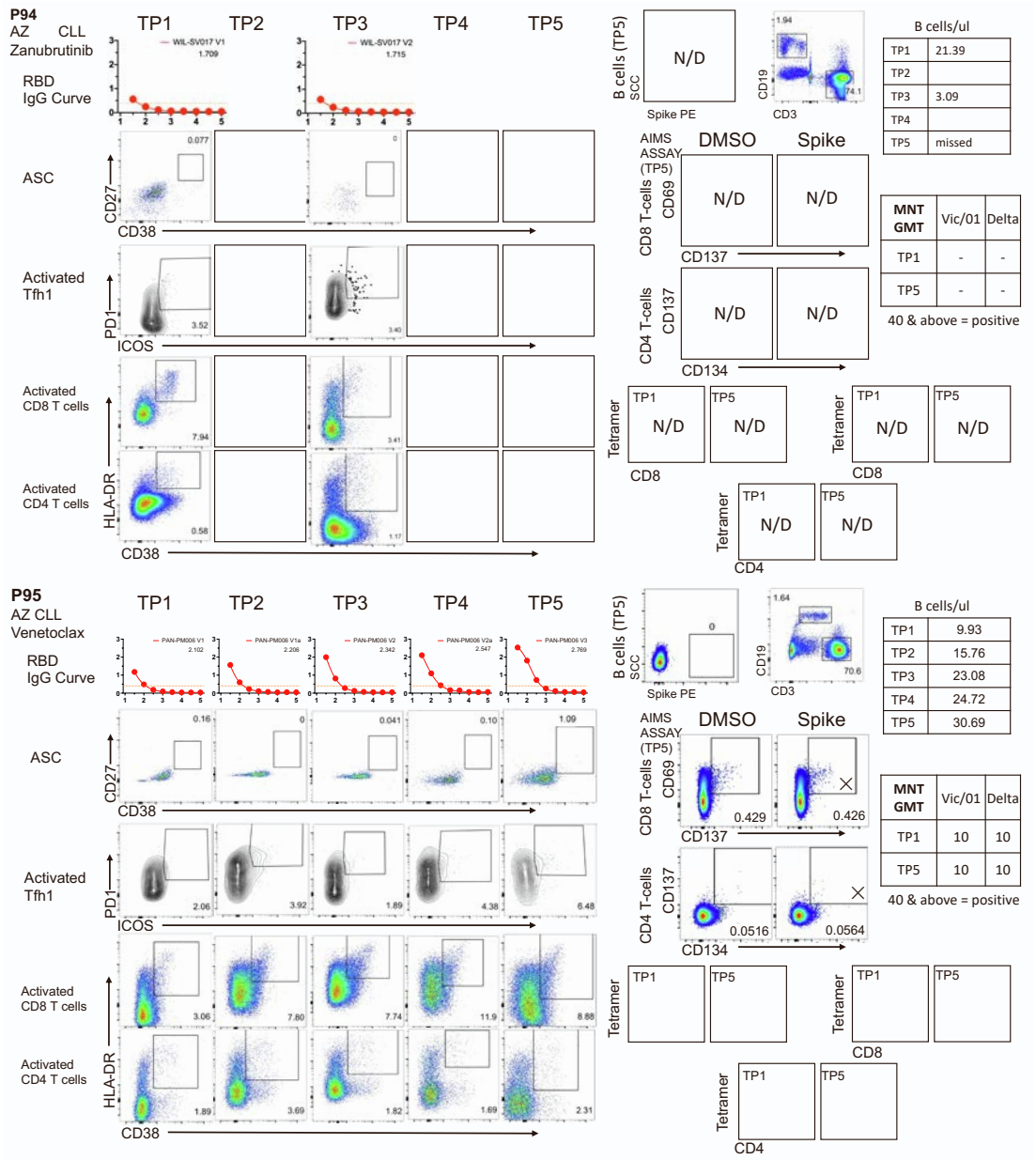

Figure S12. Individual patient's immune response following COVID-19 vaccination. T1=baseline, T2=acute response after first dose, T3=1 month post first dose, T4= acute response after second dose and T5=1 month post second dose. Due to limited sample availability, experiments were performed once for each sample. Related to Figure 1, 2, 3 and 4.